



University of HUDDERSFIELD

University of Huddersfield Repository

Elbakush, Mohamed Mostafa

Structure and function relationship in novel solid organic-inorganic hybrid base catalysts

Original Citation

Elbakush, Mohamed Mostafa (2016) Structure and function relationship in novel solid organic-inorganic hybrid base catalysts. Doctoral thesis, University of Huddersfield.

This version is available at <http://eprints.hud.ac.uk/id/eprint/30285/>

The University Repository is a digital collection of the research output of the University, available on Open Access. Copyright and Moral Rights for the items on this site are retained by the individual author and/or other copyright owners. Users may access full items free of charge; copies of full text items generally can be reproduced, displayed or performed and given to third parties in any format or medium for personal research or study, educational or not-for-profit purposes without prior permission or charge, provided:

- The authors, title and full bibliographic details is credited in any copy;
- A hyperlink and/or URL is included for the original metadata page; and
- The content is not changed in any way.

For more information, including our policy and submission procedure, please contact the Repository Team at: E.mailbox@hud.ac.uk.

<http://eprints.hud.ac.uk/>

STRUCTURE AND FUNCTION RELATIONSHIP IN
NOVEL SOLID ORGANIC-INORGANIC HYBRID
BASE CATALYSTS

MOHAMED MOSTAFA ELBAKUSH



A THESIS SUBMITTED TO THE UNIVERSITY OF HUDDERSFIELD IN PARTIAL
FULFILMENT OF THE REQUIREMENTS FOR THE DEGREE OF
DOCTOR OF PHILOSOPHY

The Department of Chemical Sciences
THE UNIVERSITY OF HUDDERSFIELD
May / 2016

Dedication

“This dissertation is lovingly dedicated to my parents for their continued support, encouragement, and constant love throughout my life”

“I would like also to dedicate my work to my loving wife, my sons Mostafa, Abdulmola and my daughter Sanabel whose love and support have accompanied me during my PhD”

Acknowledgments

First and foremost, my sincere thanks go to Allah almighty through divine direction and inspiration which helped me to attain and accomplish this academic level. I wish to express my sincere appreciation and deepest gratitude to my supervisor and advisor, Professor Robert Brown, to whom I am indebted for his guidance, motivation and support throughout this study. I would like to express my heartfelt thanks to my friend D. Ahmed Elmekawy for all his help, support and encouragement.

I would like to express my heartfelt thanks to all those individuals whose wisdom, support and encouragement made my work possible, my friends in the research office and our research group.

Abstract

The overall objective of this study was to prepare and optimise solid base catalysts for liquid phase reactions, based on silica support materials functionalised with alkyl amine groups. The study included an investigation of the effect of the pore volume, surface area and the surface chemical characteristics of the silica support on the catalyst performance. The role of surface silanol groups remaining on the silica surface after functionalisation working cooperatively with basic amine groups was also studied.

A series of silica gel supports, together with a commercially-available ordered mesoporous silica, SBA-15, were functionalized with tethered aminopropyl groups. Activities were measured in the nitroaldol reaction between nitromethane and benzaldehyde to afford nitrostyrene, and the Knoevenagel condensation reaction between benzaldehyde and ethyl cyanoacetate to form ethyl-2-cyano-3-phenylacrylate.

The results showed large variations in optimum activity depending on the support material, and its porosity in particular. All support materials exhibited an optimum catalyst loading which depended on support surface area, generally coinciding with complete coverage of the surface with a single layer of catalytic groups, based on a nominal surface area occupied by the three tethering groups linking each propylamine group to the surface.

Further experiments were performed with catalytic groups tethered by one and by two (rather than three) groups, which occupy less space on the support surface. In addition, the possible role of silanol groups was investigated by capping free silanols with non-polar methyl groups using trialkoxymethylsilane. This was found to invariably reduce the activity of the supported amine groups. Whether the role of free silanol groups was through an acid-base cooperative catalytic process or whether it was due to the hydrophilicity they impart to the catalyst surface was investigated by altering the polarity of the reaction solvent/solution. The conclusion was that the role of free silanol groups is to provide mildly acidic groups in a cooperative mechanism rather than simply through control of surface hydrophilicity/hydrophobicity.

TABLE OF CONTENTS

Chapter 1	1
1. INTRODUCTION	1
1.1. Objectives of Research	22
1.2. Heterogeneous base catalysis	2
1.3. Green chemistry and catalysis	4
1.4. Organic-inorganic hybrid materials	6
1.4.1. Organic-inorganic hybrid materials as solid catalysts	8
1.5. Role of silanol groups	9
1.6. Chemistry background and general synthesis strategies for hybrid materials	10
1.6.1. Inorganic part	11
1.6.2. Organic part	11
1.7. Hybrid interface.....	12
1.7.1. Grafting of the organic moiety onto solid surfaces.....	12
1.7.2. Direct incorporation of organic moiety.....	13
1.8. Catalyst support materials	14
1.8.1. Non-ordered mesoporous silica gel	14
1.8.2. Ordered mesoporous SBA-15 silica.....	17
1.9. Organic-inorganic hybrid catalysts in literature.....	18
1.10. Catalytic reactions used to study the catalytic activity in this work.....	20
1.11. Thesis structure.....	21
1.12. References	23
Chapter 2	29
2. INSTRUMENTAL TECHNIQUES (Background Theory)	29
2.1. Catalyst characterization.....	30

2.2.	Nitrogen Adsorption.....	30
2.3.	Adsorption isotherm models	32
2.4.	Adsorption in pores	33
2.5.	Powder X-Ray Diffraction (p-XRD).....	35
2.6.	Gas Chromatography (GC)	37
2.7.	Fourier Transform Infrared – Attenuated Total Reflectance (FTIR-ATR) Spectroscopy	38
1.	References.....	40
Chapter 3		41
3. EFFECT OF THE SILICA SUPPORT PROPERTIES ON THE PROPERTIES OF AMINE-FUNCTIONALISED CATALYSTS.....		42
3.1.	Introduction	43
3.2.	Experimental and techniques	46
3.2.1.	Materials	46
3.2.2.	Activation of silica gel	46
3.2.3.	Synthesis of amorphous mesoporous silica base catalyst (SiO ₂ -NH ₂)	47
3.2.4.	Synthesis of supported base catalysts	47
3.2.5.	Catalyst characterization	48
3.2.6.	Catalytic activity measurement.....	49
3.3.	Results and discussion:.....	51
3.3.1.	Characterisation of studied base catalysts.....	51
3.3.2.	Catalytic activities of studied base catalysts	56
3.4.	Conclusion:.....	65
3.5.	References	66
Chapter 4.....		68
4. OPTIMIZING THE ACTIVITY OF ORGANIC-INORGANIC SOLID BASE CATALYSTS BY CONTROLLING THE SURFACE COVERAGE. ..		68

4.1.	Introduction	69
4.2.	Experimental	71
4.2.1.	Material	71
4.2.2.	Activation of silica supports (EP10X, Nano-powder)	71
4.2.3.	Synthesis of solid base catalysts with (3-aminopropyl)trimethoxysilane (APTME)	71
4.2.4.	Catalyst characterization	72
4.2.5.	Catalytic activity measurement	72
4.3.	Results and discussion:	73
4.3.1.	Characterisation of studied (Nano-powder) SiO ₂ -NH ₂ (S3) base catalysts.	73
4.3.2.	Catalytic activity of studied Nano-powder (S3) base catalysts	75
4.3.3.	Characterisation of studied (EP10X) SiO ₂ -NH ₂ (S1) base catalysts	78
4.3.4.	Catalytic activity of studied EP10X (S1) base catalysts	80
4.3.5.	Discussion of monolayer optimisation:	82
4.4.	Conclusion	83
4.5.	References	84
Chapter 5		<i>Error! Bookmark not defined.</i>
5. EFFECT OF DIFFERENT AMINOPROPYLETHOXY SILANES WITH DIFFERENT GEOMETRICAL STRUCTURE AND THEIR EFFECT ON CATALYTIC ACTIVITY.		86
5.1.	Introduction	87
5.2.	Experimental and techniques	90
5.2.1.	Materials	90
5.2.2.	Activation of silica supports	91
5.2.3.	Synthesis of solid base catalysts with (3-aminopropyl)trimethoxysilane (APTMS)	91

5.2.4. Synthesis of solid base catalysts with (3-aminopropyl)triethoxysilane (APTES)	91
5.2.5. Synthesis of solid base catalysts with (3-aminopropyl)-diethoxymethylsilane (APDEMS)	91
5.2.6. Synthesis of solid base catalysts with 3-(Ethoxydimethylsilyl)propylamine (APDMES).	92
5.2.7. Synthesis of base ordered mesoporous silica (SBA-15-NH ₂).....	92
5.2.8. Catalyst characterization:.....	93
5.2.9. Catalytic activity measurement:.....	94
5.3. Results and discussion:.....	95
5.3.1. Characterisation of studied base catalysts.....	95
5.3.2. Quantification of aminopropyl groups on studied catalysts	96
5.3.3. Catalytic activities of studied base catalysts	97
5.4. Conclusion.....	106
5.5. References	107
Chapter 6	109
6. EFFECT OF SILANOL GROUPS ON THE CATALYTIC ACTIVITIES OF SOLID BASE CATALYSTS.	109
6.1. Introduction	110
6.1.1. Specific objectives	112
6.2. Experimental	114
6.2.1. Materials	114
6.2.2. Activation of silica supports (EP10X, SBA-15).....	114
6.2.3. Synthesis of solid base catalysts with APTMS (EP10X-NH ₂)	114
6.2.4. Synthesis of silylated mesoporous solid base catalysts (EP10X-NH ₂ -CH ₃)	
6.2.5. Synthesis of solid base catalysts on SBA-15 (SBA-15-NH ₂).....	115
6.2.6. Synthesis of silylated base catalysts on SBA-15 (SBA-NH ₂ -CH ₃).....	115

6.2.7. Catalyst characterization	116
6.2.8. Catalytic activity measurement	117
6.3. Results and discussion:.....	119
6.3.1. Characterisation of the base catalysts	119
6.3.2. Catalytic activity	125
6.4. Conclusion.....	138
6.5. References	139
Chapter 7	141
7. SUMMARY AND CONCLUSION.....	141
7.1. Conclusion.....	142
7.2. Recommendations for future work.....	144
9. APPENDICES	145

LIST OF FIGURES

Figure 1.1	The twelve principles of green chemistry	5
Figure 1.2	Alkene metathesis reaction	6
Figure 1.3	Arborescence representation of hybrid materials on both the academic and industrial scenes	8
Figure 1.4	Acid-Base (Cooperative)	10
Figure 1.5	Organo-functional silane hydrolysis, condensation and covalent bonding to an inorganic substrate	12
Figure 1.6	Example of grafting organosilanes onto a silanol-containing surface	13
Figure 1.7	Synthesis of polysilicic acid	15
Figure 1.8	Surface modification of silica oxide with alkoxy silanes	16
Figure 1.9	Reaction of trimethoxysilanes with (a) one, (b) two, or (c) three surface hydroxyl groups	16
Figure 1.10	Synthesis of SBA-15 mesoporous silica	18
Figure 1.11	Henry reaction (nitroaldol reaction)	21
Figure 1.12	Knoevenagel condensation reaction	21
Figure 2.1	Types of physisorption isotherms	31
Figure 2.2	Nitrogen adsorption isotherm at 77K, typical of that of mesoporous silica	35
Figure 2.3	Powder X-ray diffraction, lattice planes	37
Figure 2.4	Typical powder X-ray diffraction pattern of SBA-15	38
Figure 2.5	Schematic of (IR-ATR) Infrared Total Reflection Spectroscopy	39
Figure 3.1	Synthesis of supported base catalyst by post-synthetic (grafting)	44
Figure 3.2.	Henry reaction (nitroaldol reaction)	45
Figure 3.3	N ₂ adsorption–desorption isotherms for SiO ₂ (L1) raw silica and grafted amine-silica support SiO ₂ -NH ₂ (L1.1)	52
Figure 3.4	(A) N ₂ adsorption/desorption isotherms and (B) pore size distribution curves of the hexagonal cylindrical mesoporous SiO ₂ (S) with two different functionalised silica (S1) 1.6 mmol, (S1.1) 1.9 mmol.	53

Figure 3.5	The FTIR spectrum of SiO ₂ (S) and SiO ₂ -NH ₂ (S1)	53
Figure 3.6	Schematic diagram illustrating the functional groups grafted to silica support with small, medium, and large pore size	55
Figure 3.7	Possible grafting routes of aminopropylsilane on silica support surface	57
Figure 3.8	Kinetic data for SiO ₂ -NH ₂ (L1), SiO ₂ -NH ₂ (L1) (HCl) and SiO ₂ -NH ₂ (L1)(HNO ₃) in the nitroaldol reaction at 50 °C	57
Figure 3.9	Kinetic data for the reaction of nitromethane with benzaldehyde in the presence of o-xylene over SiO ₂ -NH ₂ (L1), SiO ₂ -NH ₂ (L2) and SiO ₂ -NH ₂ (L3)	58
Figure 3.10	First-order kinetic model of aldol reaction for different functionalised silica (APTMS)	59
Figure 3.11	Reactivity of nitromethane with benzaldehyde in the presence of o-xylene over SiO ₂ -NH ₂ (M1) and SiO ₂ -NH ₂ (M2)	60
Figure 3.12	First-order kinetic model of aldol reaction for different functionalised silica (APTMS)	61
Figure 3.13	Reactivity of nitromethane with benzaldehyde in the presence of o-xylene over SiO ₂ -NH ₂ (S1), SiO ₂ -NH ₂ (S2) and SiO ₂ -NH ₂ (S3)	62
Figure 3.14	First-order kinetic model of aldol reaction for different functionalised silica (APTMS)	63
Figure 4.1	N ₂ adsorption–desorption isotherms for silica support and grafted amine-silica support (S3)	73
Figure 4.2	Surface area vs. amine loading for amine supported on Nano-powder	74
Figure 4.3	Dependence of catalytic activity in nitroaldol reaction on amine loading for the catalysts S3, S3.1, S3.2, S3.3 and S3.4	75
Figure 4.4	First-order plots for the aldol reaction for different functionalised silica catalysts (APTMS)	76
Figure 4.5	Theoretical are occupied by functional group as % of area of Nano-powder support.	77
Figure 4.6	Schematic representation of grafted APTMS on silica surface with the possibility of amine protonation.	78
Figure 4.7	N ₂ adsorption–desorption isotherms for silica support and grafted amine-silica support (S1)	79

Figure 4.8	Surface area vs. amine loading for amine supported on SiO ₂ (S).	80
Figure 4.9	Dependence of catalytic activity in nitroaldol reaction on amine loading for silica EP10X supported amine catalysts.	80
Figure 4.10	First-order kinetic model of aldol reaction for different functionalised silica (APTMS)	81
Figure 4.11	TOF for amine supported on EP10X in the nitroaldol reaction vs the nominal (theoretical) % of the surface of the silica functionalised	82
Figure 5.1	Henry reaction (nitroaldol reaction)	88
Figure 5.2	Knoevenagel condensation reaction	88
Figure 5.3	Chemical structures and abbreviations of the silanes studied in this report	89
Figure 5.4	Kinetic data for the reaction of nitromethane with benzaldehyde in the presence of o-xylene over (T1), (T2), (T5), (S1), (S1.1) and (S1.2)	97
Figure 5.5	Activity of SiO ₂ -NH ₂ in nitroaldol reaction at 50 °C.	99
Figure 5.6	Activity of SiO ₂ -NH ₂ in nitroaldol reaction at 50 °C.	100
Figure 5.7	Activity of SiO ₂ -NH ₂ in nitroaldol reaction at 50 °C.	101
Figure 5.8	Activity of SiO ₂ -NH ₂ in nitroaldol reaction at 50 °C.	102
Figure 5.9	TOF as a function of the loading concentration of amine groups in all catalysts using the following base-catalysed reactions; nitroaldol reactions and Knoevenagel condensation reaction.	104
Figure 6.1	The silanol capping process with trimethoxymethylsilane.	110
Figure 6.2	N ₂ adsorption–desorption isotherms for S, S1.2 and S1.2-R (A) and T, T2 and T2-R (B).	118
Figure 6.3	Possibilities of linkage through one, two or three hydroxyl groups on the silica support.	121
Figure 6.4	XRD diffraction patterns of (T), (T1), (T2), (T4) and (T6).	122
Figure 6.5	Water sorption isotherm obtained at 298 K on S, S1.2 and S1.2-R.	123
Figure 6.6	Benzaldehyde conversion vs.time using T2 and S1.2 capped and uncapped in the nitroaldol reaction at 50 °C.	124

Figure 6.7	Imine catalytic mechanism for Henry reaction catalysed by amines on silica.	125
Figure 6.8	Benzaldehyde conversion vs time using SiO ₂ -NH ₂ (S1.2), SiO ₂ + APTMS and APTMS alone (all with an equivalent number of supported propylamine, 0.08 mmol) in the nitroaldol reaction at 50°C.	126
Figure 6.9	Benzaldehyde vs time for the Knoevenagal reaction studied under catalysis by SiO ₂ -NH ₂ (S1.2) , SiO ₂ +APTMS and APTMS alone (all with an equivalent number of supported propylamine, 0.08 mmol) in the nitroaldol reaction at 50°C.	127
Figure 6.10	Benzaldehyde vs. time for SiO ₂ -NH ₂ (S1, S1.1 and S1.4) and SiO ₂ -NH ₂ -CH ₃ (S1-R, S1.1-R and S1.4-R), with and without surface silanol capping in the nitroaldol reaction at 50°C.	128
Figure 6.11	First-order plots for uncapped SiO ₂ -NH ₂ (S1.4, S1.1 and S1) (A) and capped SiO ₂ -NH ₂ -CH ₃ (S1.4-R, S1.1-R and S1-R) (B) in the nitroaldol reaction.	129
Figure 6.12	Acid-base synergetic mechanism in henry reaction in different amine loading.	131
Figure 6.13	The design of experiments.	132
Figure 6.14	Benzaldehyde conversion vs time using SiO ₂ -NH ₂ (T2), in nitroaldol reaction at 50 °C.	132
Figure 6.15	Benzaldehyde vs. time for SiO ₂ -NH ₂ (S1) and SiO ₂ -NH ₂ -CH ₃ (S1-R) catalysts with nitromethane and nitroethane, with and without surface silanol capping in the nitroaldol reaction at 50°C.	134
Figure 6.16	Reactivity of nitromethane with benzaldehyde in the presence of toluene over SiO ₂ -NH ₂ .	135
Figure 6.17	First-order kinetic model of aldol reaction for uncapped SiO ₂ -NH ₂ (T2) A and capped SiO ₂ -NH ₂ -CH ₃ (T2-R) B .	135

LIST OF TABLES

Table 3.1	Silica supports used and suppliers (data from suppliers)	46
Table 3.2	Catalysts used in this chapter	48
Table 3.3	The amount of the catalyst used in each experiment	50
Table 3.4	Surface characteristics of silica supports before (raw) and after (grafted)	51
Table 3.5	The concentration of active sites on silica supports estimated by back titration.	54
Table 3.6	Elemental analysis data for three of the catalysts.	55
Table 3.7	C and N contents based on elemental analysis (MEDAC)	56
Table 3.8	Turnover frequencies for studied silica-supported catalysts with surface amine concentrations.	60
Table 3.9	Turnover frequencies for studied silica-supported catalysts with surface amine concentrations.	61
Table 3.10	The catalytic activities as TOF of catalysts and number of active sites with a small surface area.	63
Table 3.11	Surface coverage of all studied catalysts with their turn over frequencies.	64
Table 4.1	Silica support materials used (both from commercial suppliers).	71
Table 4.2	Catalysts used in this chapter.	72
Table 4.3	Textural parameters and level of functionalization for supported base catalysts.	73
Table 4.4	Number of active sites and their surface coverage on studied silica supports.	74

Table 4.5	Turnover frequencies for studied silica-supported catalysts with surface amine concentrations (Estimated by back titration) and other morphological data.	76
Table 4.6	Structural parameters for supported amine catalysts on silica EP10X.	78
Table 4.7	Measured amine concentration and their surface coverage on studied silica supports.	79
Table 4.8	The change of the activity with the surface coverage.	81
Table 5.1	Mesoporous silica supports used in this study (both from commercial suppliers).	89
Table 5.2	Catalysts have been used in this chapter are shown with shorthand names, type of support, type of amine and amount of amine that were used.	92
Table 5.3	Textural parameters for supported base catalysts.	94
Table 5.4	Concentration of amine on silica supports estimated by back titration.	95
Table 5.5	Elemental analysis data for three samples of functionalised silica EP10X.	96
Table 5.6	The number of active sites on silica EP10X supports estimated by back titration and confirmed by elemental analysis.	96
Table 5.7	The turnover frequency (TOF) and the amine contents of the catalysts used.	98
Table 5.8	Amine loading, first order rate constants and TOF values for the SiO ₂ -NH ₂ (T series) catalysts.	100
Table 5.9	Turnover frequencies with surface amine concentrations for the SiO ₂ -NH ₂ (D series) catalysts.	101
Table 5.10	Amine loading, first order rate constants and TOF values for the SiO ₂ -NH ₂ (M series) catalysts.	102

Table 5.11	Turn over frequency was calculated for each catalyst with a number of active sites.	103
Table 6.1	Silica supports used in this work.	113
Table 6.2	Catalysts have been used in this chapter are shown with shorthand names, type of support and amount of amine that were used.	115
Table 6.3	Surface characteristics of S1.2, T2 uncapped and S1.2-R, T2-R capped.	119
Table 6.4	The concentration of active sites on silica supports estimated by back titration for the (S1.2), (S1.2-R) and (T2), (T2-R) catalysts.	119
Table 6.5	Elemental analysis data for two samples of functionalised for SiO ₂ -NH ₂ (S1.2) uncapped and SiO ₂ -NH ₂ -CH ₃ (S1.2-R) capped.	120
Table 6.6	The number of active sites in two of the studied catalysts as measured by back titration and confirmed by elemental analysis.	121
Table 6.7	Elemental analysis data of base catalysts.	121
Table 6.8	First-order rate constants and TOFs for the studied catalysts in the nitroaldol reaction.	130
Table 6.9	First-order rate constants and TOFs for the studied catalysts in the nitroaldol reaction.	133
Table 6.10	The TOF was used to judge the catalytic activity of the base catalysts.	134
Table 6.11	First-order rate constants and TOFs for the studied catalysts in the nitroaldol reaction.	136

LIST OF SYMBOLS AND ABBREVIATIONS

SBA-15	Hexagonally ordered mesoporous material (SiO ₂)
APTMS	(3-Aminopropyl)trimethoxysilane
APTES	(3-Aminopropyl)triethoxysilane
APDEMS	3-Amino-propyl(diethoxy)silane
APDMES	3-(Ethoxydimethylsilyl)propylamine
TMMS	Trimethoxymethylsilane
ATR	Attenuated Total Reflectance
BJH	Barret Joyner Halenda
BET	Brunauer Emmett Teller
DVS	Dynamic Vapour Sorption
FITR	Fourier Transform Infra-Red Spectroscopy
GC	Gas Chromatography
XRD	X-ray Diffraction
TOF	Turn over frequency

Chapter 1

INTRODUCTION

In this chapter, the background and the objectives of this research are described. The structure of this thesis and a brief overview of individual chapters are also summarized.

1.1. Heterogeneous base catalysis

Heterogeneous catalysis plays an important role in many areas of the chemical and energy industries. It provides many opportunities for recovering and recycling catalysts from reaction environments.¹ These characteristics could potentially lead to improved processing steps, better process economics, and more environmentally friendly industrial manufacturing. Nevertheless, further efforts will be required in the design of new heterogeneous catalysts in order for them to reach activity and selectivity values competitive with homogeneous ones.^{2, 3}

When the catalyst and the reactants are in the same phase, the catalyst is termed *homogeneous*. The term covers both liquid and soluble solid catalysts in liquid solution, such as the mineral acid catalysts and base catalysts that are applied broadly in industrial applications.⁴ However, when the catalyst and the reactants are in different phases, then the catalyst is said to be *heterogeneous*. The term may refer to solid catalysts used with reactants in the gas or liquid phase, for instance, the platinum catalysts used in catalytic converters fitted to automobile exhausts to convert pollutants to less toxic compounds before being released into the environment.⁵ Nobel prizes were awarded in 1918, 1932, 1963 and 2007 to Fritz Haber and Carl Bosch, Irving Langmuir, Ziegler and Natta, and to Gerhard Ertl respectively, for their research achievements in heterogeneous catalysis.^{6, 7}

Each type of catalyst has its advantages and disadvantages. With homogeneous catalysts, the catalysis occurs at a specific site. These catalysts can be designed using synthesis and characterisation methods to become reaction-selective. Common reaction-selective enzymes are those enzymes found naturally within cells that have high-selectivity binding sites to specific reactants and therefore activate specifically to result in specific products. This performance has inspired and motivated the designers of homogeneous catalysts to synthesise non-biological catalysts with similar selectivity and activity to enzymatic biocatalysts.^{8, 9} However, a major drawback of using homogeneous catalysts in industry is the requirement for an additional process to separate them from the final reaction products.¹⁰ Separating catalysts is important, as their recycling is of high importance environmentally and economically; they may be expensive or, as in the case of transition metals, toxic in character.¹¹ In the production of some chiral pharmaceuticals, for instance, homogeneous organometallic catalysts are commonly used, and their consequent separation and removal to the required part per million levels is of high importance for product purity and for health purposes, as determined by the Food and Drug Administration in the United States.¹² However, in instances where only small

quantities of the catalysts are required (e.g. olefin polymerisation catalysts),¹³ where the catalyst has very high activity, or the recycling process is expensive, then recovery is not undertaken, since it is cheaper to use them once only (e.g. mineral acid/base catalysts).⁴

Unlike homogeneous catalysts, heterogeneous catalysts exist in a different phase from the reactants and the reaction. Heterogeneous catalysts can have different surface sites that differ chemically and therefore facilitate and promote their catalytic activity and are therefore named multi-sited catalysts.¹⁴ Although heterogeneous catalysts are likely to be less active and selective compared with homogeneous catalysts, they are favoured in industrial catalytic processes because of their ease of separation and re-use, which is important in continuous processes. This characteristic also leads them to be considered environmentally friendly or “green”.¹⁵ However, factors such as high calcination temperatures, and the use of homogeneous catalysts and reagents in the process of synthesising heterogeneous catalysts, make them less favoured environmentally.¹⁶

To facilitate the separation of homogeneous catalysts from reactants and reaction mixture, the technique of immobilising the catalyst on a solid support has been developed. A variety of methods have been used to immobilise homogeneous catalysts on insoluble supports, including polymer encapsulation,¹⁷ covalent tethering to a polymer backbone,¹⁸ and covalently tethering to an inorganic framework, such as silica, to form an organic/inorganic hybrid material.¹⁹ The thermal stability of the support silica and its low cost besides the variety of organosilanes used for covalent surface modification make covalently tethering to inorganic frameworks favoured and advantageous. Nylon materials have been used recently as supports for organic catalysts.²⁰ When tethered to inorganic surfaces, their behaviour is similar to their behaviour in solution. However, when designing this type of tethered catalyst, other factors relating to the catalytic reactions in which they are involved need to be considered: for instance, reactants diffusing towards the surface, reactant movement to the active catalytic sites, and desorption of products from the surface. Several reports have been published that discuss immobilised catalysis involving single organic catalytic activity fixed on a silica surface, most commonly involving acid and base groups. Enzymes and complex molecules (e.g. cinchona alkaloids)²¹ have been employed in heterogeneous catalysis fixed on a silica surface.²² Heterogeneous catalysts have been found to show better catalytic activity in some cases compared with their homogeneous analogues, owing either to their interaction with the support, to partitioning of solid/liquid that

could result in the concentration of reactants near the catalytic sites, or to other effects related to the two-dimensional concentration of active sites on their surfaces.

1.2. Green chemistry and catalysis

Awareness of the effects of chemical processes on the environment, especially those connected with industry, is increasing. There is therefore a need to find more suitable and environmentally friendly processes; this area of activity is known as “green chemistry”. Green chemistry attracts considerable attention in relation to its role in protecting the environment and natural resources, and its contribution to the economy by developing more suitable processes. Green chemistry is concerned with the impact of the chemicals themselves on the environment, as well as their production processes;^{23, 24} it therefore aims to reduce the adverse impacts that chemical processes and products may have upon the environment, and to recycle chemicals that provide significant material saving compared to traditional methods, such as recyclable heterogeneous catalysts. “Green” chemists attempt to reduce or address many of the negative effects on the environment and health of chemical processes and production.²⁵ Warner and Warner have set out the ways in which green chemistry can do this (see Figure 1.1, below).²⁶



Figure 1.1. The twelve principles of green chemistry²⁶

Catalysis played a central role in the development of the chemical industry during the twentieth century, and is likely also to have a very important role in the new greener industry of the twenty-first century. The value of catalysis can be shown not only in facilitating “green”

chemical processes directly (e.g., by replacing reagents, or by enabling more efficient processes), but also in minimising their environmental effects and costs.²⁷

Catalysis provides several green chemistry advantages such as increased selectivity, lower energy requirements, and the requirement for catalytic as opposed to stoichiometric quantities of material. Also it allows for the use of safe or less toxic materials, and reduces the use of processing and separation agents. Heterogeneous catalysis addresses the aims of green chemistry by offering ease of separation of catalyst and product, thus eliminating, for example, the need for distillation or extraction.²⁸ In addition, environmentally safe catalysts, such as zeolites and clays, may replace more hazardous catalysts currently in use. The catalysis may be utilised as a pollution prevention tool in green chemistry reactions.²⁹ Catalyst design and its application in manufacturing and processing are helping to realise the benefits of using them to the environment, human health and the economy.²⁹

It is important to be determine how chemical processes can meet the challenges of green chemistry. However, other criteria should be considered, such as chemical yield, the cost of the starting materials of the reaction, and safety in handling the chemicals.³⁰ The outputs that green chemistry can contribute to a safer and better future are outlined above (Figure 1.1).

The Nobel Prize in Chemistry 2005 was jointly awarded to Yves Chauvin, Robert H. Grubbs and Richard R. Schrock, for the discovery of a catalytic chemical process called metathesis in organic synthesis, with explicit reference to its contribution to green chemistry and "smarter production".³¹

The olefin metathesis reaction, one of the most successful organic reactions, can be considered as one in which all the carbon-carbon double bonds in an olefin (alkene) are broken and then reorganised in a statistical fashion. An example of alkene metathesis is shown in Figure 1.2.

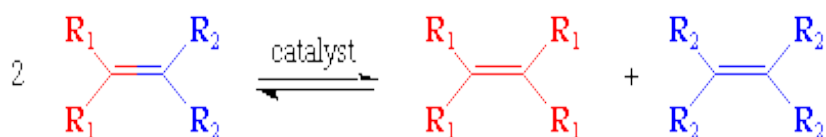


Figure 1.2. Alkene metathesis reaction

If one of the product alkenes is volatile (such as ethylene) or is otherwise easily removed, then the reaction shown above can be driven completely to the right. Likewise, using a high pressure of ethylene, internal olefins can be converted to terminal olefins.³²

In 1996 the Dow Chemical Company won the Greener Reaction Conditions award for the development of an agent used in polystyrene foam production for carbon dioxide blowing. Polystyrene foam is commonly used in packing and transporting food. In the United States alone polystyrene foam production reaches up to seven hundred million pounds. Traditional methods of foam sheet production commonly employ chlorofluorocarbons (CFCs) and other ozone-depleting materials, which have been found to present serious environmental hazards.³³

1.3. Organic-inorganic hybrid materials

Organic–inorganic hybrid materials have a very important role in the development of advanced functional materials. The research in functional organic-inorganic hybrid materials is supported through increasing interest of chemists, physicists and materials scientists who wish to take full advantage of the opportunity to invent smart materials that benefit from the best of the two realms i.e. organic and inorganic.³⁴

Hybrid organic–inorganic materials involve more than a solely physical synthesis. Hybrid organic–inorganic materials are commonly described as *nano-composites*: molecules with organic and inorganic components, carefully mixed such that the size of the components ranges from at least a few angstroms to many nanometers.³⁵ Thus, in hybrid materials their properties represent the sum of those of the individual composing materials; however, based on the nature of the interaction of the components, materials can be divided clearly into two distinct classes:

Class I: the organic and inorganic components are embedded, and only hydrogen, van der Waals or ionic bonds give cohesion to the whole structure.

Class II: the two phases are partly linked together through strong chemical covalent bonds.^{36 37}

The solid state chemistry and molecular methods of molecular and nanochemistry have attained a very high level of sophistication. Chemists can tailor many molecular types and design new functional hybrid materials with enhanced properties. Actually, many hybrid materials are synthesised and treated using “soft” chemistry approaches based on:

- The polymerisation of functional organosilanes and macromonomers³⁸
- The encapsulation of organic components within sol-gel derived organosilicas or hybrid metallic oxides³⁹
- Self-assembly or templated growth, such as microporous metal organic frameworks (MOFs).⁴⁰

The potential of these hybrid materials prepared by various methods is reflected in the fact that many of them are being brought to market for a range of purposes, evidence of the increasing impact of hybrid materials science, both on the academic and industrial scene, is represented in Fig 1.3.



Figure 1.3. Arborescence representation of hybrid materials on both the academic and industrial scenes.⁴¹

1.3.1. Organic-inorganic hybrid materials as solid catalysts

Catalysts used in industry for their essential role in chemical processes and impact on the environment are available in a wide range of forms, including the heterogeneous type (porous solids form), homogeneous type (liquid form dissolved in the reaction mixture) and biological type (enzyme form).⁴²

Many efforts have focused within the last decade on utilising hybrid catalysts (organic-inorganic materials) as solid catalysts, particularly within the fields of materials science and catalytic applications.⁴³

Solid catalysts are quite often environmentally benign: they are noncorrosive, can be easily separated from liquid products, and cause fewer disposal problems, in addition to their ability to be repeatedly re-used.⁴⁴ Moreover, they can be designed to provide a long catalyst life, high activity and selectivity.^{45, 46}

There are many advantages of hybrid organic-inorganic catalysts over other types of solid catalysts, such as those on polymer supports and those based on metal oxides. Polymer supports have a number of disadvantages, such as loss of mechanical stability, swelling, and sensitivities towards many chemical environments. These disadvantages are not present in hybrid organic-inorganic catalysts.⁴⁷ In the case of metal oxides it is very difficult, although not impossible, to control the heterogeneity of their active surface sites. This results in a negative impact on their selectivity, which is the most important feature in catalysis.

An important feature of organic-inorganic hybrid solid materials is that they can be easily designed as single-site catalysts, combining the advantages of both heterogeneous and homogeneous catalysts.⁴⁸ Furthermore, metal oxides require very high temperatures of >500 °C to activate the catalysts during preparation, and if they are left exposed to the atmosphere for a long period of time it is possible for them to become poisoned; organic-inorganic hybrid catalysts, by contrast, can be activated with comparatively low temperatures of 120 °C.⁴⁹

1.4. Role of silanol groups

The high activity of heterogeneous amine catalysts compared to homogeneous amines suggests that the silica surface play an important catalytic role.⁵⁰

The surface of silica materials can be functionalised with a variety of organic groups, via a reaction of the silanol groups on the silica surface with functional alkoxy silanes to anchor the organic group to the silica support.⁵¹

Mesoporous silica functionalised with 3-aminopropyl groups can be prepared either by co-condensation of 3-aminopropyltrialkoxysilane with a silica precursor, or by post-synthetic grafting on to the surface of a mesoporous silica support. In the process of post-synthetic grafting using mesoporous silicates, the surface silanol groups, which can be present in high concentration, act as convenient anchoring points for organic functionalised.^{52, 53}

The silanol groups at one end of hydrolysed 3-aminopropyl trialkoxysilane can bind with OH groups exposed on the material surface, while its amine group can be exploited for further covalent derivatisation with organic molecules; the mechanism of the silanol condensation is well-established.⁵⁴

Recently, investigations showed that the surface silanols of the mesoporous silica were beneficial to the catalytic performances for the synergetic catalytic effects with the introduced reactive groups such as amines.⁵⁵

The synergetic interactions between different functional groups are a feature of catalytic activity, and are increasingly being exploited in developing chemical catalysts that display high selectivity and specificity. Recently, a new research approach is working to improve the reactivity of heterogeneous catalysts through enhancing the cooperation between multiple functional groups;⁵⁶ for instance, it was recently shown that the silanol groups on the surface of mesoporous silica are likely to improve catalytic performance.⁵⁷ Addition of organic groups may improve cooperative catalytic activity.⁵³

The weakly acidic silanol groups (residual silanol) can form hydrogen bonds with reactants, leading to cooperative catalysis with surface organic groups, as shown in Figure 1.4 below.⁵⁶

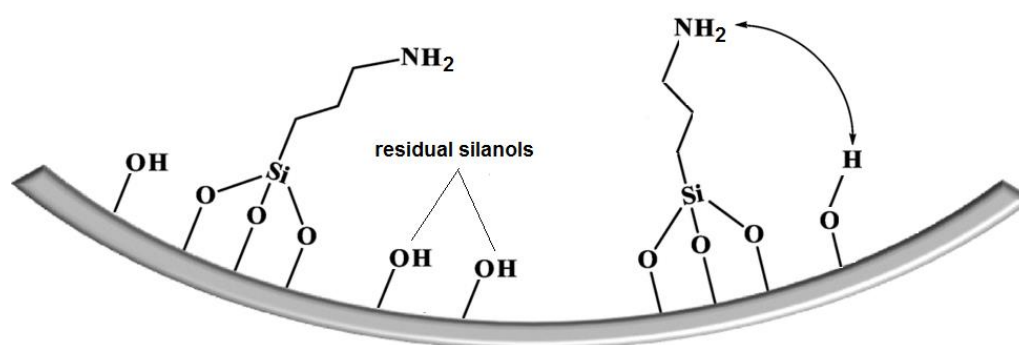


Figure 1.4 Acid-base (cooperative)⁵⁸

Many attempts have been made to investigate catalytic activity by blocking, removing or otherwise decreasing the number of residual silanols in the silica surface. One of the most common processes is that of capping with trimethylsilyl (TMS) groups as a means of determining the effects of the silanol groups on catalytic activity. The capping produces an important decrease in the number of surface silanols, although it does not completely remove them.^{59, 60}

The cooperative effect of silanol groups has been investigated for various C-C bond-forming reactions such as the nitroaldol (Henry) condensation, Knoevenagel condensation and Michael addition.⁶¹

The goal of the present work is to determine whether silanol groups can cooperatively participate in the key steps of the catalytic activity. Their effects are discussed in more detail in Chapter 6.

1.5. Chemistry background and general synthesis strategies for hybrid materials

Hybrid materials are constituted by organic components (molecules) or networks (organic polymers) intimately mixed at the molecular or nanoscopic level with inorganic components, predominantly metal oxides but also phosphates, carbonates, chalcogenides and allied derivatives.

One hybrid catalyst is based on the association between a metal oxide and organic molecules such as bio-components; this type of catalyst has become established successfully in industry.⁴¹

A comprehensive description of all the chemical reactions involved in the production of organic and inorganic components is outside the scope of this work; however, some important reviews in this area have been published.^{37,62} Therefore, a discussion of chemical reactions with the background material, including reactions of class II hybrid materials, in which organic molecules and the inorganic support are covalently bonded, is specifically included. In the following sections, the constituents of hybrid materials will be presented independently in order to facilitate the chemical description of the organic and inorganic components.

1.5.1. Inorganic component

In this work, commercial silica gel (SiO_2) was used as the support material, as it is available in numerous forms. Silica gel has many advantages over other types of support materials. It is robust, and can exhibit specific surface areas; it also has a resistance to organic solvents and does not swell.⁶³⁻⁶⁵ Moreover, the hydrophilic surface can stabilise polar reactive intermediates and transition states at the active site.⁶⁶ Attachments of organic functional groups to a silica surface is often easier than attachments to other supports.⁶³ There is a wide variety of silylating agents that allow functional groups of different types to be immobilised on silica surfaces.⁶⁵ Amorphous silica gel will be described in Section 1.7.1.

1.5.2. Organic component

In the case of adding organic components to the hybrid material as a network former, this can be performed by using pre-synthesised functional macromonomers. These are made compatible with the inorganic component via two main strategies: either through chemical grafting, or by embedding within the growing inorganic network in a common solvent known as co-condensation. In both methods, the silane molecules hydrolyse easily with water to form silanol Si-OH groups. These silanol groups subsequently either condense with each other to form polymeric structures incorporating very stable siloxane Si-O-Si bonds (co-condensation method), or they can condense with hydroxyl groups on the surface of metal oxides to form stable Si-O-M bonds ($\text{M} = \text{Si}, \text{Al}, \text{Fe}, \text{etc.}$).

Figure 1.5 shows a series of reactions of a typical alkoxy silane molecule, $\text{RSi}(\text{MeO})_3$, as it is hydrolysed and then proceeds to condense with silanol groups on the surface of a silica or other oxide support or substrate.

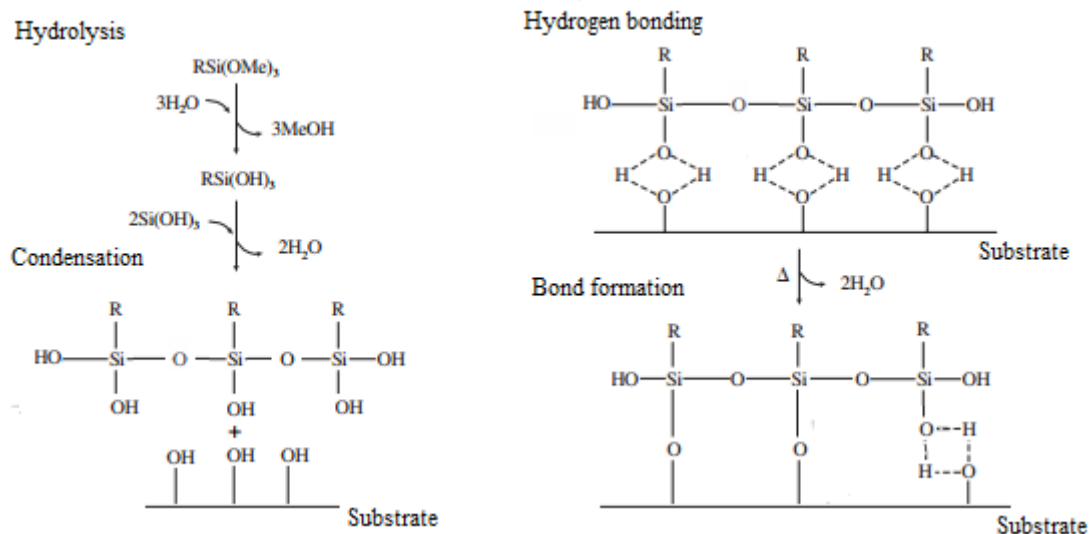


Figure 1.5. Organo-functional silane hydrolysis, condensation and covalent bonding to an inorganic substrate.⁵⁷

1.6. Hybrid interface

1.6.1. Grafting of the organic moiety on to solid surfaces

Recently, several methods have been used to bind organic groups to silica surfaces via the formation of covalent bonds. One method is the chlorination of the silica surface followed by subsequent use of Grignard reagents to form silicon-carbon bonds. However, the use of Grignard reagents could potentially limit the range of functional groups that can be tethered to the solid surface.⁶⁷ Nevertheless, consequent to the stability of the Si-C bonds, the formation of a silicon-carbon bond between the solid surface and the organic moieties is desirable.⁶⁷ The other method of silica surface functionalisation is the grafting of organic groups to surface silanol using a trialkoxy- or trichloro-organosilane (Figure 1.6), a reaction that is broadly similar to that shown in the figure above (Figure 1.5).

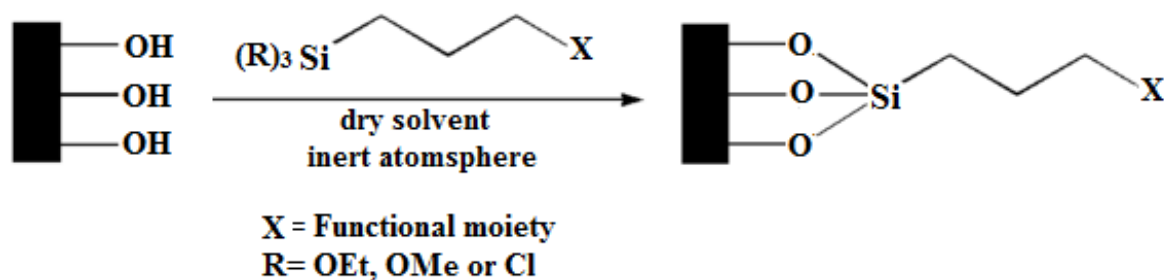


Figure 1.6. Example of grafting organosilanes onto a silanol-containing surface⁶⁸

The availability of the silanol groups can determine whether the grafted silicon atom is tethered via one, two, or three silicon-oxygen bonds.⁶⁹ Numerous papers have been published on grafting of silicas. The organic groups covalently linked can be modified to create a diversity of catalytic sites and, in addition, can readily to be adequately stable for recycling and reuse.⁶⁸

1.6.2. Direct incorporation of organic moiety

Though grafting of organosilanes to surfaces via hydroxyl groups has been intensively studied, and is a frequently used method of forming hybrid (organic-inorganic) materials, the tethering is done via covalent linking between an organosilane and a surface silicon atom via the silicon (surface)-oxygen-silicon (external) bond in the organosilane. The organic functional group is then bound to the external silicon atom.

The silicon-oxygen bond is then external to the surface and can be broken under conditions encountered in some catalytic reactions.⁶⁷ Certainly, when this happens, the solids will not retain the ability to function as recyclable catalysts. It would be desirable instead to have the carbon bound directly to a silicon atom on the surface. Through the combination between the organosilane and the synthesis mixture during the formation of the solid, the functional group anchored on the surface and the silicon in the silicon-carbon bond in the organosilane is on the surface of the material.⁷¹ This creates a more uniform dispersion throughout the solid. Organosilanes can be condensed and cohydrolysed with other reagents, such as tetraalkoxysilanes, and other suitable organising molecules used to synthesise ordered mesoporous materials as well as zeolites; this method, named “one-pot”, is used in creating synthesised mixtures. Factors such as the stability of organic functional groups under the reaction conditions and during the extraction procedures, the extractability of organising and structure-directing agents (SDAs) following the reaction, and the solubility of the organosilane in the mixture, are important considerations in designing the preparation.⁶²

In this work, the preferred strategy for functionalisation was grafting, in which functional groups react with the silica support. A decision was made not to employ the condensation sol-gel approach, in which functionalisation takes place simultaneously with the silica gel precipitation. This followed a review of the existing literature, from which it was concluded that catalysts obtained by the grafting route are generally more active than those obtained by a direct incorporation method.¹³ The base sites on the surface silica were generated by using (3-aminopropyl) trimethoxysilane (APTMS), on account of its ability to form an amine-reactive layer that is tightly attached to the surface.⁷²

products. The gel is referred to as *hydrogel*, or *alcogel* if an alcohol has been used as the solvent.⁷⁶ The nature of the gel and the solid silica formed from it is governed by temperature, the pH of the reaction medium, the nature of the solvent and any electrolyte present, as well as the starting materials.⁷⁷ Control of pore size, pore volume, and specific surface area can be obtained through these variables.^{77, 78}

The surface chemistry of silica gel has been studied by Hofmann,⁷⁹ Kiselev⁸⁰ and Carman.⁸¹ They showed that hydroxyl (silanol) groups, Si-OH, are present on the surface. Yaroslavsky⁸² proved for the first time the existence of hydroxyl groups on the silica surface (porous glass) by infrared spectroscopy. The acidic nature of the silanol groups is responsible for the adsorption properties of these materials, and is exploited for chemical modifications in several different fields including catalysis. The enhanced acidity of the silica surface gives it a high degree of chemical reactivity; thus, it can react with many coupling agents to immobilise organo-functionalised alkoxy-silanes (Figure 1.8),

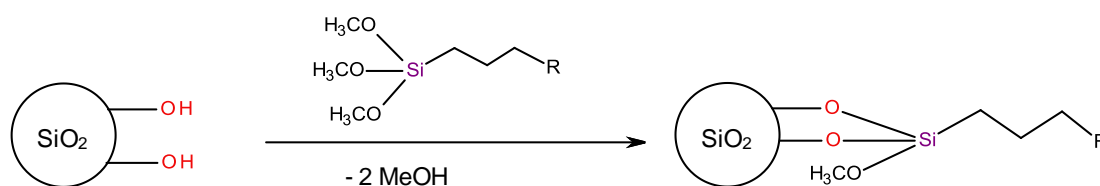


Figure 1.8. Surface modification of silica oxide with alkoxy-silanes

This reaction generally uses methoxy- or ethoxysilanes, as C3 or higher alkoxy groups tend to be less reactive due to their increased bulkiness. This reaction forms a covalent Si-O-Si bond between the solid support and functional group. The functional group on the alkoxy-silane can be any number of chemically reactive species. Common commercially available examples include amines, alcohols, carbonyls, halogens, thiols, olefins, etc.

Reaction of typical trialkoxy-silanes with solid supports can result in the condensation of one, two, or three surface hydroxyl groups (Figure 1.9).

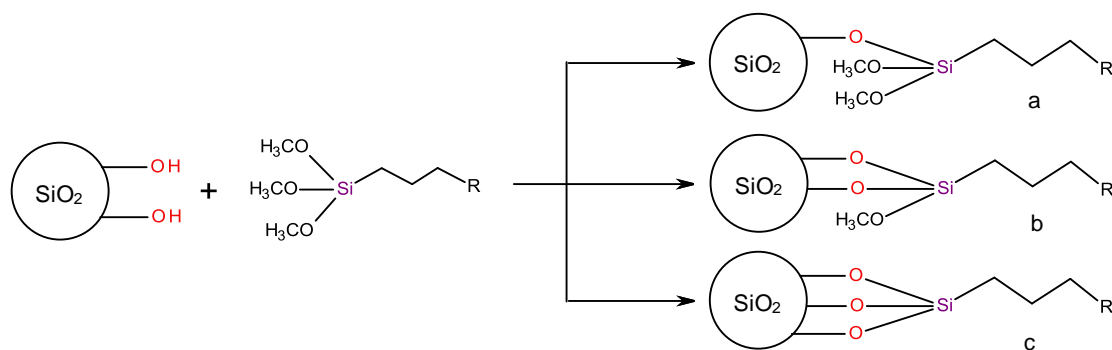


Figure 1.9 Reaction of trimethoxysilanes with (a) one, (b) two, or (c) three surface hydroxyl groups

It has been found that if water is present during the reaction, it can hydrolyse the alkoxy groups of the silane, forming hydroxyl groups. These hydroxyl groups can react with other alkoxy silanes, forming multi-layers of functional groups instead of monolayers of functional groups. Depending on the user's desire for a material with higher loading and less uniform surface coverage, or a material with lower loading and a better-defined monolayer coverage, water may or may not be included in the grafting procedure. Should monolayer coverage be required, the inorganic oxide must be pre-dried at a high temperature to remove all water, as these materials tend to be highly hygroscopic. Finally, silica-immobilised organic materials have many properties that are important when they become the basis for supported catalysts:

- The physical rigidity of their structures
- Negligible swelling in both aqueous and organic solutions
- High biodegradation, photochemical and thermal stability
- Slower poisoning by irreversible side reactions
- Readily modified by a variety of functional groups.

However, there are some notable drawbacks of silica-immobilised organic materials, such as leaching of the functional groups from the support surface into the solution upon treatment with acidic solutions, as the surface bonds are hydrolysed.

1.7.2. Ordered mesoporous SBA-15 silica

Studies on ordered mesoporous materials have attracted considerable attention since the discovery of the M41S family of mesoporous materials in 1992. Out of these, two materials have been highlighted, MCM-41, obtained in basic media, and SBA-15, obtained in acid media.⁸³

SBA-15 (Santa Barbara Amorphous) materials, developed in 1998 by Stucky *et al.*, have attracted intense interest due to their large surface areas, well-defined pore structures, inert frameworks, nontoxicity, high biocompatibility⁸⁴ and thermal and hydrothermal stability, which allows them to be used in catalysis, adsorption, chemical sensing, immobilisation, drug delivery systems, and separation by chromatographic techniques such as high-performance liquid chromatography (HPLC).⁸⁵ One critical achievement in this area was the use of commercially available block copolymers to synthesise mesoporous silica of the type SBA-15 with large pores ordered.⁸⁹ It was reported that, using tri-block copolymers as a structure-directing agent, it was possible to synthesise ordered mesoporous silica in a wide range of pore sizes. Preparation for synthesising a silica surfactant composite generally begins with an ageing step under hydro-thermal conditions, followed by filtration, a washing step, and subsequent calcinations to remove the organic template. Under acidic conditions, the cooperative self-assembly between the template, which consists of micellar rods formed of tri-block copolymer, and the silica precursor, is the basis of this process of synthesis. A schematic pathway for the formation of SBA-15 silica material is shown in Figure 1.10.

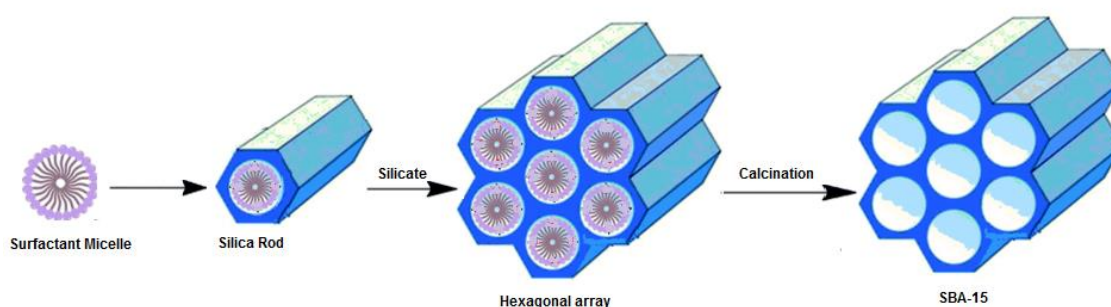


Figure 1.10. Synthesis of SBA-15 mesoporous silica

SBA-15 materials have a hexagonal network of pores as shown in Figure 1.10, with uniform pore sizes which are usually of diameters of about 8 nm (as compared to MCM-41, which has a pore diameter of about 4 nm). However, depending on the template compound used, pore

size can be as large as 30 nm.⁸⁷ The specific surface areas and specific pore volumes are somewhat smaller than those of MCM-41 materials, but pore walls are thicker (between 3.1 and 6.4 nm).⁸⁸ One result is that the thermal and hydrothermal stability of these materials are better than those of MCM-41.

1.8. Organic-inorganic hybrid catalysts in literature

In the last 20 years, solid basic organic–inorganic hybrid catalysts have been widely studied, and the scientific literature on the subject is becoming more extensive owing to its importance in the chemical industry. The examples in the following section provide more insight into the role of base catalysis in chemical reactions.⁸⁹

Solid-base catalysts show higher activities and selectivity for many types of reactions, including some condensation, alkylation, cyclisation and isomerisation reactions, than conventional homogeneous-base catalysts. Furthermore, many of the homogeneous-base catalysts used in industry require stoichiometric amounts of the liquid base for conversion to the required product. Replacement of these liquid-base- with solid-base catalysts would permit the separation from the product in addition to possible regeneration and reuse of the catalyst.^{3, 55, 90}

Aminopropyl functionalised silicas and their catalytic application have been the organic-inorganic hybrid solids most widely studied as solid base catalysts. Consequently, researchers have extensively studied these materials, attempting to identify the key properties that control the type of material stability, activity and selectivity in different reactions. Walcarius⁴³ investigated the chemical reactivity and stability of aminopropyl-grafted silica in an aqueous medium. It was found that in the case of a high local concentration of aminopropylsilane (~2.0 mmol g⁻¹), a fast hydrolysis reaction of Si-O-Si bonds occurred in the aqueous medium, resulting in the leaching of aminopropylsilane in the external solution, even in buffered solutions at pH 5.7.

It was established that the amount of organic component strongly influences the composition and textural properties of the hybrid organic–inorganic materials. Sartori⁹¹ observed that when the aminopropylsilane to tetrathoxysilane ratio was increased to more than 40% by the co-condensation method, the pore volume collapsed. Using FT-IR revealed a significant decrease in the interaction with benzaldehyde reagent. An interesting study was conducted by Macquarrie and Sartori⁹² to investigate the influence of the immobilisation procedure on the

catalytic activity of aminopropylsilicas in C–C forming reactions. This study showed aminopropylsilica catalysts exhibiting different activity in nitroaldol and nitro Michael reactions, depending on the method followed for their preparation.

Catalysts prepared by co-condensation were less active than those obtained using the grafting approach. Although there were high amounts of propylamine in the catalysts prepared by the co-condensation method, they did not show high catalytic activity. This was accounted for as resulting from the fact that most of the propylamine groups were incorporated within the siliceous framework where the reactants were unable to reach them. By contrast, in the catalysts prepared by grafting, despite a reduction in the pore size, the aminopropyl groups were directly linked to the surface, and consequently, the majority of them were easily accessible to the reagents and able to function within the reaction.⁹²

Primary and secondary amines with silica support base catalysts with different loadings and reactions were also investigated.⁵⁵ The results showed the existence of an optimum amine loading amount. The optimum organoamine loading amount showed little difference for different reactions. Moreover, the optimum amine loading amount was in the order of $\text{NH}_2\text{-MCM} > \text{NHCH}_3\text{-MCM} > \text{NH}_2\text{NH-MCM} > \text{NHPh-MCM}$, where MCM refers to the ordered mesoporous silica support. However, group work showed that there was no significant difference in the catalytic activity between the ordered and non-ordered silica support.⁵⁵

Although this optimum loading was observed in many of the studies, few researchers have attempted to offer an explanation for it. Most authors relate catalytic activity to the available surface area and sometimes to pore volume; however, some of the more recent investigations relate the catalytic performances to the synergetic catalytic effect of surface silanols with the introduced reactive groups, such as amines.⁹³⁻⁹⁷ Hruby *et al.*⁹⁷ claimed that the residual silanols may transfer a proton for its weakly acidic quality. A synergetic acid-base catalytic mechanism was also proposed for aminopropyl-functionalised silica gel for a Henry reaction. Due to the existence of the silanol-amine acid-base synergetic effect, the balance in amounts between amine and silanol groups needs to be considered when the catalytic activities of the functionalised catalysts are evaluated. Therefore the number of silanol groups on the surface consumed in the process of functionalisation should be minimised. This was done by using aminopropylsilane with one or two alkoxy groups.

Bruhweiler *et al.*⁹⁸ studied the extent of loading of different propylsilane precursors with one, two, and three alkoxy groups on a silica surface in an anhydrous solvent. They observed a correlation between the tendency to yield a homogeneous distribution of grafting sites and the number of alkoxy groups per aminopropylsilane molecule. They demonstrated that monoalkoxysilanes were distributed more uniformly than di- and trialkoxysilanes. The explanation offered for this was that monoalkoxysilanes are more mobile on account of their weaker interaction with the surface, and are therefore better able to reach less accessible sites located in the pores compared with other precursors.

Furthermore, silanes with more than one alkoxy group per molecule have the tendency to form aminopropylsilane islands. This contributes to a non-uniform distribution of the grafting sites.⁹⁸⁻¹⁰⁰ No existing studies have investigated the effect of surface coverage of the organic precursor on its catalytic performance. It is well known that aminopropylsilane covers a surface of 0.50 nm^2 , so the surface coverage can be calculated for each support according to its surface area.⁴³ Thus, the optimum amount of aminopropylsilane can initially be practically related to the surface coverage of any silica support, then theoretically calculated for other supports.

1.9. Catalytic reactions used to study catalytic activity in this work

In this work, the catalytic performances of the amino-functionalised catalysts were investigated for two carbon-carbon coupling reactions.⁵⁵ The first of these was the aldol condensation reaction between nitromethane and benzaldehyde to produce nitrostyrene, as shown in Figure 1.11.

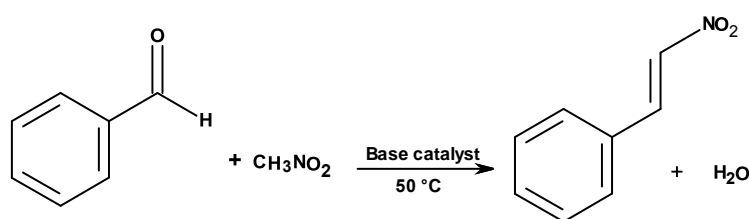


Figure 1.11. Henry reaction (nitroaldol reaction)

The mechanism includes the base site withdrawing a proton from the nitromethane to produce the nitromethane anion (CH_2NO_2^- ion), which can then attack the carbonyl group on benzaldehyde. This then proceeds to form nitrostyrene, with the elimination of water through the recovery of the proton from the catalyst.

The second test reaction (Figure 1.12) is the Knoevenagel condensation reaction between benzaldehyde and ethyl cyanoacetate in the presence of toluene as the solvent and *o*-xylene as an internal standard to produce ethyl 2-cyano-3-phenylacrylate.

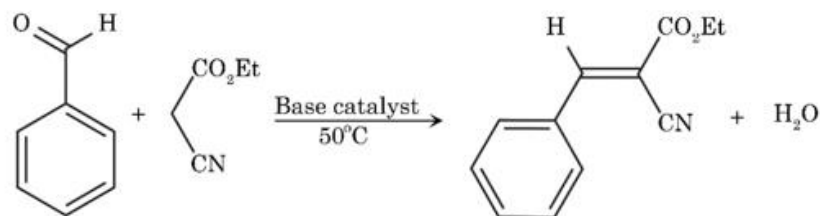


Figure 1.12. Knoevenagel condensation reaction

1.10. Thesis structure

This thesis consists of seven chapters. Chapter 1, the introduction, explains the background of the study, the literature review, the report structure and the research objectives. In Chapter 2, the characterisation methods used in this thesis are explained. Chapter 3 describes the preparation of different types of silica supports by grafting 3-aminopropyl (trimethoxysilane) (APTMS), prepared from different amorphous silica gel with various structural parameters, such as surface area and porosity and tested in the Henry reaction, and compares their activity before and after functionalisation with aminopropylsilane groups. Chapter 4 describes the preparation of various samples of aminopropyl-functionalised silica via grafting an organosilane precursor, 3-aminopropyl-triethoxysilane (APTES), on to the surface of silica gel. The amine group content of the material was adjusted by varying the amount of APTES in the reaction. The catalytic activities showed a level of dependency on surface area, amount of active sites, pore size and pore volume. However, one of the key variables affecting the catalytic activity was the surface coverage. The highest specific catalytic activity was obtained at a level of functionalisation corresponding to the saturation of the support surface with a single layer of functional groups. Chapter 5 describes the preparation of several aminopropyl-functionalised silicas using the grafting method for three types of aminopropylalkoxysilanes which varied in their number of ethoxy groups (one, two and three), with two different supports. The two supports were the amorphous silica EP10X and the ordered mesoporous molecular sieve silica SBA-15. On the basis that the fractional coverage of the silica surface by

catalytically active groups was key to controlling overall catalytic activity in base-catalysed reactions, this study showed that the maximum activity of supported amines (at the optimum loading in all cases around 1.0 mmol g⁻¹) varied a great deal depending on the amine tether precursor. The amines originating from 3-aminopropyltrialkoxysilanes, and therefore held to the surface by three tethering groups, showed the highest activity, followed by those held by “two” and then by “one”. Chapter 6 highlights the effect of silanol groups on the catalytic activity in nitroaldol reactions. The surface silanols were capped with trimethoxymethylsilane (TMMS) to determine the effects of the silanol groups on catalytic activity. The capped catalysts were further investigated and compared with un-capped catalysts in different reactions designed to explore the reasons of this drop-off in the activity. Chapter 7 offers recommendations for future work.

1.11. Objectives of Research

The overall objectives of the work reported in this thesis are as follows:

- a) To develop new, active and selective supported solid base catalysts for liquid phase reactions of industrial importance.
- b) To develop these catalysts using amorphous and ordered silica supports and supported aminoalkyl groups attached via grafting aminoalkyltrialkoxysilane compounds.
- c) To investigate the relationships between the physical and chemical characteristics of the silics supports and the activities of the catalysts prepared from them
- d) To investigate the relationships between the surface loadings of catalytic groups and catalytic activities
- e) To investigate the effects of silica surface modification on the activities of supported amine groups.
- f) To investigate the relationship between the nature of the supported amine and catalytic activity.
- g) To develop a theoretical model to explain the dependence of catalytic properties on the nature of the supported catalysts.

1.12. References

1. K. Bahrami, M. M. Khodaei and M. Roostaei, *New Journal of Chemistry*, 2014, **38**, 5515-5520.
2. V. Dal Santo, F. Liguori, C. Pirovano and M. Guidotti, *Molecules*, 2010, **15**, 3829-3856.
3. K. Akutu, H. Kabashima, T. Seki and H. Hattori, *Applied Catalysis A: General*, 2003, **247**, 65-74.
4. E. G. Garrido-Ramírez, B. K. G. Theng and M. L. Mora, *Applied Clay Science*, 2010, **47**, 182-192.
5. D. N. Belton and K. C. Taylor, *Current Opinion in Solid State and Materials Science*, 1999, **4**, 97-102.
6. C. T. Campbell, *Surface Science*, 2007, **601**, ix.
7. J. Ross, *Applied Catalysis A: General*, 1992, **92**, N3-N4.
8. R. Breslow, *Science*, 1982, **218**, 532-537.
9. J. A. Gladysz, *Chemical Reviews*, 2002, **102**, 3215-3216.
10. R. Mat, R. A. Samsudin, M. Mohamed and A. Johari, *Bulletin of Chemical Reaction Engineering and Catalysis*, 2012, **7**, 142-149.
11. D. J. Cole-Hamilton, *Science*, 2003, **299**, 1702-1706.
12. A. Thayer, *Chemical & Engineering News*, 2005, **83**, 55-58.
13. X. J. Yin and S. L. Lu, *Xiandai Huagong/Modern Chemical Industry*, 2013, **33**, 9-13.
14. D. Rosenthal, *Physica Status Solidi (A) Applications and Materials Science*, 2011, **208**, 1217-1222.
15. I. Fechete, Y. Wang and J. C. Védrine, *Catalysis Today*, 2012, **189**, 2-27.
16. A. Shanaghi, *Surface Review and Letters*, 2012, **19**.
17. W. F. Liu, Z. X. Guo and J. Yu, *Gaofenzi Cailiao Kexue Yu Gongcheng/Polymeric Materials Science and Engineering*, 2009, **25**, 67-70.
18. Y. Xiao, D. Chen, N. Ma, Z. Hou, M. Hu, C. Wang and W. Wang, *RSC Advances*, 2013, **3**, 21544-21551.
19. X. S. Zhao, X. Y. Bao, W. Guo and F. Y. Lee, *Materials Today*, 2006, **9**, 32-39.
20. J.-W. Lee, T. Mayer-Gall, K. Opwis, C. E. Song, J. S. Gutmann and B. List, *Science*, 2013, **341**, 1225-1229.
21. K. M. Kacprzak, N. M. Maier and W. Lindner, *Tetrahedron Letters*, 2006, **47**, 8721-8726.

22. D. Moelans, P. Cool, J. Baeyens and E. F. Vansant, *Catalysis Communications*, 2005, **6**, 307-311.
23. R. A. Sheldon, I. Arends and U. Hanefeld, *Green chemistry and catalysis*, John Wiley & Sons, 2007.
24. K. Moller and T. Bein, *Chemistry of Materials*, 1998, **10**, 2950-2963.
25. M. Poliakoff, J. M. Fitzpatrick, T. R. Farren and P. T. Anastas, *Science*, 2002, **297**, 807-810.
26. P. T. Anastas and J. C. Warner, *Green chemistry: theory and practice*, Oxford university press, 2000.
27. I. R. Shaikh, *Journal of Catalysts*, 2014, **2014**, 1-35.
28. R. H. Crabtree, *Handbook of Green Chemistry, Green Catalysis, Biocatalysis*, John Wiley & Sons, 2009.
29. P. T. Anastas, M. M. Kirchhoff and T. C. Williamson, *Applied Catalysis A: General*, 2001, **221**, 3-13.
30. M. Nosonovsky and B. Bhushan, *Green Tribology*, Springer, 2012.
31. R. S. Silberglitt, A. Wong and S. Bohandy, *The Global Technology Revolution, China, In-depth Analyses: Emerging Technology Opportunities for the Tianjin Binhai New Area (TBNA) and the Tianjin Technological Development Area (TEDA)*, Rand Corporation, 2009.
32. A. M. Rouhi, *Chemical & engineering news*, 2002, **80**, 29-38.
33. R. Awasthi and D. Shikha, *ChemInform*, 2015, **46**, 2-8.
34. C. Sanchez, B. Julian, P. Belleville and M. Popall, *Journal of Materials Chemistry*, 2005, **15**, 3559-3592.
35. S. Wu, Z. Tang, B. Guo, L. Zhang and D. Jia, *RSC Advances*, 2013, **3**, 14549-14559.
36. C. Sanchez, B. Julián, P. Belleville and M. Popall, *Journal of Materials Chemistry*, 2005, **15**, 3559-3592.
37. A. Mehdi, C. Reye and R. Corriu, *Chemical Society Reviews*, 2011, **40**, 563-574.
38. J. Zhang, A. Wang and S. Seeger, *Polymer Chemistry*, 2014, DOI: 10.1039/c3py01293j.
39. F. de Clippel, M. Dusselier, S. Van de Vyver, L. Peng, P. A. Jacobs and B. F. Sels, *Green Chemistry*, 2013, **15**, 1398-1430.
40. A. Dhakshinamoorthy, M. Opanasenko, J. Cejka and H. Garcia, *Catalysis Science & Technology*, 2013, **3**, 2509-2540.

41. C. Sanchez, P. Belleville, M. Popall and L. Nicole, *Chemical Society Reviews*, 2011, **40**, 696-753.
42. M. H. Siadati, G. Alonso, B. Torres and R. R. Chianelli, *Applied Catalysis A: General*, 2006, **305**, 160-168.
43. M. Etienne and A. Walcarius, *Talanta*, 2003, **59**, 1173-1188.
44. T. Setoyama, *Catalysis Today*, 2006, **116**, 250-262.
45. K. Tanabe and W. F. Hölderich, *Applied Catalysis A: General*, 1999, **181**, 399-434.
46. S. Huh, H.-T. Chen, J. W. Wiench, M. Pruski and V. S. Y. Lin, *Journal of the American Chemical Society*, 2004, **126**, 1010-1011.
47. P. K. Jal, S. Patel and B. K. Mishra, *Talanta*, 2004, **62**, 1005-1028.
48. U. Díaz, M. Boronat and A. Corma, *Proceedings of the Royal Society A: Mathematical, Physical and Engineering Science*, 2012, DOI: 10.1098/rspa.2012.0066.
49. I. E. Wachs and C. A. Roberts, *Chemical Society Reviews*, 2010, **39**, 5002-5017.
50. I. G. Shenderovich, G. Buntkowsky, A. Schreiber, E. Gedat, S. Sharif, J. Albrecht, N. S. Golubev, G. H. Findenegg and H.-H. Limbach, *The Journal of Physical Chemistry B*, 2003, **107**, 11924-11939.
51. M. Luechinger, R. Prins and G. D. Pirngruber, *Microporous and mesoporous materials*, 2005, **85**, 111-118.
52. A. Walcarius, M. Etienne and B. Lebeau, *Chemistry of materials*, 2003, **15**, 2161-2173.
53. S. Shylesh, A. Wagner, A. Seifert, S. Ernst and W. R. Thiel, *Chemistry—A European Journal*, 2009, **15**, 7052-7062.
54. L. Russo, F. Taraballi, C. Lupo, A. Poveda, J. Jiménez-Barbero, M. Sandri, A. Tampieri, F. Nicotra and L. Cipolla, *Interface focus*, 2014, **4**, 20130040.
55. W. Lang, B. Su, Y. Guo and L. Chu, *Science China Chemistry*, 2012, **55**, 1167-1174.
56. E. L. Margelefsky, R. K. Zeidan and M. E. Davis, *Chemical Society Reviews*, 2008, **37**, 1118-1126.
57. B. Arkels, *Inc, Morrisville, Silane coupling agents: Connecting across boundaries PA*, 2006, **2**, 2-72.
58. G. Musso, E. Bottinelli, L. Celi, G. Magnacca and G. Berlier, *Physical Chemistry Chemical Physics*, 2015, **17**, 13882-13894.

59. J. M. Herrero-Martínez, A. Méndez, E. Bosch and M. Rosés, *Journal of Chromatography A*, 2004, **1060**, 135-145.
60. A. Cauvel, G. Renard and D. Brunel, *The Journal of organic chemistry*, 1997, **62**, 749-751.
61. X. Yu, X. Yu, S. Wu, B. Liu, H. Liu, J. Guan and Q. Kan, *Journal of Solid State Chemistry*, 2011, **184**, 289-295.
62. A. P. Wight and M. E. Davis, *Chemical Reviews*, 2002, **102**, 3589-3614.
63. L. N. H. Arakaki, L. M. Nunes, J. A. Simoni and C. Airoidi, *Journal of Colloid and Interface Science*, 2000, **228**, 46-51.
64. I. P. Alimarin, V. I. Fadeeva, G. V. Kudryavtsev, I. M. Loskutova and T. I. Tikhomirova, *Talanta*, 1987, **34**, 103-110.
65. A. R. Sarkar, P. K. Datta and M. Sarkar, *Talanta*, 1996, **43**, 1857-1862.
66. H. C. Zeng, *Nanotechnology*, 1988, 2539-2551.
67. P. M. Price, J. H. Clark and D. J. Macquarrie, *Journal of the Chemical Society, Dalton Transactions*, 2000, DOI: 10.1039/a905457j, 101-110.
68. M.-C. Durrieu, D. Quemener, C. Baquey and V. Sabaut-Heroguez, *Journal*, 2005.
69. A. Arranz, C. Palacio, D. García-Fresnadillo, G. Orellana, A. Navarro and E. Muñoz, *Langmuir*, 2008, **24**, 8667-8671.
70. K. Chen, Y. Zhao and X. Yuan, *Progress in Chemistry*, 2013, **25**, 95-104.
71. A. P. Alves, M. G. Fonseca and A. F. Wanderley, *Materials Research*, 2013, **16**, 891-897.
72. Q. H. Yang, M. P. Kapoor and S. Inagaki, *Journal of the American Chemical Society*, 2002, **124**, 9694-9695.
73. H. J. Lee, B. Ramaraj, S. M. Lee and K. R. Yoon, *Journal of Polymer Science Part A: Polymer Chemistry*, 2008, **46**, 1178-1184.
74. in *Studies in Surface Science and Catalysis*, eds. P. V. D. V. E.F. Vansant and K. C. Vrancken, Elsevier, 1995, vol. Volume 93, pp. 3-30.
75. I. M. El-Nahhal and N. M. El-Ashgar, *Journal of Organometallic Chemistry*, 2007, **692**, 2861-2886.
76. V. A. Felonov, V. Y. Gavrilov and L. G. Simonova, in *Studies in Surface Science and Catalysis*, eds. P. G. G. Poncelet and P. A. Jacobs, Elsevier, 1983, vol. Volume 16, pp. 665-674.

77. B. Handy, K. L. Walther, A. Wokaun and A. Baiker, in *Studies in Surface Science and Catalysis*, eds. P. A. J. P. G. G. Poncelet and B. Delmon, Elsevier, 1991, vol. Volume 63, pp. 239-246.
78. J. Limpo, M. C. Bautista, J. Rubio and J. L. Oteo, in *Studies in Surface Science and Catalysis*, eds. F. R.-R. K. S. W. S. J. Rouquerol and K. K. Unger, Elsevier, 1994, vol. Volume 87, pp. 429-437.
79. U. Hofmann, K. Endell and D. Wilm, *Angewandte Chemie*, 1934, **47**, 539-547.
80. A. V. Kiselev, *Kolloidn. Zh.*, 1936, **2**, 17-26.
81. P. C. Carman, *Transactions of the Faraday Society*, 1940, **36**, 964-973.
82. N. G. Yaroslavsky and A. N. Terenin, *Dokl. Akad. Nauk SSSR*, 1949, **66**.
83. S. M. L. dos Santos, K. A. B. Nogueira, M. de Souza Gama, J. D. F. Lima, I. J. da Silva Júnior and D. C. S. de Azevedo, *Microporous and Mesoporous Materials*, 2013, **180**, 284-292.
84. W. Zhao, J. Gu, L. Zhang, H. Chen and J. Shi, *Journal of the American Chemical Society*, 2005, **127**, 8916-8917.
85. X. Wang, K. S. Lin, J. C. Chan and S. Cheng, *The Journal of Physical Chemistry B*, 2005, **109**, 1763-1769.
86. L. Gibson, *Chemical Society Reviews*, 2014, **43**, 5163-5172.
87. J. C. Groen, L. A. Peffer and J. Pérez-Ramírez, *Microporous and Mesoporous Materials*, 2003, **60**, 1-17.
88. U. Ciesla and F. Schüth, *Microporous and Mesoporous Materials*, 1999, **27**, 131-149.
89. S. Hitz and R. Prins, *Journal of Catalysis*, 1997, **168**, 194-206.
90. S.-Y. Chen, C.-Y. Huang, T. Yokoi, C.-Y. Tang, S.-J. Huang, J.-J. Lee, J. C. C. Chan, T. Tatsumi and S. Cheng, *Journal of Materials Chemistry*, 2012, **22**, 2233-2243.
91. G. Sartori, F. Bigi, R. Maggi, R. Sartorio, D. J. Macquarrie, M. Lenarda, L. Storaro, S. Coluccia and G. Martra, *Journal of Catalysis*, 2004, **222**, 410-418.
92. D. J. Macquarrie, R. Maggi, A. Mazzacani, G. Sartori and R. Sartorio, *Applied Catalysis A: General*, 2003, **246**, 183-188.
93. J. D. Bass, A. Solovyov, A. J. Pascall and A. Katz, *Journal of the American Chemical Society*, 2006, **128**, 3737-3747.
94. K. K. Sharma, R. P. Buckley and T. Asefa, *Langmuir*, 2008, **24**, 14306-14320.
95. K. K. Sharma and T. Asefa, *Angewandte Chemie*, 2007, **119**, 2937-2940.

Chapter 1

96. K. K. Sharma, A. Anan, R. P. Buckley, W. Ouellette and T. Asefa, *Journal of the American Chemical Society*, 2007, **130**, 218-228.
97. S. L. Hruby and B. H. Shanks, *Journal of Catalysis*, 2009, **263**, 181-188.
98. H. Salmio and D. Brühwiler, *The Journal of Physical Chemistry C*, 2006, **111**, 923-929.
99. N. Gartmann and D. Brühwiler, *Angewandte Chemie International Edition*, 2009, **48**, 6354-6356.
100. H. Ritter and D. Brühwiler, *The Journal of Physical Chemistry C*, 2009, **113**, 10667-10674.

Chapter 2

INSTRUMENTAL TECHNIQUES (Background Theory).

In this chapter, the techniques used to characterize and test the catalysts are covered.

The aim of this chapter is to discuss the techniques and methods that have been used to characterize the solid materials considered in this thesis. The first objective is to determine the structure, morphology, porosity, and chemical composition of the materials. The second objective of the chapter is to reveal the characteristics of the surface in relation to its reactivity.

2.1. Catalyst characterization

Nitrogen adsorption measurements were carried out to establish porosities and surface areas. Powder X-ray diffraction (p-XRD) was utilised to determine the crystal structures for some of the catalysts under study. Elemental analysis (C, H, and N) was then carried out to determine the loading of active sites on the catalyst surface. Dynamic vapour sorption (DVS) was also utilized to examine the hydrophilicity and hydrophobicity characteristics of the catalysts. Infra-red spectroscopy was done to certify the existence of functional organic groups on the surface of the catalyst. Gas chromatography (GC) was utilized to oversee the reaction rates using quantitative analysis of the reactants and products. Finally, gas chromatography-Mass spectrometry (GC-MS) was utilized to certify the final products in the Henry reaction.

2.2. Nitrogen Adsorption

It can be argued the most significant characterization method used in this study is Nitrogen Adsorption. This can be used to find out the definite surface area pore volume and the pore size distribution. The Nitrogen Adsorption method is deemed to be one of the most powerful techniques for establishing the porosity in solid materials, and this is due to the results being very accurate, and the fact that interpreting the results is easy to do. Therefore, it is one of the most widely used tools.¹

In using the adsorption of an inert gas onto a solid surface, it is possible to measure the surface area of the solid. Nitrogen is usually used as an adsorbate, and an adsorption isotherm is produced by calculating the level of nitrogen absorbed by the solid, as a result of the pressure of nitrogen equilibrium in the solid product. The pressure is given as P/P_0 – P represents the pressure of nitrogen and P_0 stands for the saturated vapour pressure at the temperature of adsorption. In general, adsorption isotherms are usually report to be higher than the P_0 range of zero to 1.0. In terms of nitrogen, the adsorption isotherms are taken at 77 K, which is when the saturated vapour pressure P_0 is 1.0 in the atmosphere.

The adsorption of a gas onto a solid can be done either through van der Waals (physical) or covalent (chemical) interactions. Currently, there are six different types of adsorption isotherm that are categorized in relation of their nature (porosity) of the adsorbent (Figure 2.1).

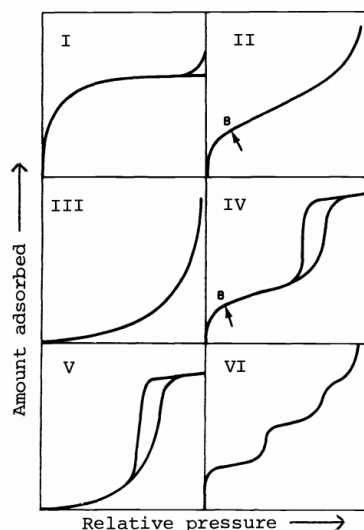


Figure 2.1 – Types of physisorption isotherms²

Type I isotherms are present when a monolayer developed on the surface. This is usually the case with microporous adsorbents (where pore widths are not greater than 2 nm). The adsorption occurs at somewhat low pressure and the isotherm depresses when a monolayer of adsorbate is generated, and only increases again when P/P_0 reaches 1.0 and condensation takes place. Type II isotherms are commonplace in non-porous (or macroporous) solids in which multilayer adsorption takes place. Type III isotherms do not show any point at which a monolayer is formed. These are present when the heat of the adsorption is lower than that of liquefaction. This kind of isotherm is not common. The IV isotherm is a characteristic of mesoporous solids (pores widths 2 nm – 50 nm). Hysteresis loops are existent, and this is because the capillary condensation that occurs in mesoporous solids is not reproduced at the same level of pressure as in the desorption process. It appears that pores fill at higher pressures during adsorption, and then at lower pressures during desorption. At the beginning, Type IV isotherms are similar to Type I isotherms, due to the fact a monolayer is developed, however, steadily multilayer formation occurs as the pores fill up. Type V isotherms are not very common and are attained when there is very little cooperation between the adsorbent and the adsorbate. Type VI isotherms are also not very common; due to the fact the associated sites are typically not the same in terms of their size and energetics. The stages that are seen in this isotherm reveal that there are sets pores of different sizes.

2.3. Adsorption isotherm models

The most straightforward model for the adsorption process of gas molecules onto a surface was developed by Langmuir in 1918.³ This model assumes the following:

- It is not possible for adsorption to developed more than one molecular layer on the surface.
- All adsorption sites are homogenous.
- The likelihood of a site adsorbing a molecule is the same, regardless of whether the neighbouring sites are unengaged or not.
- All adsorption sites can house only one molecule of adsorbate.
- Molecules of the adsorbate do not communicate with each other.
- Balance is achieved between the rates of absorption and desorption of the species from the surface.

Therefore, it can be argued adsorption is a progressive process. However these assumptions made by Langmuir are not suitable for many of the porous materials many efforts have been made to create a model that does not depend so greatly on them, one of these is the BET (Braunauer, Emmett and Teller) model.⁵ The BET equation is underpinned by the Langmuir model however, it has different assumptions:

- The adsorbate can develop more than a one layer on the surface.
- The value of the initial monolayer is precise value.
- The heat of adsorption of the second and others layers of adsorbed gas molecules is the same as the heat of condensation of the gas.
- The interactions that take place between the vapour and surface only coincide with adsorption and desorption.
- The molecules that are adsorbed molecules cannot move from one layer to another.

The BET equation is:

$$\frac{P}{V(P_0 - P)} = \frac{1}{V_m c} + \frac{(c - 1)}{V_m c} \cdot \frac{P}{P_0} \quad \text{Equation 2.1}$$

P Stands for the equilibrium pressure of the adsorbate and P_0 represents the saturated vapour pressure. V is the volume of gas adsorbed at P/P_0 . V_m is the volume of gas adsorbed to

develop a monolayer and the constant c is linked with the net heat of adsorption. The straight line that is normally between P/P_0 values of 0.05-0.35 is attained by plotting:

$$\frac{P}{V(P_0 - P)} \text{ vs. } \frac{P}{P_0} \quad \text{Equation 2.2}$$

The intercept, $\frac{1}{V_m c}$ and the slope, $\frac{c-1}{V_m c}$ can be used to calculate V_m and the surface area of the solid can then be calculated using the same equation as before.

$$V_m = \frac{1}{\text{slope} + \text{intercept}} \quad \text{Equation 2.3}$$

In Figure 2.2, there is an example of a nitrogen adsorption/desorption isotherm of a mesoporous silica structure – which is a kind of IV isotherm. The surface area is usually computed using the desorption isotherm.

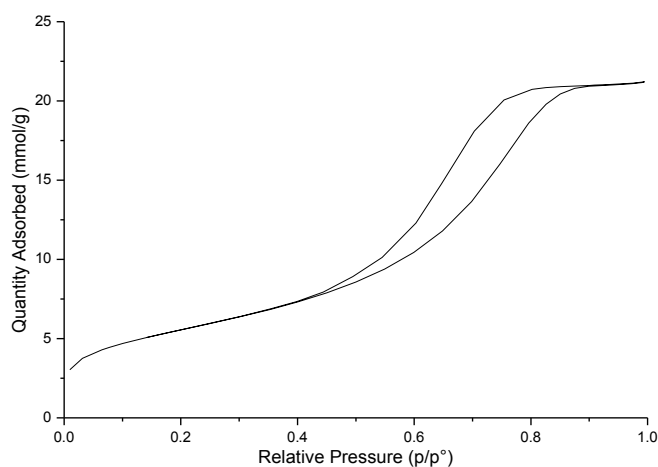


Figure 2.2 – Nitrogen adsorption isotherm at 77K, typical of that of mesoporous silica.

2.4. Adsorption in pores

Pore size distribution of porous samples is determined using the method named BJH abbreviate Barrett, Joyner and Halenda.⁶ Here is used to characterise mesoporous materials supported by the Kelvin equation. There assumptions are:

- The pores are of the same shape.
- Each of the pores is in the mesoporous range (with pore widths ranging.

- The existence of pores in an adsorbent solid can influence the shape of an adsorption/desorption isotherm as the equilibrium vapour pressure above condensed liquid in a (cylindrical) pore, in which the surface of the liquid is curved, is lower than that above a liquid with a flat surface.

The Kelvin equation is associated with the equilibrium vapour pressure of a liquid in a small cylindrical pores, whereby the surface of the liquid is a regular curvature. The Kelvin equation portrays the reliance of the equilibrium vapour pressure of a liquid in the pore on the radius of the pore, r , as well as the contact angle, θ . As the equilibrium vapour pressure above a curved surface is less than above a flat surface, vapour condenses in pores at lower P/P_0 values than when on a flat surface, and narrow pores fill at lower pressures than wide pores do. The radius of the pores can be calculated from the pressure at which condensation occurs. The Kelvin equation is provided below. In the equation, P/P_0 is the relative vapour pressure at which condensation takes place in pores of radius r ; with the contact angle of the condensed liquid with the pore walls θ . (θ is presumed to be zero for pores in the size range studied). The other constants values are γ , the surface tension of the condensed liquid, V_{molar} the molar volume of the liquid, R and T .

$$\ln \frac{P}{P_0} = \frac{-2 \cdot \gamma \cdot V_{molar}}{r \cdot R \cdot T} \cos \theta \quad \text{Equation 2.4}$$

The BJH method comprises of a correction of the pore radius provided by the Kelvin equation in order to enable a film of condensed vapour on the pore walls, and this means that the pore radius is somewhat bigger than the radius of curvature of the meniscus. The data shown that are provided in this study is BJH corrected pore diameter.

2.5. Powder X-Ray Diffraction (p-XRD)

Powder X-Ray Diffraction (p-XRD) was utilised to portray some of the catalysts in this study and the mesoporous silica (SBA-15) has been used to support this. X-ray was discovered in 1912 by Laue, Friederich and Knipping and later developed by W. H. Bragg and W. L. Bragg.^{7, 8}

It is possible to diffract a monochromatic beam of x-rays via atoms in a crystal. The angle at which intense reflections are detected is governed by interferences between x-ray beams reflected by adjacent planes of atoms in the crystal. From these angles, the spacing between the various planes of atoms can be determined. Diffraction patterns (intensity of reflections vs. 2θ , where θ is both the incident and reflected angle between the x-ray beam and the planes of the atoms) recorded for individual crystalline materials can be interpreted in terms of the crystal structure of the materials.

Reflected x-rays from a set of planes interfere constructively when the Bragg condition is met, (Equation 2.1 and Figure 2.3).

$$n\lambda = 2d_{hkl} \sin \theta \quad \text{Equation 2.1}$$

Where: d the distance between the planes; θ the angle between both incident and emulated beams and the plane; n an integer the order of reflection; h , k and l are Miller indices linked to the planes based on the reciprocal lattice vectors.

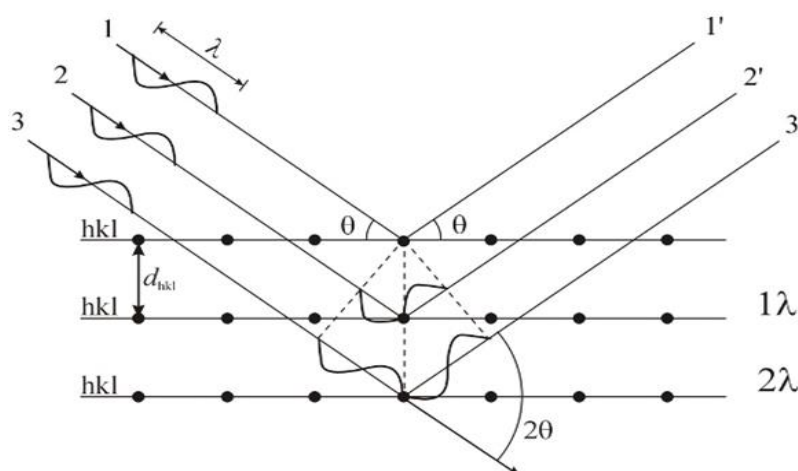


Figure 2.3 – Powder X-ray diffraction, lattice planes.

There are various groups of planes of atoms in a crystal that cause diffraction. Every set of plane is determined by Miller indices, h , k and l . These are linked to how planes traverse the three axes, x , y and z correspond to the dimensions of the crystal unit cell. The diffraction patterns that were taken from powdered (polycrystalline) samples comprise of less information than the one that were obtained from single crystals, however sometimes they provide information about specific lattice spacings, and this helps characterize the powdered material. Powder XRD patterns are commonly used in fingerprint crystal structures. The p-XRD pattern of a typical SBA-15 is shown in Figure 2.4.

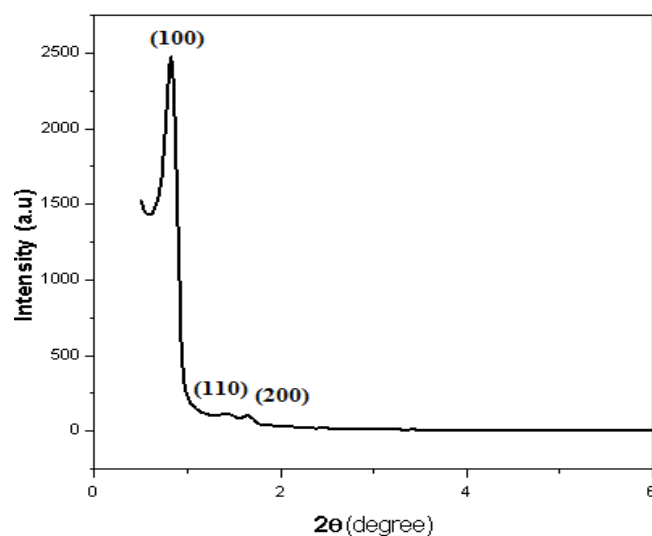


Figure 2.4 – Typical powder X-ray diffraction pattern of SBA-15.

Typically, powder X-ray diffraction patterns of SBA-15 with long-range order presents three peaks which can be recorded on a hexagonal unit cell to (100), (110) and (200) compared to the literature.⁹ The level of crystallization of SBA-15 can be determined through the diffraction intensities of these peaks. The higher the ordered hexagonal porosity is, the higher the intensities are.

2.6. Gas Chromatography (GC)

In this analytical technique a mixture of compounds in their vapour/gas state can be separated and quantified. After injecting the sample to the system it will be transferred to vapour under high temperatures designed in the injector. Consequently, the vaporized sample will flow towards the column directed by the use of a carrier gas.

The column inner walls are then covered with an adsorbent material, which is the stationary phase. Interactions between the sample and the stationary phase leads to the individual compounds in the mixture passing through the column at different rates and they get to the detector at different times; the stronger the interaction between the compound and the stationary phase is, the more time it takes for the compound to get to the detector. It is possible to subject the column to a temperature program if there is a need to separate the materials with wide ranging boiling points. Stationary phases are chosen depending on the compounds that require separation. Generally, the polar compounds will communicate greatly with polar stationary phases and thus there will be longer retention times. Several other factors influence the separation process in GC systems such as the column length, the carrier gas and its flow rate, injection volume. Different types of detectors can be used in can be used in GC systems including electron capture (ECD), flame ionization detector (FID) and thermal conductivity detector (TCD).

For all experiments in this current study, FID has been utilized. An FID can be used to identify organic compounds that have high hydrocarbon contents, and can be used with a hydrogen-air flame. Organic compounds that are generated from the column are burnt in the flame and the ions developed in the flame are identified through growth electrical conductivity across the gas flow. A likely difference of 200-300 V is activated across the flowing gas and the current that flows is measured, amplified and shown as a peak on the chromatograph.

2.7. Fourier Transform Infrared – Attenuated Total Reflectance (FTIR-ATR) Spectroscopy

FTIR-ATR Spectroscopy has been used in this thesis to study the spectroscopic behaviour of the chemical constituents of the prepared catalysts in a qualitative manner. It is a surface sensitive method which generates interaction of electromagnetic radiation with solids, liquids or gaseous molecules within $4000 - 400\text{cm}^{-1}$ region of the electromagnetic spectrum.¹⁰ Infrared spectra can be expressed in terms of wavelength or as wavenumber (in cm^{-1}) which is used more commonly as it varies corresponding to the light energy.¹¹ Resulted spectra produced utilizing mathematical algorithm in this method named fourier transform. Light interact with the molecules and causes vibration to the covalent bonds appears as bends or stretches.¹² The essential principle of operation in a standard FTIR-ATR technique is portrayed according to Figure. 2.5 and equation 2.1.

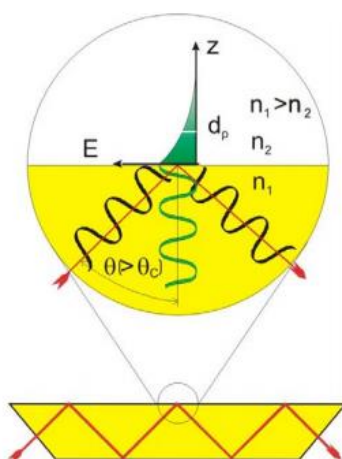


Figure 2.5-Schematic of (IR-ATR) Infrared Total Reflection Spectroscopy.

$$n_1 \sin\theta_1 = n_2 \sin\theta_2 \quad \text{Equation 2.1}$$

Where: n_1 crystal's refractive index; n_2 is sample's refractive index; θ_1 is angle of incident light; θ_2 is the refracted angle.

An infrared light, set at a specific angle of incidence is directed through a sample that is placed next to a crystal (for example, ZnSe) which has a rather high refractive index. The light is then reflected from the internal surface of the crystal and permeates into a less dense medium (which is the sample) with small refractive index and creates a process known as total internal

CHAPTER 2

reflection (TIR), which proposes that the angle of incidence is higher than the critical angle. This process then ultimately produces an evanescent wave which then generates some energy that gets absorbed by the sample and emulated beam, which then weakens and goes to the detector as interferograms and is modified into infrared spectrum by the Fourier Transform¹³

1. References

1. M. Kruk and M. Jaroniec, *Chemistry of Materials*, 2001, **13**, 3169-3183.
2. K. S. W. Sing, D. H. Everett, R. A. W. Haul, L. Moscou, R. A. Pierotti, J. Rouquerol and T. Siemieniewska, in *Handbook of Heterogeneous Catalysis*, Wiley-VCH Verlag GmbH & Co. KGaA, 2008, DOI: 10.1002/9783527610044.hetcat0065.
3. I. Langmuir, *Journal of the American Chemical Society*, 1918, **40**, 1361-1403.
4. H. Kral, J. Rouquerol, K. S. Sing and K. Unger, *Characterization of porous solids*, Elsevier, 1988.
5. S. Brunauer, P. H. Emmett and E. Teller, *Journal of the American Chemical Society*, 1938, **60**, 309-319.
6. E. P. Barrett, L. G. Joyner and P. P. Halenda, *Journal of the American Chemical Society*, 1951, **73**, 373-380.
7. W. H. Bragg, *Journal of the Franklin Institute*, 1930, **210**, 9-14.
8. W. L. Bragg, *Journal of the Franklin Institute*, 1925, **199**, 761-772.
9. N. P. Hung, N. T. Hoan and N. V. Nghia, *Nanoscience and Nanotechnology*, 2013, **3**, 19-25.
10. B. Schrader, *Infrared and Raman spectroscopy: methods and applications*, John Wiley & Sons, 2008.
11. N. J. Harrick, *Internal reflection spectroscopy*, Harrick Scientific Corp., 1967.
12. J. Fahrenfort, *Spectrochimica Acta Part A: Molecular Spectroscopy*, 1989, **45**, 251-263.
13. M. Fan, D. Dai and B. Huang, *Fourier transform–materials analysis. InTech*, 2012.

Chapter 3

EFFECT OF THE SILICA SUPPORT PROPERTIES ON THE PROPERTIES OF AMINE-FUNCTIONALISED CATALYSTS.

3.1. Introduction

In this chapter work on silica-supported base catalysts is reported. The silica supports are functionalised with alkylamino groups so that the catalytic centres are amine groups tethered via alkyl (propyl) groups chemically bound to the silica surface as described later. Silica is widely used as support for catalysts. The silica supports physical properties such as surface area, pore volume, and radius of curvature or average pore diameter should be designed and developed during support preparation.¹

Several experimental and theoretical works have been undertaken to understand the effect of silica support on the properties of supported catalysts.²

The physical properties of silica make it one of the best supports available for application in many catalytic processes. It is considered to be chemically inert, stable at a high temperature, and has high pore volume and surface area that allows it to host a large number of active sites in the particles. In addition, the physical properties of the silica can be tailored during the synthesis in order to suit the targeted application. Furthermore, silica is relatively inexpensive; it is therefore considered a good choice for catalyst production. There are many forms of silica including anhydrous crystalline forms such as quartz, tridymite, and cristobalite. However, the most common kind used in catalyst supporting is the amorphous form.^{3,4}

The physical properties of the silica play a very important role in controlling the catalyst performance. The chemical properties of the silica are very important for the catalyst activity, especially in terms of how active sites of the catalyst are anchored on the surface of the pores. This is generally controlled by the silanol groups on the silica's surface.⁵

There have been various studies seeking to understand the relationship between structural properties and catalytic activity such as morphologies and porous structures. One of the most important structural properties is the porosity, which not only affects the surface area but also affects the adsorption and diffusion of reactant molecules.⁶ In general, materials with pores in the mesopore size range are considered the most useful, the pores being large enough to accommodate reactant molecules but small enough to ensure that the catalyst surface area remains relatively high.

Some studies showed that as the pore volume of the support increases the catalytic activity of solid base catalyst will also increase. Catalyst supports with large pore size will allow the active sites to be anchored through the catalyst particle.⁷

There are two major main routes available for the synthesis of porous hybrid materials based on organosilica: post-synthetic surface transformations (grafting) and direct synthesis procedures (co-condensation, one-pot synthesis).⁸ Post-synthetic surface functionalization is usually carried out under anhydrous conditions (Figure 3.1).

The co-condensation method involves the simultaneous condensation of the corresponding silica and organosilica precursors. There are other strategies, for instance hydrosilylation¹¹ which can also be used, but they are less common than surface grafting.⁹

The co-condensation route generally leads to a good, even distribution of functional groups throughout the silica material. A disadvantage is that some of the functional groups end up in the bulk of the silica rather than in accessible sites on the surface. The grafting method on the other hand ensures that all functional groups end up on the catalyst surface but there is the possibility that functionalisation leads to preferential functionalization of the most readily accessible sites, i.e., sites on the external particle surface and sites on the pore surface close to the pore entrances.^{9, 10}

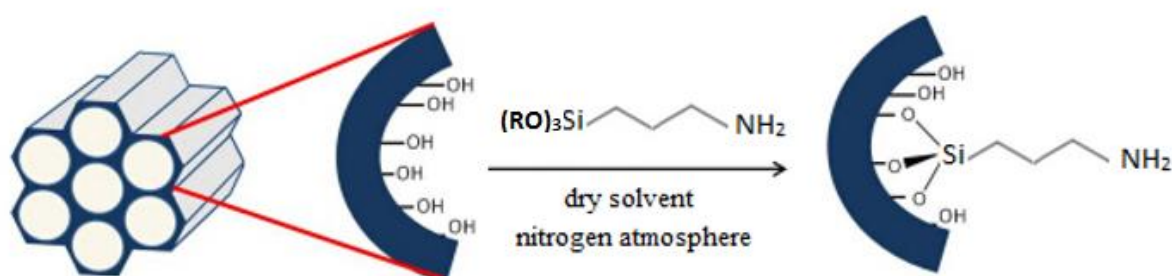


Figure 3.1. Synthesis of supported base catalyst by post-synthetic (grafting).¹¹

The physical properties of functionalized silica can vary within a wide range depending on the nature of the silylating agent used. There are a large number of functional groups that can be used for different applications in various materials. The most common groups of silanes used to functionalize mesoporous silica are the alkoxy silanes.¹²

(3-Aminopropyl)trimethoxysilanes and similar compounds are widely used as coupling agents and among the most commonly used precursors for the modification of silica surfaces due to

their bifunctional nature. In addition they are available at reasonable prices and they behave predictably in the silanization reactions.³

The objectives of the work reported in this chapter were as follows:

- 1) To investigate the influences of physical properties of the support on the catalytic activities of supported amine groups.
- 2) To study the dependence of the supported amine catalysts' activities on the extent of functionalization.
- 3) To identify the key properties of silica supports that control the activities of grafted amine groups.

A range of silica supports have been studied and all have been functionalised with 3-aminopropyltrimethoxysilane. All catalysts were fully characterized. The effect of the properties of the silica support and the properties of the catalysts made from them on the catalytic activities were studied.

Catalytic activities have been assessed using the base-catalysed nitroaldol condensation between nitromethane and benzaldehyde to afford nitrostyrene (Figure 3.2).

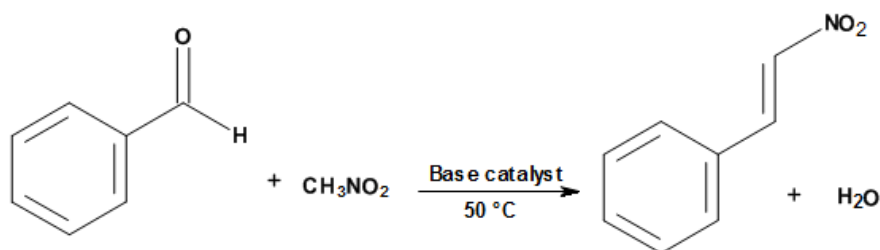


Figure 3.2. Henry reaction (nitroaldol reaction)

3.2. Experimental and techniques

3.2.1. Materials

Eight types of commercial amorphous silica gel solids were used. They are divided into three groups, the L, M and S groups. The letters L, M and S represent the surface areas, L is large surface area, M is medium surface area and S is small surface area.

Table 3.1. Silica supports used and suppliers (data from suppliers).

Materials	BET Surface area (m ² /g)	Pore volume /(cm ³ /g)	Average Pore size (nm)	Suppliers
Silica 717185 (L1)	505	0.8	4.8	Sigma Aldrich
Silica 9536 (L2)	529	0.3	3.2	Johnson Matthey
Silica 214396 (L3)	556	0.4	3.2	Sigma Aldrich
Silica kieselgel (M1)	340	0.8	7.0	MerckMillipore
Silica 236845 (M2)	312	1.1	11.0	Sigma Aldrich
Silica EP10 X (S1)	290	1.6	17.3	INEOS Silicas
Silica Fumed (S2)	193	1.4	26.3	Sigma Aldrich
Silica nano-powder (S3)	199	1.3	25.5	Sigma Aldrich

The average uncertainty for these measurements is approximately +/- 5% for surface area, 2% for average pore size and 0.2% for pore volume.

Benzaldehyde was purchased from Acros; (3-aminopropyl)trimethoxysilane, nitromethane, o-xylene, dry toluene and ethanol 99.5% were purchased from Sigma Aldrich and HCl at 37%, and concentrated HNO₃ solution were purchased from Fischer. Deionized water was used in all experiments.

3.2.2. Activation of silica gel

The silica gel was treated by different acids where 30 g raw silica gel was refluxed in 150 ml of stock HCl (37%) or HNO₃ (60%) for 4 h at 100 °C. The treated silica gel was washed with

distilled water and dried in the oven for 24 h at 120 °C. The activated silica samples were denoted SiO₂ (HCl) and SiO₂ (HNO₃). The non-activated silica was denoted SiO₂.¹³

3.2.3. Synthesis of amorphous mesoporous silica base catalyst (SiO₂-NH₂)

A sample of 5 g of silica gel (activated or non-activated) was suspended in 50 ml of dry toluene and (3-aminopropyl)trimethoxysilane APTMS (1.75 ml, 2.0 mmol g⁻¹) was added to this suspension. The mixture was refluxed under dry nitrogen atmosphere for 72 h at 110 °C and the modified silica gel was filtered off, washed twice with toluene, and dried under vacuum at room temperature. The catalysts were named as follows: SiO₂-NH₂ (L1) for non-activated silica gel, SiO₂-NH₂ (L1) (HCl) and SiO₂-NH₂ (L1) (HNO₃) for activated silica gel with HCl and HNO₃ respectively.

3.2.4. Synthesis of supported base catalysts

A sample of 5 g of activated silica gel was suspended in 50 ml dry toluene, and (1.75 ml, 2.0 mmol g⁻¹) (3-aminopropyl)trimethoxysilane was added to this suspension. The mixture was refluxed in a nitrogen atmosphere (using the Schlenk line technique) for 72 h at 110 °C and the modified silica gel was filtered off, washed with toluene and dried for 24 h.¹⁴ All synthesized materials were named SiO₂-NH₂ and to differentiate between them, brackets were added after the name with one letter and number, where the letters were L (L1, L2 and L3) for the silica with a large surface area, M (M1 and M2) for the silica with a medium surface area and S (S1, S2 and S3) for the silica with a small surface area and catalyst (S1.1) were prepared with the same support of S1. A list of the catalysts appears in Table 3. 1. Note that the target amine content of each catalyst is shown based on the amount of APTMS used but also figures are shown for the measured amount of surface amine are given. The way this was measured is given below. Although this data should really be in the Results section, the fact that subsequent experimental detail requires a knowledge of the amine content, it is given here so that the basis on which the amounts of catalysts used (Table 3. 2) were calculated can be seen.

Table 3.2. Catalysts used in this chapter.

Names of catalysts	Type of Support	Type of Amine	Amount of Amine (measured) mmol/g ^a	Amount of Amine (target) mmol/g
SiO ₂ -NH ₂ (L1)	Silica 717185	(APTMS)	0.7	2.0
SiO ₂ -NH ₂ (L1) (HNO ₃)	Silica 717185	(APTMS)	0.9	2.0
SiO ₂ -NH ₂ (L1) (Non-activated)	Silica 717185	(APTMS)	1.3	2.0
SiO ₂ -NH ₂ (L2)	Silica 9536	(APTMS)	0.9	2.0
SiO ₂ -NH ₂ (L3)	Silica 214396	(APTMS)	0.8	2.0
SiO ₂ -NH ₂ (M1)	Silica kieselgel	(APTMS)	1.6	2.0
SiO ₂ -NH ₂ (M2)	Silica 236845	(APTMS)	1.3	2.0
SiO ₂ -NH ₂ (S1)	Silica EP10X	(APTMS)	1.6	2.0
SiO ₂ -NH ₂ (S1.1)	Silica EP10X	(APTMS)	1.9	2.1
SiO ₂ -NH ₂ (S2)	Silica Fumed	(APTMS)	1.3	2.0
SiO ₂ -NH ₂ (S3)	Silica nano-powder	(APTMS)	2.0	2.0

(a) Estimated by back titration and each value represents the average of three repeats (all values are to +/- 0.1 mmol g⁻¹)

3.2.5. Catalyst characterization

Nitrogen adsorption–desorption isotherms were measured at 77 K on a Micrometrics ASAP-2020 after evacuation at 423 K for 5 h. The surface area was calculated using the BET method as before,¹⁵. BJH analysis, based on the Kelvin equation (see Chapter 2), was applied to the desorption branch for the mesopore and small macropore size range to give pore size distributions, average pore diameters and pore volumes.^{15, 16}

Levels of functionalization were assessed by two methods. The first method was via carbon, hydrogen and nitrogen elemental analysis (MEDAC Ltd), which provided the total amount of amine groups on the surface. The second method was aqueous back titration, where a sample of 100 mg of base catalyst was stirred in 20 ml 0.0100 mol dm³ HCl solution for 4 hr. Then 10 ml of the supernatant solution was extracted and added to 10 ml deionised water and then titrated with 0.0100 mol dm³ of NaOH solutions using phenolphthalein indicator. A comparison between the volumes of NaOH solution required to neutralize HCl which had not been in contact with the catalyst and HCl which had been in contact with the catalyst allowed the

concentration of NH_2 groups on the catalyst surface to be determined. Note that the results from this second method (back titration) are shown above in Table 3.2.

Infrared spectra of the solid samples were recorded on a Nicolet 380 FTIR single reflection (The solid samples were dried at $120\text{ }^\circ\text{C}$ for 2h to remove any physisorbed water and carbon dioxide). Nicolet spectrometer recording attenuated total reflectance infrared (ATR IR) spectra over the range $400\text{-}4000\text{ cm}^{-1}$ under atmospheric conditions, to investigate the chemical nature of the catalyst surface.

3.2.6. Catalytic activity measurement

Catalysts were ground in a pestle and mortar and then activated before use under static air at $120\text{ }^\circ\text{C}$ for 2 h in still air. A mixture of benzaldehyde (0.1 ml), nitromethane (5 ml) and o-xylene as an internal standard (0.1 ml) were kept at $50\text{ }^\circ\text{C}$ under an atmosphere of nitrogen and magnetic stirring was undertaken for 30 min. The reaction vessel was a 100 ml round bottom flask, fitted with a condenser and with a dry nitrogen feed. Temperature was controlled using an oil bath in which the flask was immersed on a hotplate controlled by a temperature probe immersed in the oil and feeding back to the hotplate. The amount of the catalyst used in each experiment was determined on the basis of the functional group loading value as measured by analysis (see Table 3.2 above) in order to introduce the same number of supported propylamine equivalents in the different experiments (Table 3.3). The activated catalyst was added to the reaction mixture while held at the reaction temperature and continuously stirred. Small aliquots of the mixture (small enough not to affect the overall relative concentration of catalyst significantly) were removed with a filter syringe at regular intervals. The filter ensured that reaction mixture was separated from catalyst at the time of extraction. The samples were stored at $0\text{ }^\circ\text{C}$ in an ice bath and analysed by gas chromatography (FID, 25 m BPI column) which was calibrated previously (see appendix C). The final product was fully identified by GC-MS in advance of the experiments and it was established that nitrostyrene was the exclusive product. Kinetic data was henceforth reported in terms of the conversion of benzaldehyde, the limiting reagent. Pseudo first order kinetics were assumed as nitromethane was in large excess.

Table 3.3 The amount of the catalyst used in each experiment.

Samples	Amount of catalyst used in experiment (mg) ^a
SiO ₂ -NH ₂ (L1)	114 +/- 0.35
SiO ₂ -NH ₂ (L1) (HNO ₃)	89 +/- 0.25
SiO ₂ -NH ₂ (L1) (Non-activated)	62 +/- 0.2
SiO ₂ -NH ₂ (L2)	89 +/- 0.25
SiO ₂ -NH ₂ (L3)	100 +/- 0.35
SiO ₂ -NH ₂ (M1)	50 +/- 0.15
SiO ₂ -NH ₂ (M2)	62 +/- 0.2
SiO ₂ -NH ₂ (S1)	50 +/- 0.15
SiO ₂ -NH ₂ (S1.1)	42 +/- 0.1
SiO ₂ -NH ₂ (S2)	62 +/- 0.2
SiO ₂ -NH ₂ (S3)	40 +/- 0.1

(a)The amount of the catalyst used in each experiment has been determined on the basis of the value of amine functional groups present on the surface of SiO₂-NH₂ (**S1**).

3.3. Results and discussion:

3.3.1. Characterisation of studied base catalysts

3.3.1.1. Surface area and pore size determination by nitrogen porosimetry

Eight Silica gel supports were functionalised using (3-aminopropyl)trimethoxysilane (APTMS) at a range of loadings. Their surface areas, pore volumes and pore size distributions before (raw) and after grafting with aminopropylsilane (grafted) were calculated from their N₂ adsorption/desorption isotherms. The results are summarised in Table 3.4 Data for the raw silicas is that provided by the suppliers.

Table 3.4. Surface characteristics of silica supports before (raw) and after (grafted).

Samples	BET surface area /(m ² /g)		Average pore size /(nm)		Average Pore volume /(cm ³ /g)	
	Raw	Grafted	Raw	Grafted	Raw	Grafted
SiO ₂ -NH ₂ (L1)	505	402	4.8	4.3	0.8	0.5
SiO ₂ -NH ₂ (L1) (HNO ₃)	505	356	4.8	4.1	0.8	0.4
SiO ₂ -NH ₂ (L1) (Non-activated)	505	273	4.8	4.0	0.8	0.3
SiO ₂ -NH ₂ (L2)	529	304	3.2	3.1	0.3	0.2
SiO ₂ -NH ₂ (L3)	556	365	3.2	3.1	0.4	0.3
SiO ₂ -NH ₂ (M1)	340	262	7.0	5.2	0.8	0.6
SiO ₂ -NH ₂ (M2)	312	302	11.0	6.0	1.1	0.8
SiO ₂ -NH ₂ (S1)	290	230	17.25	15.9	1.57	1.3
SiO ₂ -NH ₂ (S1.1)	290	219	17.25	15.0	1.57	1.0
SiO ₂ -NH ₂ (S2)	193	161	26.3	24.4	1.4	1.2
SiO ₂ -NH ₂ (S3)	199	77	25.5	25.0	1.5	0.6

The average uncertainty for these measurements is approximately +/- 5% for surface area, 2% for average pore size and 0.2% for pore volume.

All samples were mesoporous silicas with mesopores with diameters in the range 3 to 25 nm. In most cases, the pore size was reduced a little by the grafting of aminopropylsilane. Surface

areas and pore volumes were also decreased. This suggests that the organic moieties were successfully incorporated by grafting and at least some of the added groups occupy a volume inside the pore space of silica, thereby decreasing the pore volume of silica.

In the present case, three catalysts, $\text{SiO}_2\text{-NH}_2$ (L1), $\text{SiO}_2\text{-NH}_2$ (S1), $\text{SiO}_2\text{-NH}_2$ (S1.1) before and after functionalization, were used to illustrate more fully the effect of grafting, through the N_2 adsorption/desorption isotherms of the support and the functionalised support (Figure. 3.3) and (Figure 3.4).

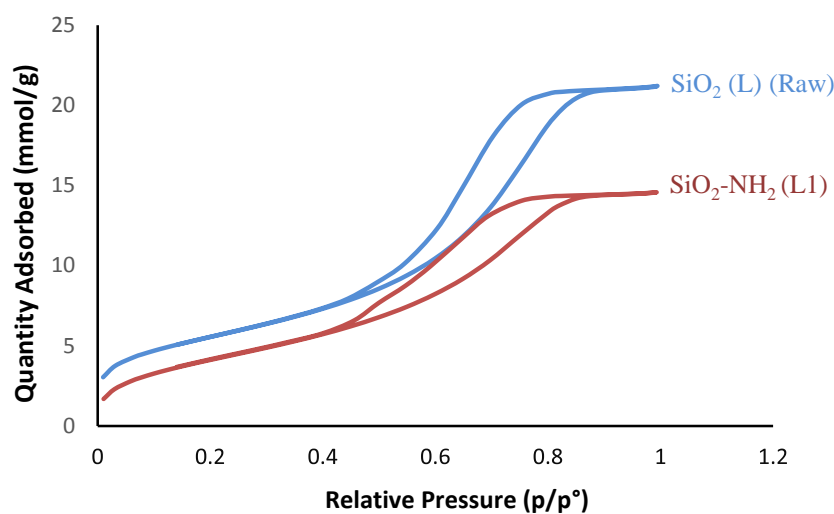


Figure 43.3. N_2 adsorption–desorption isotherms at 77 K for SiO_2 (L) raw silica and grafted amine-silica support $\text{SiO}_2\text{-NH}_2$ (L1)

As shown in Figure 3.3, SiO_2 (L) and $\text{SiO}_2\text{-NH}_2$ (L1) both show type IV isotherms according to the IUPAC classification.¹⁷ The increase of nitrogen uptake at $P/P^\circ \approx 0.4$ is a characteristic of type IV.¹⁸ The other supports showed the same behaviour as $\text{SiO}_2\text{-NH}_2$ (L1) which was expected.

Samples with low (approximately 1.6 mmol g^{-1}) and high amino content (approximately 1.9 mmol g^{-1}) were prepared by adding the corresponding amounts of APTMS to a suspension of the mesoporous silica in dry toluene.

Adsorption/desorption isotherms with pore size distributions, for the raw silica (S) and the same support with 1.6 mmol g^{-1} (S1) and 1.9 mmol g^{-1} (S1.1) amine loading are shown in Figure 3.4. It is clear that by increasing the amount of organic groups leads to a decrease in the surface area of the support, the pore volume is reduced and the average pore size distribution also decreased.

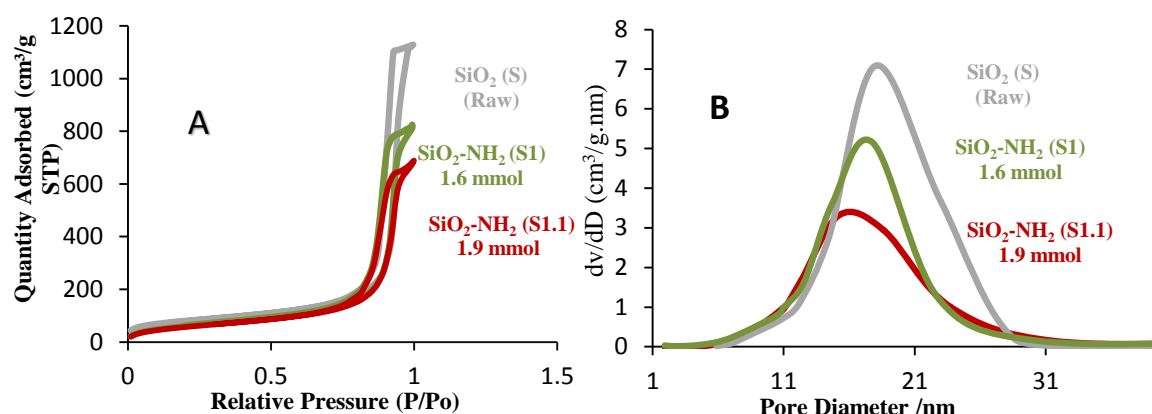


Figure 3.4. (A) N_2 adsorption/desorption isotherms and (B) pore size distribution curves of the hexagonal cylindrical mesoporous SiO_2 (S) with two different functionalised silicas SiO_2-NH_2 (S1) 1.6 mmol g^{-1} , SiO_2-NH_2 (S1.1) 1.9 mmol g^{-1} .

3.3.1.2. The chemical nature of the catalyst surface by FTIR

The FTIR spectra of all catalysts were found to be similar with some differences in the intensities of the bands. However, infrared spectroscopy was used in this study simply to confirm the presence of aminopropylsilane on the surface qualitatively not quantitatively. Therefore, only one example of FTIR spectra of the catalysts is shown in Figure 3.5.

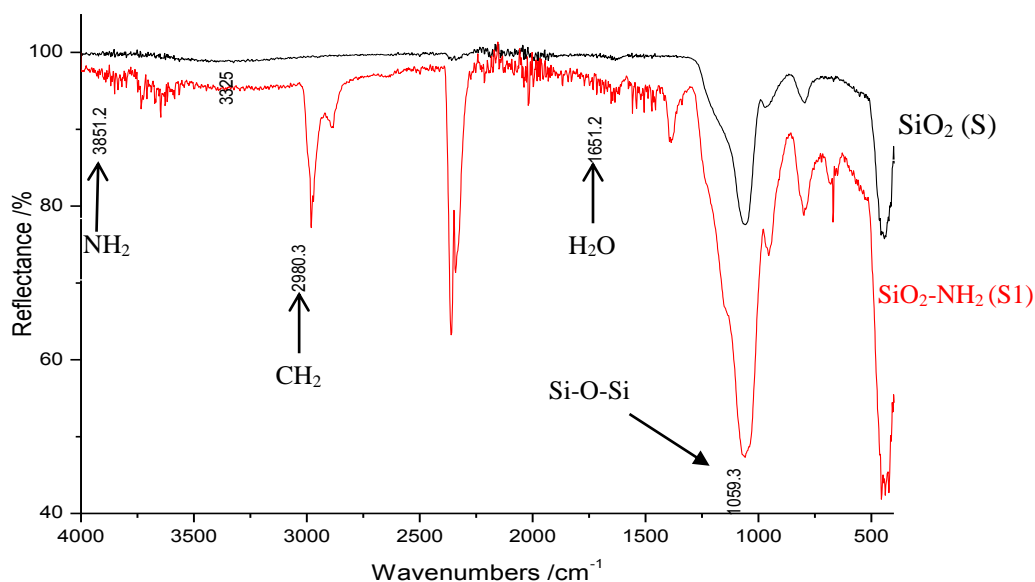


Figure 3.5. The FTIR spectrum of SiO_2 (S) and SiO_2-NH_2 (S1).

SiO_2-NH_2 (S1) spectra showed a broad band at 3325 cm^{-1} which is characteristic of the silanol group (Si-OH). SiO_2-NH_2 showed two bands, stretching vibration band at 2980 cm^{-1} and a

bending vibration band at 1471 cm^{-1} characteristic of the CH_2 groups of the propyl chain of the silylating agent and the weak band at 3851 cm^{-1} , is characteristic of the NH_2 (NH vibrations).¹⁹ However, their low frequencies are acceptable since the spectra were taken in the solid phase. The vibrations of Si–O–Si can be seen at 1059 cm^{-1} (asymmetric stretching), 791 cm^{-1} (symmetric stretching) and 437 cm^{-1} (bending). The band at 1651 cm^{-1} in both spectra is assigned to the deformation vibrations of water.^{19, 20} These results confirmed the successful grafting of amines onto the silica supports.

3.3.1.3. Quantification of aminopropyl groups on studied catalysts.

The concentration of surface amine groups on the catalysts was estimated by the back titration method. (Data is given in Table 3.2 in the Experimental section as well as here.)

Table 3.5. The concentration of active sites on silica supports estimated by back titration.

Samples	Amine concentration (mmol/g) ^a
$\text{SiO}_2\text{-NH}_2$ (L1)	0.7
$\text{SiO}_2\text{-NH}_2$ (L2)	0.9
$\text{SiO}_2\text{-NH}_2$ (L3)	0.8
$\text{SiO}_2\text{-NH}_2$ (M1)	1.6
$\text{SiO}_2\text{-NH}_2$ (M2)	1.3
$\text{SiO}_2\text{-NH}_2$ (S1)	1.6
$\text{SiO}_2\text{-NH}_2$ (S2)	1.3
$\text{SiO}_2\text{-NH}_2$ (S3)	2.0

(a) Estimated by back titration all values are to $\pm 0.1\text{ mmol g}^{-1}$

The results in Table 3.5 show that there is a general trend in which the actual level of functionalization of the silica supports appears to increase as the surface area of the support decreases as shown in Table 3.4. This is surprising. It may be the case that the effectiveness of functionalization is more dependent on pore size than on overall surface area, and it is the case that effective functionalization seems to be related to the pore diameter. The highest loading was 2.0 mmol g^{-1} for $\text{SiO}_2\text{-NH}_2$ (S3) which has the largest pore size (25.5 nm) while, the lowest loading was 0.8 mmol g^{-1} for $\text{SiO}_2\text{-NH}_2$ (L3) which has the smallest pores (3.1 nm). It might be expected that there is a steric effect by grafted APTMS molecules on the surface of the pore entrance which restricts the diffusion of other APTMS to enter the pores. This can be seen in the smaller pores silica where these smaller pores easily become blocked during the functionalisation reaction. (Figure 3.6).

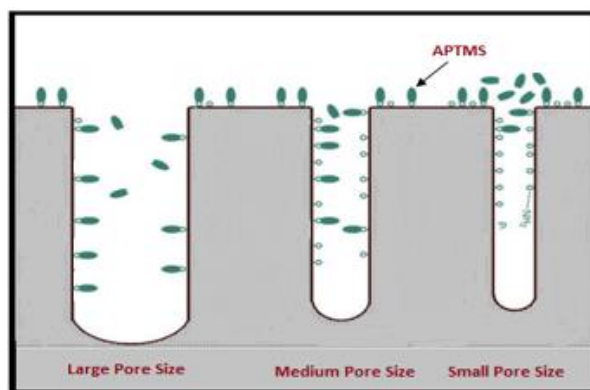


Figure 3.6. Schematic diagram illustrating the functional groups grafted to silica support with small, medium, and large pore size.

Elemental analysis results for the three representative catalysts appear in Table 3.6, showing nitrogen and carbon % w/w values (MEDAC Ltd). Nitrogen content reflects the amine content and the carbon content, or more specifically the molar ratio of carbon to nitrogen, can be used to identify the way in which the functional group is bound to the silica surface.

Amine group concentrations were calculated as shown in Equation 1 and carbon contents were determined in a similar way.

$$C_{\text{NH}_2} = (\text{N}\% / 14.0) \times 10 \text{ mmol g}^{-1} \quad (\text{Equation 1})$$

Table 3.6. Elemental analysis data for three of the catalysts.

Samples	N% w/w	mmol/g	C% w/w	mmol/g	(C/N molar ratio) ^a
SiO ₂ -NH ₂ (S1)	2.27	1.6	5.88	4.9	3.0
SiO ₂ -NH ₂ (S3)	2.97	2.1	7.95	6.6	3.1
SiO ₂ -NH ₂ (L2)	1.30	0.9	3.58	2.9	3.1

(a) Each value represents the average of several repeats +/- 0.1.

Table 3.7. C and N contents based on elemental analysis (MEDAC).

Base catalysts	Number of active sites (mmol g ⁻¹)	
	By titration (NH ₂ /mmol g ⁻¹)	By elemental analysis (NH ₂ /mmol g ⁻¹)
SiO ₂ -NH ₂ (S1)	1.6	1.6
SiO ₂ -NH ₂ (S3)	2.0	2.1
SiO ₂ -NH ₂ (L2)	0.9	0.9

In Table 3.7, the concentrations of amine groups determined by back titration and by elemental analysis are shown. It is clear that, within experimental error, values from the two methods are in agreement.

The carbon to nitrogen molar ratio is approximately 3.0 in each case (Table 3.6). A simple interpretation of this is that, on average, the three methoxy groups on each APTMS molecule have reacted with surface silanols with loss of methanol in each case (so that the only carbon atoms left are the three making up the propyl chain) effectively forming a monolayer on the silica surface.²¹ (Figure 3.7, route 1). An alternative model that would still explain this C/N ratio could involve some groups reacting with silanol groups on neighbouring silane molecules to form siloxane bonds (Si-O-Si).²² Silanol groups can be formed by partial hydrolysis of APTMS molecules in the presence of residual water during the silanization process. This alternative mechanism could lead to the formation of a multilayer or a polymerized siloxane network attached to the silica support surface by less chemical bonds than the monolayer way (Figure 3.7, route 2). It is worth saying that other mechanisms, such as the formation of hydrogen bonds between adjacent amino groups or between amino and residual silanol groups, have also been proposed to explain the possible formation of a three dimensional APTMS networks (Figure 3.7 route 3).

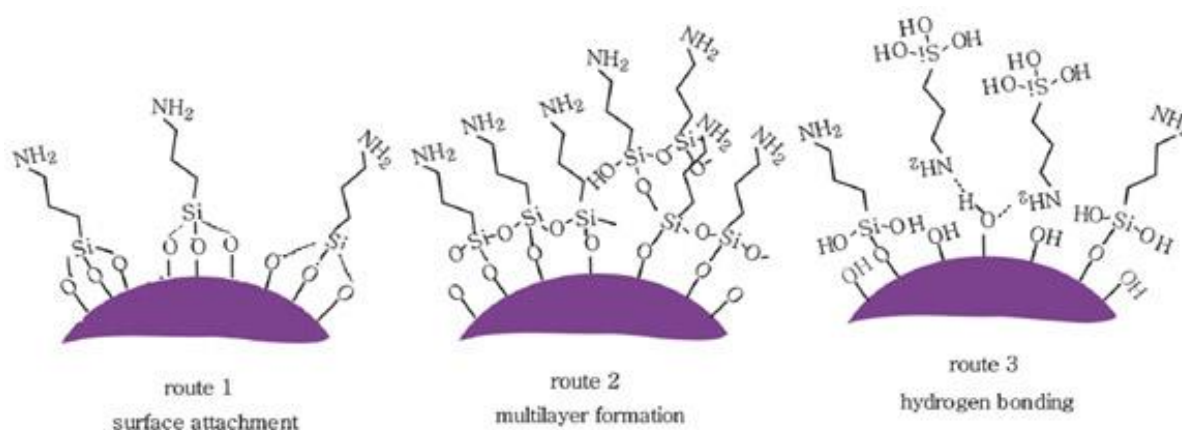


Figure 3.7. Possible grafting routes of aminopropylsilane on silica support surface.

3.3.2. Catalytic activities of studied base catalysts

All synthesised catalysts were studied in the nitroaldol condensation reaction between nitromethane and benzaldehyde to produce nitrostyrene. The conversion of benzaldehyde was plotted against the time of reaction.

3.3.2.1. Effect of silica acid treatment on the activity of supported amine catalyst

SiO₂-NH₂ (L1)

Catalytic activities of SiO₂-NH₂ (L1) (HCl), SiO₂-NH₂ (L1) (HNO₃) and SiO₂-NH₂ (L1) in the nitroaldol reaction at 50° C were measured and the kinetic data were recorded as shown in Figure 3.8.

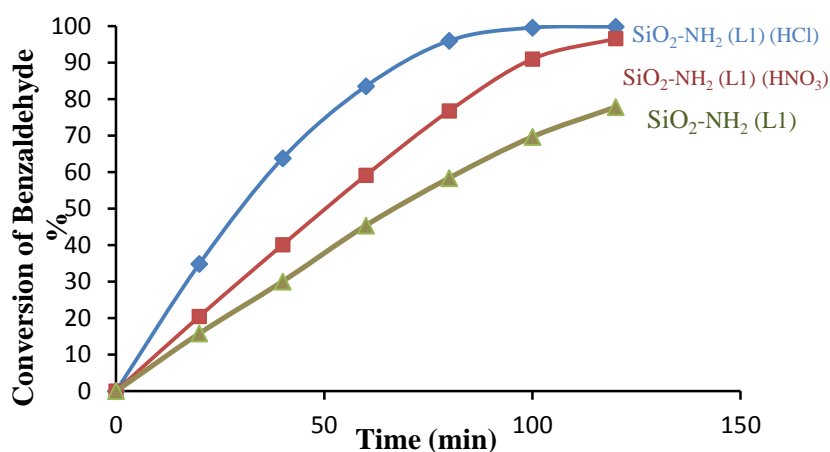


Figure 3.8. Kinetic data for SiO₂-NH₂ (L1), SiO₂-NH₂ (L1) (HCl) and SiO₂-NH₂ (L1)(HNO₃) in the nitroaldol reaction at 50 °C.

The kinetic data shows that the catalyst prepared with SiO₂ (L1) subjected to HCl treatment is the most active material, followed by the catalyst prepared with HNO₃ and the catalyst prepared without any treatment. The number of active sites in SiO₂-NH₂ (L1) (HCl) was lower than the catalyst prepared with HNO₃ and the catalyst prepared without any treatment by 20% and 50% respectively as shown in (Table 3.2). A possible explanation for why this catalyst was the most active is linked to the possibility that more silanol groups are on the surface than other catalysts. Therefore, a cooperative acid-base mechanism may be involved²³ as mentioned in section 1.5 (chapter 1). Comprehensive study of the co-operative mechanism of silanol and amine groups in nitroaldol reaction is covered in chapter 6.

3.3.2.2. Catalytic activity of studied catalysts with large surface area support (L)

The catalytic activities of catalysts prepared using the three silicas with the largest surface areas are shown in Figure 3.9.

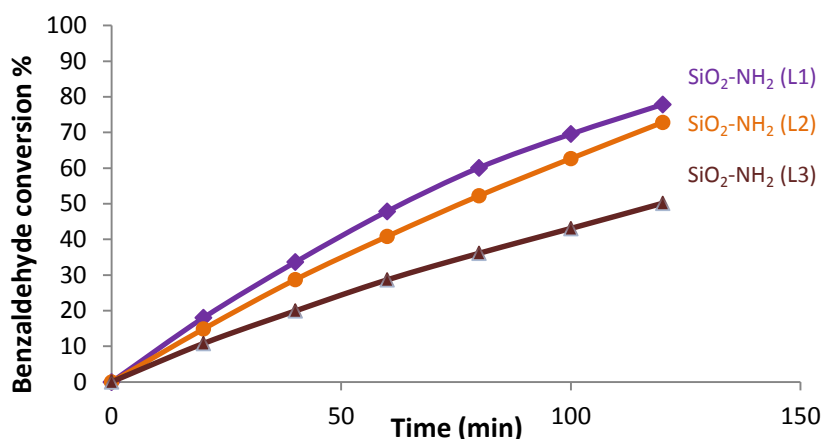


Figure 3.9. Kinetic data for the reaction of nitromethane with benzaldehyde in the presence of *o*-xylene over SiO₂-NH₂ (L1), SiO₂-NH₂ (L2) and SiO₂-NH₂ (L3).

As different concentration of active sites were present in the three catalysts shown in Figure 3.9. To allow for this, the turnover frequency (TOF) at the beginning of the reaction has been calculated which is the total number of moles transformed into the desired product by one mole of active site per hour (Equation 3.5).

Turn over frequency (TOF) was calculated for all studied catalysts by using the rate of reaction assuming pseudo-first order kinetics as in equation 3.2.

$$\text{Rate} = \frac{d[\text{BZ}]}{dt} = -k[\text{Nm}][\text{BZ}] \quad \text{Equation 3.1}$$

Where, Nm = Nitromethane and BZ = benzaldehyde.

$$\frac{d[\text{BZ}]}{dt} = -k'[\text{BZ}] \quad \text{where } [\text{Nm}] \gg [\text{BZ}] \text{ and } k' = k[\text{Nm}] \quad \text{Equation 3.2}$$

By integration of equation 2,

$$\ln [\text{BZ}] = \ln [\text{BZ}]_0 - k't \quad \text{Equation 3.3}$$

Since [BZ] \propto [100 - % conversion]

$$\ln [100 - \% \text{conversion}] = \ln [100] - k't \quad \text{Equation 3.4}$$

Therefore by drawing $\ln [100 - \% \text{conversion}]$ against time (t), a straight line with a slope equal to $-k'$ will be obtained. Then by using k' , TOF can be calculated by using equation 3.5.

$$\text{TOF} = \frac{k' \times 60 \times \text{Initial moles of reactant (mmol)}}{\text{mmol of NH}_2} = h^{-1} \quad \text{Equation 3.5}$$

The reaction progress curves for different functionalised silica (APTMS) in figure 3.9 were used and the rate of the reaction was estimated by using equation 3.5 as shown in Figure 3.10.

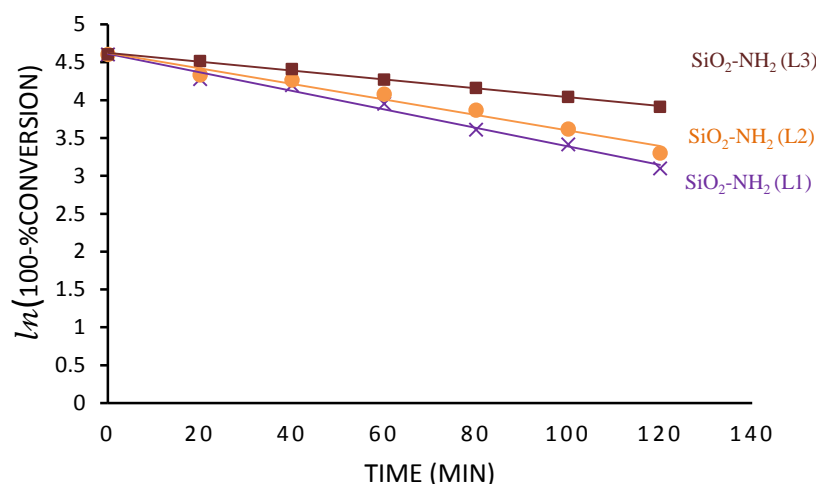


Figure 3.10. First-order kinetic model of aldol reaction for different functionalised silica (APTMS).

From data shown in Figure 3.10, it seems clear that the linear fittings are good for all catalysts in our reaction conditions as R^2 is close to 1.0. The intercept for all regression lines is approximately 4.6. These data were then analysed using the linear regression and the results are used to estimate the rate of the reaction and turn over frequency (TOF), and the results are summarised in Table 3.8

Table 3.8. Turnover frequencies for studied silica-supported catalysts with surface amine concentrations.

Samples	Amine concentration (mmol/g) (-NH ₂) ^a	Linear regression Equation of the first order rate	1st order rate constant k (h ⁻¹) ^b	TOF (h ⁻¹) ^{b*} 1 st Order Kinetics
SiO ₂ -NH ₂ (L1)	0.7	$y = -0.0122x + 4.6108$ $R^2 = 0.9865$	0.0122	8.9 +/- 0.46
SiO ₂ -NH ₂ (L2)	0.9	$y = -0.0102x + 4.6251$ $R^2 = 0.9764$	0.0102	7.5 +/- 0.38
SiO ₂ -NH ₂ (L3)	0.8	$y = -0.0059x + 4.6234$ $R^2 = 0.9976$	0.0059	4.3 +/- 0.22

(a) Estimated by back titration, (b, b*) Confidence limits on k values and on TOF values are approximately +/- 5%.

The notable feature of this data is that SiO₂-NH₂ (L3) is significantly less active (in terms of TOF) than the other two. The concentration of active sites on all three catalysts are similar so, although possible, it seems unlikely that this is a consequence of something related simply to the concentration of active sites on the surface. It is more likely that it is linked to a difference in the morphology of L3 compared to the other two but what this difference might be cannot easily be identified from the data here.

3.3.2.3. Catalytic activities of studied catalysts with medium surface area support

(M)

The catalytic activities of catalysts made using silicas with medium surface area support are shown in Figure 3.11.

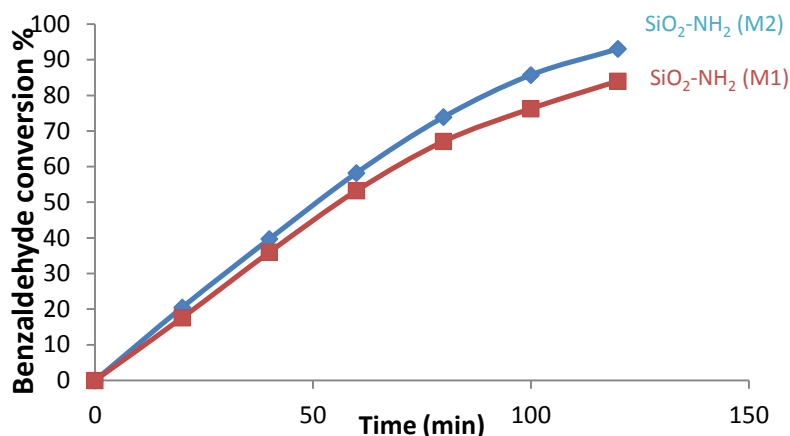


Figure 3.11: Reactivity of nitromethane with benzaldehyde in the presence of *o*-xylene over SiO₂-NH₂ (M1) and SiO₂-NH₂ (M2)

As different amount of active sites were present in each support, the turnover frequency (TOF) which is the total number of moles transformed into the desired product by one mole of active site per hour was calculated for each catalyst as a universal measure of its activity (Equation 3.5) (section 3.3.2.2)

The reaction progress curves for different functionalised silica (APTMS) in figure 3.11 were used as an indicator of the activity of the catalyst and the rate of the reaction was estimated by using equation 3.5 (section 3.3.2.2) as shown in Figure 3.12.

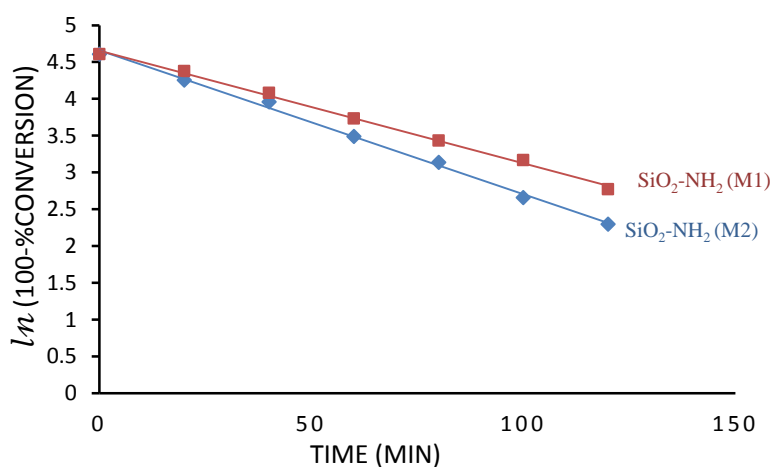


Figure 3.12. First-order kinetic model of aldol reaction for different functionalised silica (APTMS).

From data shown in Figure 3.12, appears clearly that the linear fittings are good for all catalysts in our reaction conditions as R^2 is close to 1.0. The intercept for all regression lines is approximately 4.6. These data were then analysed using the linear regression and the results are used to estimate the rate of the reaction and turn over frequency (TOF), and the results can be seen in Table 3.9.

Table 3.9. Turnover frequencies for studied silica-supported catalysts with surface amine concentrations.

Samples	Amine concentration (mmol/g) (-NH ₂) ^a	Linear regression Equation of the first order rate	1st order rate constant (k /h ⁻¹) ^b	TOF (h ⁻¹) ^{b*} 1 st Order Kinetics
SiO ₂ -NH ₂ (M1)	1.6	$y = -0.0153x + 4.6548$ $R^2 = 0.9968$	0.015	11 +/- 0.57
SiO ₂ -NH ₂ (M2)	1.3	$y = -0.0195x + 4.6577$ $R^2 = 0.9968$	0.020	14 +/- 0.70

(a)Estimated by back titration, (b, b*) Confidence limits on k values and on TOF values are approximately +/- 5%.

The results in Table 3.9 show SiO₂-NH₂ (M2) slightly higher activity than SiO₂-NH₂ (M1) by 20%. The reason could be that SiO₂-NH₂ (M2) has larger pore size (11.0 nm) than SiO₂-NH₂ (M1) pore size (7.0 nm). On the other hand, the major observation is that the values of TOFs here are far higher than with those the (L) supports by 35 %. It is clear the effect of pore size play important role in catalytic activity, despite that (L) supports have slightly larger surface area than with those (M) supports (See Figure 3.2).

3.3.2.4. Catalytic activity of studied catalysts with small surface area support (S)

The catalytic activities of catalysts with medium surface area support are shown in Figure 3.13.

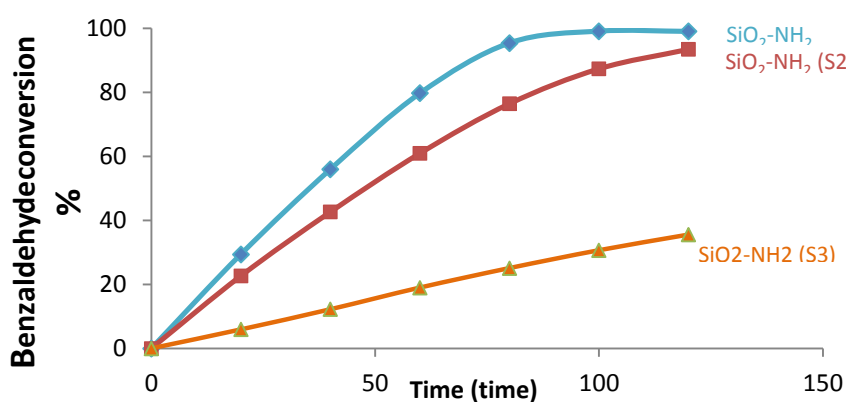


Figure 3.13. Reactivity of nitromethane with benzaldehyde in the presence of o-xylene over SiO₂-NH₂ (S1), SiO₂-NH₂ (S2) and SiO₂-NH₂ (S3).

As different amount of active sites were present in each support. The reaction progress curves for different functionalised silica (APTMS) in figure 3.13 were used as an indicator of the activity of the catalyst and the rate of the reaction was estimated by using equation 3.5 (section (3.3.2.2)) as shown in Figure 3.14.

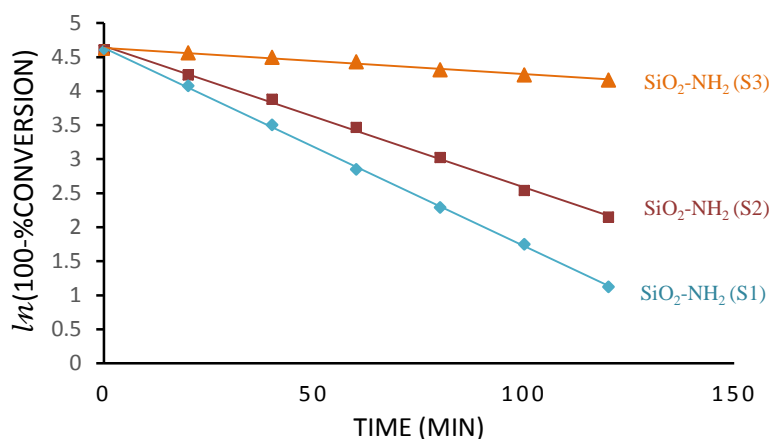


Figure 3.14. First-order kinetic model of aldol reaction for different functionalised silica (APTMS).

From data shown in Figure 13, it appears clear that the linear fittings are good for all catalysts in our reaction conditions as R^2 is close to 1.0. The intercept for all regression lines is approximately 4.6. These data were then analysed using the linear regression and the results are used to estimate the rate of the reaction and turn over frequency (TOF), and the results can be seen in Table 3.10.

Table 3.10. The catalytic activities as TOF of catalysts and number of active sites with a small surface area.

Samples	Amine concentration (mmol/g) (-NH ₂) ^a	Linear regression Equation of the first order rate	1st order rate constant (k /h ⁻¹) ^b	TOF (h ⁻¹) ^{b*} 1 st Order Kinetics
SiO ₂ -NH ₂ (S1)	1.6	$y = -0.0291x + 4.6335$ $R^2 = 0.9994$	0.029	21.2 +/- 1.1
SiO ₂ -NH ₂ (S2)	1.3	$y = -0.0207x + 4.66$ $R^2 = 0.9977$	0.020	14.7 +/- 0.75
SiO ₂ -NH ₂ (S3)	2.0	$y = -0.0038x + 4.6333$ $R^2 = 0.9868$	0.004	2.7 +/- 0.14

(a) Estimated by back titration, (b, b*) Confidence limits on k values and on TOF values are approximately +/- 5%.

The SiO₂-NH₂ (S3) showed a much lower level of activity (2.7 h⁻¹) than other catalysts, despite the amount of amine groups on the surface which was very high (2.0 mmol g⁻¹) compared to the other catalysts, regardless of the large pore size which allow the diffusion of

reactants inside the pores and thus reach the aminopropyl groups. But the results for the other two materials, S1 and S2, are high compared to the M and L catalysts a rate ranging between 80% and 20%. There seems to be a trend with specific activities increasing as the surface area of the support is reduced and the size of the pores is increased.

3.3.2.5. Discussion of activity results

The turn over frequency for the studied catalyst varied from 21.2 h^{-1} to 2.7 h^{-1} although the same functional group was grafted on all catalysts. This result confirms that the inorganic support morphology has a very significant effect on the activity of the functional group, in line with previous reports.^{5,6} However, it was very difficult to assign the overall change in activity to a single property of the support. Three factors found to be very important were surface area, pore size and the amount of organic groups on the surface. It appears that by increasing the surface area of the support, the amount of organic groups decrease, in line with other reports.²⁴⁻²⁶ Concomitantly, the specific activity of the amine groups (as TOF) also seems to fall. However, increasing the support surface area leads to a decrease in pore diameter and there is a correlation between the decreasing pore size and the decreasing activity of the amine groups. This does not seem unreasonable and may be because reactant accessibility depends on the size of the catalyst pores when they are in the mesoporous range as those studied here are. The small pore diameter may also facilitate the blocking of pores by the catalytic functional groups located at the pore entrances, therefore preventing other molecules access to sites deep inside the pores, which is a disadvantage to catalytic activity of catalysts.^{27,28} In contrast, with a large pore size the amino group can easily diffuse inside the pores and the grafting occurs on the internal surface of the pores and thus increasing catalytic activity, this observation is consistent with reported work.^{7, 27-29} The importance of the role of the silica surface alone as a factor in controlling activity, it is possible to estimate the proportion of the surface covered by functional groups. It is well known that one aminopropylsilane group covers approximately 50 nm^2 of the silica surface.^{30,31} therefore the surface coverage can be calculated for each support according to its surface area. Thus, the optimum amount of aminopropylsilane can firstly, be practically related to the surface coverage of any silica support then, theoretically calculated for other supports (Calculate the theoretical amount of aminopropyl on the silica surface, see appendix B).

Table 3.11 Surface coverage of all studied catalysts with their turn over frequencies.

Samples	BET surface area(m ² /g) of SiO ₂ (raw)	Amine concentration (mmol/g) (-NH ₂)	(Surface Coverage) Area occupied by amine at 0.50 nm ² per molecule (m ² /g)	TOF (h ⁻¹) 1st Order Kinetics
SiO ₂ -NH ₂ (L1)	505	0.7	211	8.9 +/- 0.46
SiO ₂ -NH ₂ (L2)	529	0.9	271	7.5 +/- 0.38
SiO ₂ -NH ₂ (L3)	556	0.8	240	4.3 +/- 0.22
SiO ₂ -NH ₂ (M1)	340	1.6	482	11.2 +/- 0.57
SiO ₂ -NH ₂ (M2)	312	1.3	391	14.3 +/- 0.70
SiO ₂ -NH ₂ (S1)	290	1.6	482	21.2 +/- 1.1
SiO ₂ -NH ₂ (S2)	193	1.3	391	14.7 +/- 0.75
SiO ₂ -NH ₂ (S3)	199	2.0	602	2.7 +/- 0.14

As shown in Table 3.11, the lowest activity was the catalyst with the surface coverage of active sites (602 m²/g) higher than the surface area available by the support (199 m²/g). That this very large apparent excess coverage is linked to the lowest, by far, specific activity of supported amine groups does suggest that the nominal coverage factor (surface area needed for the amine groups as a monolayer compared to the available surface area on the support in this case (602:199) might be important. We might expect a multilayer of aminopropylsilane groups on the surface which could be the reason for the lower activity. The same principle can be used to explain other catalysts with different activities. However, a proper study of the relationship between specific amine activity and nominal surface coverage as a percentage of available surface area is presented in the following chapters, where one of the variables specifically studied is the loading of amine on selected supports, and it will be shown that this relationship does turn out to be an important one in determining the activity of the amine groups tethered to the silica surface to optimise the catalytic activity.

3.4. Conclusion:

The effect of the physical properties of the support on the catalytic activity of solid catalysts was studied, by using eight silica gel supports which have been functionalised by grafting 3-aminopropyl (trimethoxysilane) (APTMS).

The obtained results showed that variations of structural properties of the catalyst supports have a significant effect on their activity, since they influence the dispersion of the active sites, but the most interesting results were the activity of silica nano-powder $\text{SiO}_2\text{-NH}_2$ (S3) which was much lower than other catalysts, despite the amount of amine groups on the surface which was very high (2.0 mmol g^{-1}) comparing to other catalysts. This lower activity may be a result of multilayer formation of aminopropylsilane on the silica support surface. This multilayer may be created when the methoxy groups from two APTMS molecules are displaced, and a siloxane bond is formed between them.²²

In the following chapter, the effect of the loading amount of aminopropylsilane on the same support $\text{SiO}_2\text{-NH}_2$ (S3) has been studied by varying the amount of APTMS to obtain different surface coverage, which was then correlated to the total surface area as a percentage.

3.5. References

1. A. Ayrál, A. Julbe, V. Rouessac, S. Roualdes and J. Durand, *Inorganic Membranes: Synthesis, Characterization and Applications*, volume, 2008, **13**, 33-459.
2. P. B. Amama, A. E. Islam, S. M. Saber, D. R. Huffman and B. Maruyama, *Nanoscale*, 2016, **8**, 2927-2936.
3. P. Zucca and E. Sanjust, *Molecules*, 2014, **19**, 14139-14194.
4. R. Oosthuizen and V. Nyamori, *Platinum Metals Review*, 2011, **55**, 154-169.
5. F. Fakhfakh, L. Baraket, A. Ghorbel, J. M. Fraile, C. I. Herrerías and J. A. Mayoral, *Journal of Molecular Catalysis A: Chemical*, 2010, **329**, 21-26.
6. W. Tang, Y. Deng, W. Li, J. Li, G. Liu, S. Li, X. Wu and Y. Chen, *Catalysis Science & Technology*, 2016, **6**, 1710-1718.
7. M. McDaniel, *Advances in Catalysis*, 1985, **33**, 47-98.
8. T. Kugita and H. Higuchi, *Chemistry Letters*, 2006, **35**, 906-907.
9. K. K. Sharma, R. P. Buckley and T. Asefa, *Langmuir*, 2008, **24**, 14306-14320.
10. A. Stein, B. J. Melde and R. C. Schroden, *Advanced Materials*, 2000, **12**, 1403-1419.
11. M. D. Esquivel Merino, P. Van Der Voort and F. Romero-Salguero, *AIMS Materials Science*, 2014, **1**, 70-86.
12. H. Zhu, D. J. Jones, J. Zajac, R. Dutartre, M. Rhomari and J. Rozière, *Chemistry of materials*, 2002, **14**, 4886-4894.
13. A. N. Kursunlu, E. Guler, H. Dumrul, O. Kocyigit and I. H. Gubbuk, *Applied Surface Science*, 2009, **255**, 8798-8803.
14. A. G. Prado and C. Airoidi, *Journal of colloid and interface science*, 2001, **236**, 161-165.
15. S. Brunauer, P. H. Emmett and E. Teller, *Journal of the American Chemical Society*, 1938, **60**, 309-319.
16. R. Denoyel, M. Barrande and I. Beurroies, in *Studies in Surface Science and Catalysis*, eds. F. R.-R. J. R. P.L. Llewellyn and N. Seaton, Elsevier, 2007, vol. Volume 160, pp. 33-40.
17. K. S. W. Sing, D. H. Everett, R. A. W. Haul, L. Moscou, R. A. Pieroti, J. Rouquerol, T. Siemieniowska. *Pure Appl. Chem.*, (1985), **57**, 603-619.
18. H. Alsyouri, M. Abu-Daibes, A. Alassali and J. Lin, *Nanoscale Research Letters*, 2013, **8**, 484.

19. M. R. Mello, D. Phanon, G. Q. Silveira, P. L. Llewellyn and C. M. Ronconi, *Microporous and Mesoporous Materials*, 2011, **143**, 174-179.
20. W. Kaleta and K. Nowinska, *Chemical Communications*, 2001, DOI: 10.1039/b007111k, 535-536.
21. A. Arranz, C. Palacio, D. García-Fresnadillo, G. Orellana, A. Navarro and E. Muñoz, *Langmuir*, 2008, **24**, 8667-8671.
22. S.-H. Choi and B.-m. Zhang Newby, *Surface Science*, 2006, **600**, 1391-1404.
23. M. Hartmann and X. Kostrov, *Chemical Society Reviews*, 2013, **42**, 6277-6289.
24. Yoncheva, K.; Popova, M.; Szegedi, A.; Mihály, J.; Tzankov, B.; Lambov, N.; Konstantinov, S.; Tzankova, V.; Pessina, F.; Valoti, M., *Journal of Solid State Chemistry 2014*, **211**, 154-161.
25. Clerici, M. G.; Kholdeeva, O. A., *Liquid phase oxidation via heterogeneous catalysis: organic synthesis and industrial applications*. John Wiley & Sons: 2013.
26. Bonneviot, L.; Kaliaguine, S., *Zeolites: A Refined Tool for Designing Catalytic Sites*. Elsevier: 1995, **97**.
27. Melde, B. J.; Johnson, B. J.; Charles, P. T., *Sensors* 2008, **8**, 5202-5228
28. Ritter, H.; Brühwiler, D., Accessibility of amino groups in postsynthetically modified mesoporous silica. *The Journal of Physical Chemistry C* **2009**, *113* (24), 10667-10674.
29. Xia, K.; Ferguson, R. Z.; Losier, M.; Tchoukanova, N.; Brüning, R.; Djaoued, Y., *Journal of hazardous materials* 2010, **183** , 554-564.
30. M. Etienne and A. Walcarius, *Talanta*, 2003, **59**, 1173-1188.
31. E. F. Vansant, P. Van Der Voort and K. C. Vrancken, *Characterization and chemical modification of the silica surface*, Elsevier, 1995.

Chapter 4

OPTIMIZING THE ACTIVITY OF ORGANIC-INORGANIC SOLID BASE CATALYSTS BY CONTROLLING THE SURFACE COVERAGE.

The objective of this chapter is to obtain the optimum activity of organic-inorganic base catalyst by varying the amount of catalytic active groups on the surface.

4.1. Introduction

Mesoporous materials have received a great deal of attention because of their controllable structures and compositions, which make them suitable for many potential applications as supports for catalysis, separation, selective adsorption, novel functional materials.¹

Mesoporous silicas as supports may enhance the catalytic properties if the material is suitably designed. Thus, the design of efficient organocatalytic mesoporous silica requires not only a good understanding of the mechanisms behind the catalytic processes but also an ability to control the synthesis and characterization tools for silica-based materials.²

The pore size of mesoporous silica is large enough and sufficiently uniform to host large molecules. In addition, the existence of high concentration of silanol groups on the pore wall is helpful to introduction of functional groups with a high level of coverage.^{3,4}

One of important method of modifying the chemical and physical properties of mesoporous silica is the incorporation of organic components, either on the silica surface, as part of the silica walls, or trapped within the channels.⁵

In numerous cases where mesoporous materials have been used, further functionalization of these materials on their surface has been done, usually in order to improve their chemical and physical properties.⁶ It is expected that an increase in the amount of functional groups on the mesoporous silica surface while retaining the open space would result in a higher activity. However, such functionalized silica exhibits poorer structural ordering than non-functionalized mesoporous silica materials.⁷ Meanwhile, uneven distribution of functional groups in the mesoporous adversely affects the performance of the catalyst because the high density of functional groups on the surface may prevent the diffusion of molecules in the mesopores. Therefore, the balance of the high loading of functional groups should be attained as a whole.^{8,9}

Surface modification with functional groups is desired so that the coverage of functional groups on the surface may increase without affecting the diffusion of molecules in the mesopores to obtain catalysts that give a high performance.^{10,11} The ability to cover mesoporous materials with high quality functionalized monolayers is a powerful synthetic tool in the development of high surface area heterogeneous catalysts.¹²

The most common groups of silanes used to functionalize mesoporous silica are alkoxysilanes. The incorporation of the functional groups into the mesoporous silica can be obtained either during the synthesis (co-condensation) or after the synthesis (grafting).¹³

Aminopropylsilanes are among the most commonly used precursors for the modification of silica surfaces. In anhydrous media, reaction of the silane alkoxy group (usually methoxy or ethoxy) with surface hydroxyl groups proceeds with concurrent loss of the corresponding alcohol.¹⁴

In this study, most of the work has involved the (3-aminopropyl)trimethoxysilane precursor for controlling the amount, the distribution, and the stability of the grafted aminopropyl moieties on the mesoporous silica surface.¹⁴

The objective of the work in this chapter is to investigate the relationships between the surface loadings of catalytic groups and catalytic activities. The approach taken has been to calculate the optimum loading by controlling the level of functionalization to obtain a monolayer coverage. Two types of silica supports have been selected: Nano-powder (S3) and EP10X (S1).

The reason for choosing these two silica supports over all other silica supports is that the base catalyst with EP10X support gave the highest activity while the base catalyst with Nano-powder silica support gave the lowest activity although the level of active base sites (amine groups) in the later was two times higher than the former catalyst. Therefore the aim of this chapter is to optimise silica Nano-powder catalyst (increase its activity) by controlling the level of functionalization to obtain a monolayer coverage. This was done by varying the amount of catalytic active groups on the surface. On the basis that the fractional coverage of the silica surface by catalytically active groups is key to controlling overall catalytic activity in base-catalysed reactions.

All catalysts were fully characterized. The effect of the synthesis method, support textural parameters and reaction conditions on the catalytic activities were studied.

Catalytic activities have been assessed using the base-catalysed reactions; nitroaldol condensation between nitromethane and benzaldehyde to afford nitrostyrene (as mentioned in section 3.1 (chapter 3)).

4.2. Experimental

4.2.1. Material

(3-aminopropyl)trimethoxysilane (APTMS), dry toluene, o-xylene, nitromethane, and ethanol 99.5%, were purchased from Sigma Aldrich. Benzaldehyde was purchased from Acros and HCl at 37% was purchased from Fischer. Unless noted otherwise, all chemicals were at least 99% pure and used as received. Deionized water was used in all experiments.

Table 4.1. Silica support materials used (both from commercial suppliers).

EP10X Silica (INEOS Silicas)	Nano-powder silica (Sigma Aldrich)
Average Surface area = 290 m ² /g	Average Surface area = 199 m ² /g
Average Pore volume = 1.57 cm ³ /g	Average Pore volume = 1.30 cm ³ /g
Average pore size = 17.25 nm	Average Average pore size = 25.50 nm

4.2.2. Activation of silica supports (EP10X, Nano-powder)

Silica gel was treated by acid where 30.0 g of raw silica support was refluxed in 150 ml stock HCl (37%) for 4 h at 100 °C to generate silanols groups on the surface and dissolve any metal impurities which could be active in the reactions. The activated silica support was washed in copious amounts of distilled water to remove all acid residues before being dried in the oven for 24 h at 120 °C.¹⁵

4.2.3. Synthesis of solid base catalysts with (3-aminopropyl)trimethoxysilane (APTME)

A sample of 5 g of activated silica gel was suspended in 50 ml dry toluene, and 1.0 ml APTMS was added to this suspension. The mixture was refluxed in a nitrogen atmosphere (using the Schlenk line technique) for 72 h at 110 °C and the modified silica gel was filtered off, washed with toluene and dried for 24 h.¹⁶ Similar catalysts were prepared by the same method. The catalysts have been named according to amount of amine used in each catalyst, as follows: (S3, S3.1, S3.2, S3.3 and S3.4.) and (S1, S1.1, S1.2, S1.3 and S1.4). The catalysts are summarised in Table 4.2.

Table 4.2. Catalysts used in this chapter.

Type of Silica Support EP10X			Type of Silica Support Nano-powder		
Names of catalysts	Amine concentration (mmol/g)(NH ₂) ^a	Type of amine	Names of catalysts	Amine concentration (mmol/g) (-NH ₂) ^a	Type of amine
SiO ₂ -NH ₂ (S1)	1.6	APTMS	SiO ₂ -NH ₂ (S3)	2.0	APTMS
SiO ₂ -NH ₂ (S1.1)	1.9	APTMS	SiO ₂ -NH ₂ (S3.1)	1.3	APTMS
SiO ₂ -NH ₂ (S1.2)	1.0	APTMS	SiO ₂ -NH ₂ (S3.2)	1.1	APTMS
SiO ₂ -NH ₂ (S1.3)	0.9	APTMS	SiO ₂ -NH ₂ (S3.3)	0.7	APTMS
SiO ₂ -NH ₂ (S1.4)	0.6	APTMS	SiO ₂ -NH ₂ (S3.4)	0.5	APTMS

(a)Estimated by back titration and each value represents the average of three repeats (all values are to +/- 0.1 mmol g⁻¹)

4.2.4. Catalyst characterization

Nitrogen adsorption–desorption isotherms were measured at 77 K on a Micrometrics ASAP-2020 after evacuation at 423 K for 5 h. The surface area was calculated using the BET method¹⁷ from the adsorption leg and porosity was evaluated using the BJH method¹⁸, based on the Kelvin equation, using the desorption leg, both as described in Chapter 2.

Levels of functionalization were assessed by two methods. The first method was via nitrogen, carbon and hydrogen elemental analysis, which provided the total amount of amine groups on the surface. Elemental analysis was provided by MEDAC Ltd.

The second method was assessed by back titration where a sample of 100 mg of dried base catalyst was stirred in 20 ml HCl 0.01 mol dm³ for 4 h. Then 10 ml of the HCl solution was added to 10 ml distilled water along with 2 drops of phenolphthalein as indicator. The mixture was titrated with standardized 0.01 mol dm³ of NaOH solutions.

4.2.5. Catalytic activity measurement

Catalysts were activated before use under static air at 120 °C for 2 h. A mixture of benzaldehyde (0.1 ml), nitromethane (5 ml) and *o*-xylene as internal standard (0.1 ml) were kept at 70 °C under an atmosphere of nitrogen and magnetic stirring for 30 min. After that, 50 mg of the selected catalyst was added to the mixture to start the reaction. The reaction mixture was then stirred under an atmosphere of nitrogen and aliquots of the sample mixture were removed with a filter syringe. The samples were stored at 0°C in an ice bath and analysed by a calibrated gas chromatography-flame ionisation detector (GC-FID) as soon as possible (invariably within minutes of extraction). The final product was fully identified by GC-MS.

4.3. Results and discussion:

4.3.1. Characterisation of studied (Nano-powder) SiO₂-NH₂ (S3) base catalysts.

Several samples of aminopropyl-functionalised silica were prepared by grafting different amount of (3-aminopropyl)trimethoxysilane (APTMS) onto the surface of silica nano-powder. The aminopropyl group content of the materials has been adjusted by varying the amount of APTMS in the reaction medium. The catalysts labelled S3, S3.1, S3.2, S3.3 and S3.4. N₂ adsorption–desorption isotherms were obtained for the silica support samples before and after grafting the amine groups. The results are listed in Table 4.3.

Table 4.3. Textural parameters and level of functionalization for supported base catalysts.

Samples	BET surface area (m ² /g)		Average pore size /(nm)		Average pore volume /(cm ³ /g)	
	Raw	Grafted	Raw	Grafted	Raw	Grafted
SiO ₂ -NH ₂ (S3)	199	77	25.5	25	1.45	0.56
SiO ₂ -NH ₂ (S3.1)	199	160	25.5	24	1.45	1.04
SiO ₂ -NH ₂ (S3.2)	199	162	25.5	25.2	1.45	1.28
SiO ₂ -NH ₂ (S3.3)	199	169	25.5	25	1.45	1.4
SiO ₂ -NH ₂ (S3.4)	199	183	25.5	25.4	1.45	1.39

The average uncertainty for these measurements is approximately +/- 5% for surface area, 2% for average pore size and 0.2% for pore volume

From Table 4.3, it is clear that all samples are mesoporous silica with high pore sizes 25 nm. All silica supports show type V isotherms before and after grafting the amine groups, which indicates the presence of mesopores, as shown in Figure 4.1.

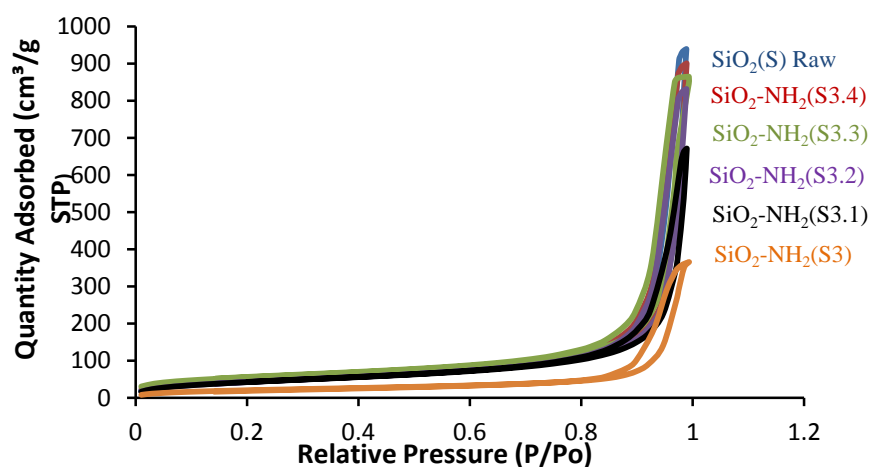


Figure 4.1. N₂ adsorption–desorption isotherms for silica support and grafted amine-silica support (S3)

From Table 4.3, by increasing the level of functionalization, the surface area decreases. The relation between the surface area and the amount of NH_2 on the surface is shown in Figure 4.2.

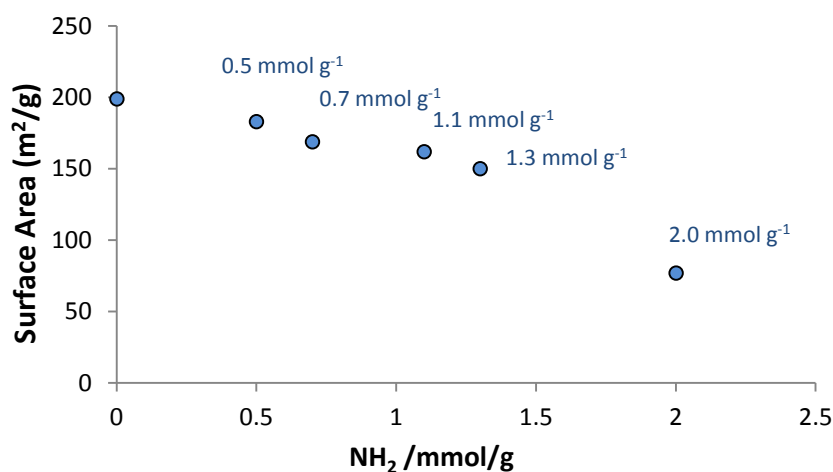


Figure 4.2. Surface area vs. amine loading for amine supported on Nano-powder.

According to figure 4.2, the surface area drops by 60% when the amount of NH_2 on the surface reaches 2.0 mmol g^{-1} . In Table 4.4 the area occupied by functional groups on nano-powder catalysts has been calculated, based on the premise that each functional group occupies 0.50 nm^2 ^{219, 20}.

Table 4.4. Number of active sites and their surface coverage on studied silica supports.

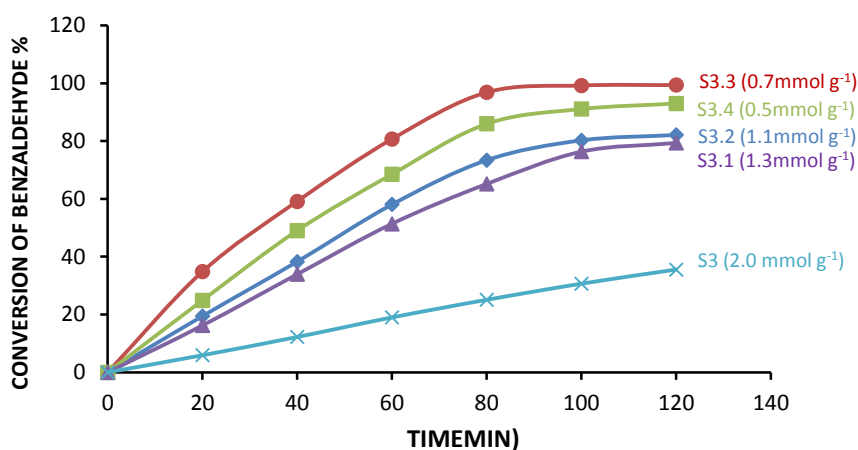
Types of base catalysts	Amine concentration (mmol/g) ($-\text{NH}_2$) ^a	(Surface Coverage) Area occupied by amine at 0.50 nm^2 per molecule (m^2/g)
$\text{SiO}_2\text{-NH}_2$ (S3)	2.0	602
$\text{SiO}_2\text{-NH}_2$ (S3.1)	1.3	391
$\text{SiO}_2\text{-NH}_2$ (S3.2)	1.1	331
$\text{SiO}_2\text{-NH}_2$ (S3.3)	0.7	211
$\text{SiO}_2\text{-NH}_2$ (S3.4)	0.5	151

(a) Estimated by back titration and all values are to $\pm 0.1 \text{ mmol g}^{-1}$

4.3.2. Catalytic activity of studied Nano-powder (S3) base catalysts

The conversions of benzaldehyde in the nitroaldol reaction over the catalysts were studied where the amount of the catalyst utilized in each experiment was carefully determined on the basis of the loading value in order to introduce the same amount of supported propyl amine in the different experiments and the results are summarised in Table 4.5.

Figure 4.3 shows conversion vs time data for experiments performed to determine the initial rate of the aldol reaction catalysed by the catalysts.



IS I

Figure 4.3. Dependence of catalytic activity in nitroaldol reaction on amine loading for the catalysts S3, S3.1, S3.2, S3.3 and S3.4.

The catalyst with 0.7 mmol of NH_2 showed the highest activity as 100% of benzaldehyde was converted to the final product. By increasing the amount of amine groups on the surface the activity decreases. This could be because the formation of multilayer on aminopropylsilane on the surface which mean that the grafted aminopropylsilane are more than the available surface of the support (as seen in chapter 3).

Turn over frequency (TOF) was calculated for all studied catalysts by using the rate of reaction where the rate of the reaction can be estimated by applying the First-order kinetic model as shown in Figure 4.4, on the basis that the kinetics are first order in benzaldehyde and, with nitromethane in excess, can be described as pseudo first order overall.

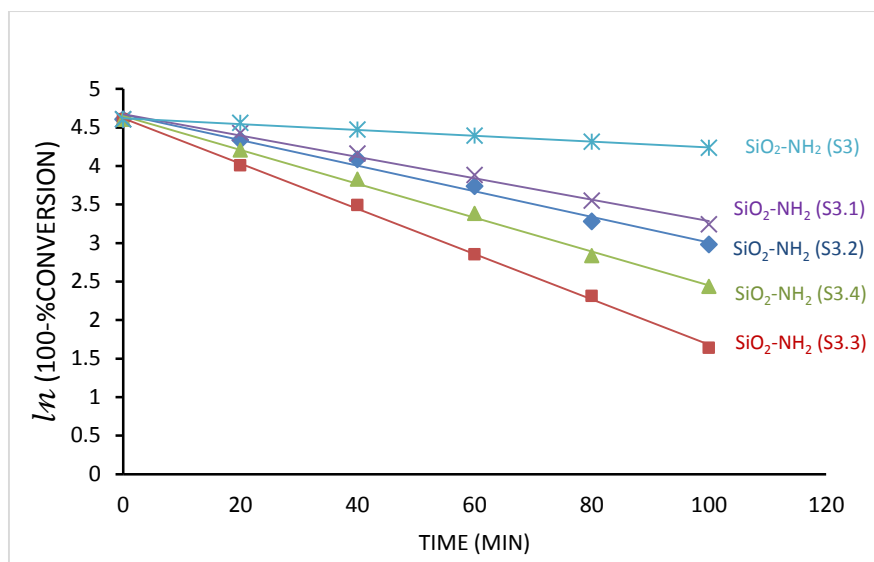


Figure 4.4. First-order plots for the aldol reaction for different functionalised silica catalysts (APTMS).

From data shown in Figure 4.4, it appears clear that the linear fittings are good for all catalysts in our reaction conditions as R^2 is close to 1.0. The intercept for all regression lines is approximately 4.6. These data were then analysed using the linear regression and the results are used to estimate the rate of the reaction and turn over frequency (TOF) and the results can be seen in Table 4.5.

Table 4.5. Turnover frequencies for studied silica-supported catalysts with surface amine concentrations (Estimated by back titration) and other morphological data

Samples	BET surface area (m ² /g)		Amine Concentration (measured) (mmol/g) (NH ₂)	(Theoretical Surface Coverage) ^a (m ² /g)	Theoretical Surface Coverage (%)	Linear regression Equation of the first order rate	TOF (h ⁻¹) ^b
	Raw	Grafted					
SiO ₂ -NH ₂ (S3)	199	77	2.0	602	303	y = -0.0038x + 4.6204 R ² = 0.9949	2.7 +/- 0.14
SiO ₂ -NH ₂ (S3.1)	199	160	1.3	391	196	y = -0.0139x + 4.6723 R ² = 0.9918	10.2 +/- 0.51
SiO ₂ -NH ₂ (S3.2)	199	162	1.1	331	166	y = -0.0166x + 4.6698 R ² = 0.99	12.2 +/- 0.61
SiO ₂ -NH ₂ (S3.3)	199	169	0.7	211	103	y = -0.0294x + 4.6207 R ² = 0.9989	21.6 +/- 1.10
SiO ₂ -NH ₂ (S3.4)	199	183	0.5	151	76	y = -0.022x + 4.6488 R ² = 0.9967	16.1 +/- 0.82

(a) Area occupied by amine at 0.50 nm² per molecule, (b) confidence limits on TOF +/- 0.05

For each catalyst the percentage of the available surface of the silica support that is functionalised has been calculated based on the assumption that each aminopropylsilane group occupies an area of 0.50 nm^2 . This is the area that has been reported to be occupied by three tethering groups bound to three adjacent silanol groups on the surface^{19,20}. It turns out that, on this basis, an amine loading of about 0.7 mmol g^{-1} corresponds to the amount of functionalisation that would cover the 211 m^2 on a single gram of support. The nominal area that each of the amine loadings would require for complete monolayer coverage is calculated and appears in Table 4.5. The TOF values for each catalyst are then plotted against the theoretical “% coverage” assuming monolayer formation in Figure 4.5 the support according to the standard BET method.

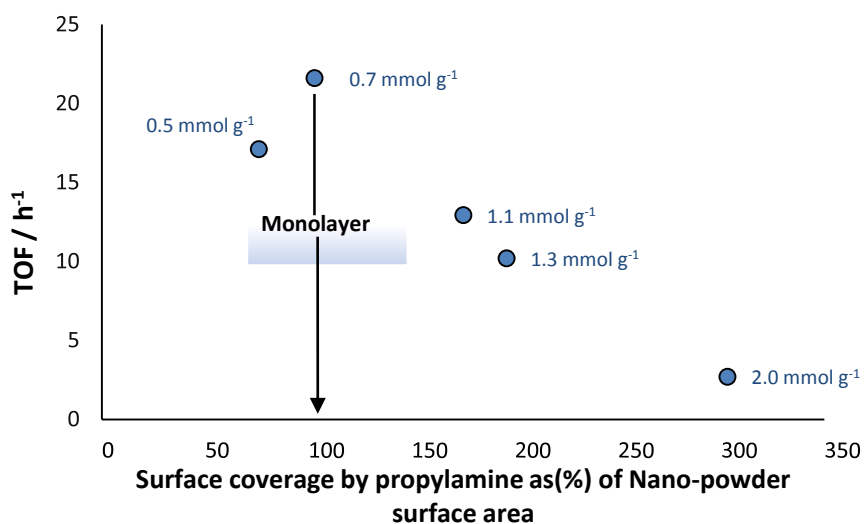


Figure 4.5. Theoretical are occupied by functional group as % of area of Nano-powder support.

As stated above the highest specific catalytic activity was obtained at a level of functionalization corresponding to 100% coverage, in which the amount of APTMS was calculated to completely cover the support surface in a monolayer (~100% surface coverage). The catalyst with the surface coverages higher than this show progressively lower activity, which suggests that the formation of multilayers of functional molecules reduces activity. It looks like even the catalysts with lower amount of propylamine groups with lower surface coverage also show reduced TOF. This reduced activity of amine groups may result from the protonation of some amine groups on the surface with silanols groups. It is known that aminopropylsilane prefer to lay on the surface if there is available space as shown in Figure 4.6.

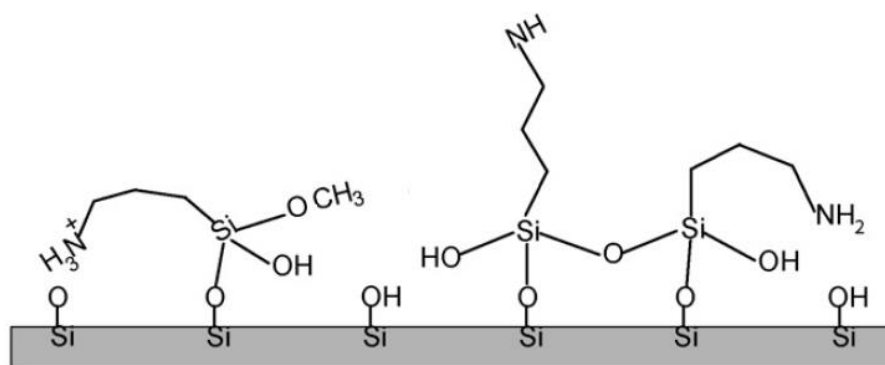


Figure 4.6. Schematic representation of grafted APTMS on silica surface with the possibility of amine protonation.

4.3.3. Characterisation of studied (EP10X) SiO_2-NH_2 (S1) base catalysts

The results obtained section 4.3.1 showed that the most active catalyst was the catalyst with 100% surface coverage of aminopropylsilane groups.

To confirm this result we used another silica support (EP10X) SiO_2-NH_2 (S1) and estimated the amount of amino propyl needed to cover 100% support surface (Calculate the theoretical amount of aminopropyl on the silica surface, see appendix B). Other catalysts was also prepared with aminopropylsilane groups content higher or lower than the amount needed for 100% surface coverage for comparison. The catalyst with 100% surface coverage is SiO_2-NH_2 (S1.2). The catalysts are labelled S1, S1.1, S1.2, S1.3 and S1.4.

The surface areas were calculated according to the BET method and porosities determined using the BJH method. The results are listed in Table 4.6.

Table 4.6. Structural parameters for supported amine catalysts on silica EP10X

Samples	BET surface area (m^2/g)		Average pore size /(nm)		Average pore volume /(cm ³ /g)	
	Raw	Grafted	Raw	Grafted	Raw	Grafted
SiO_2-NH_2 (S1)	290	230	17.25	15.91	1.57	1.27
SiO_2-NH_2 (S1.1)	290	219	17.25	14.96	1.57	1.06
SiO_2-NH_2 (S1.2)	290	257	17.25	17.17	1.57	1.55
SiO_2-NH_2 (S1.3)	290	267	17.25	17.20	1.57	1.53
SiO_2-NH_2 (S1.4)	290	284	17.25	17.15	1.57	1.56

The average uncertainty for these measurements is approximately +/- 5% for surface area, 2% for average pore size and 0.2% for pore volume

From Table 4.6, it is clear that all samples are mesoporous (pore sizes 17 nm). All silica supports show type V isotherms before and after grafting the amine groups, which indicates the presence of mesoporous, as shown in Figure 4.7.

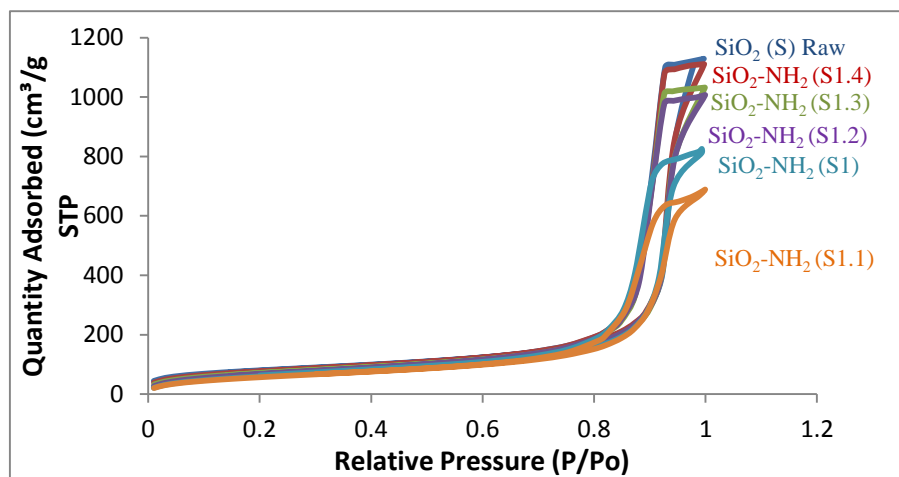


Figure 4.7. N₂ adsorption–desorption isotherms for silica support and grafted amine-silica support (S1)

The amine loadings of the catalysts was estimated by back titration and the surface coverage was calculated in the same way as before on the basis that one aminopropylsilane group covers approximately 0.50 nm² (Table 4.7).

Table 4.7. Measured amine concentration and their surface coverage on studied silica supports.

Types of base catalysts	Amine concentration (mmol/g) ^a	(Surface Coverage) Area occupied by amine at 0.50 nm ² per molecule (m ² /g)
SiO ₂ -NH ₂ (S1)	1.6	481
SiO ₂ -NH ₂ (S1.1)	1.9	571
SiO ₂ -NH ₂ (S1.2)	1.0	301
SiO ₂ -NH ₂ (S1.3)	0.9	271
SiO ₂ -NH ₂ (S1.4)	0.6	181

(a) Estimated by back titration and all values are to +/- 0.1 mmol g⁻¹

Similar to those catalysts based on the silica EP10X, increasing the level of functionalization in silica EP10X leads to a decrease in the surface area (Figure 4.8), quite possibly as a result of some pore filling or pore blocking.

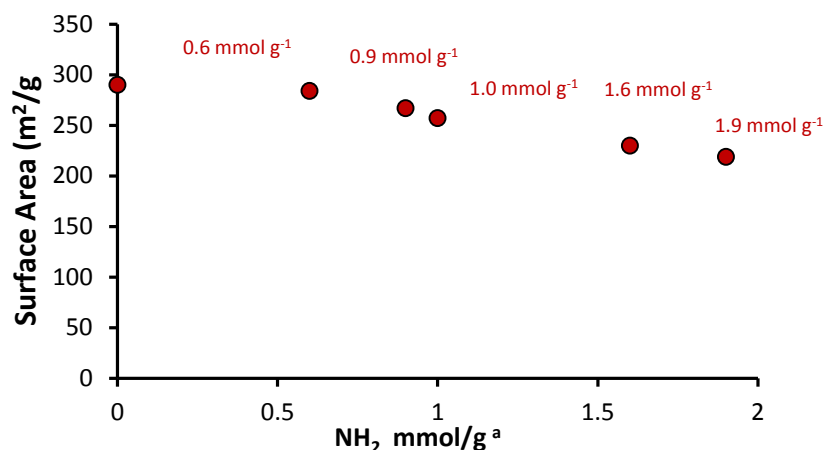


Figure 4.8. Surface area vs. amine loading for amine supported on EP10X

4.3.4. Catalytic activity of studied EP10X (S1) base catalysts

The conversions of benzaldehyde in the nitroaldol test reaction over the various catalysts were studied where the amount of the catalyst utilized in each experiment was carefully determined on the basis of the loading value in order to introduce the same supported propyl amine equivalents in the different experiments.

Figure 4.9 shows a typical kinetic data.

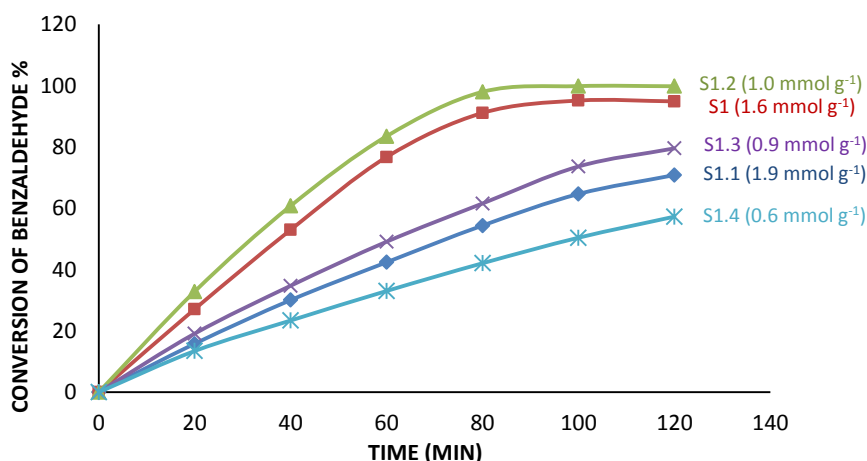


Figure 4.9. Dependence of catalytic activity in nitroaldol reaction on amine loading for silica EP10X supported amine catalysts.

As shown in Figure 4.9, the catalyst with 1.0 mmol of NH₂ showed the highest activity with both higher and lower loadings resulting in reduced activities. This data was treated as first order in benzaldehyde and on the assumption that nitromethane was in excess. Applying pseudo first order kinetics (Figure 4.10) rate constants were determined and turnover frequencies calculated at time zero (Table 4.8).

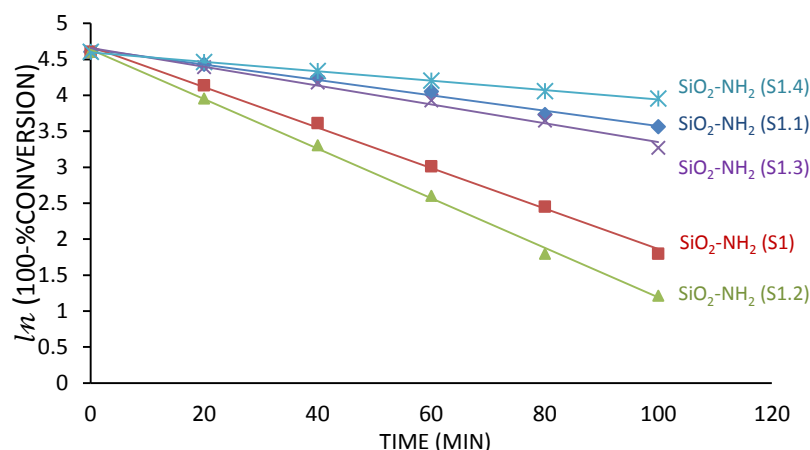


Figure 4.10. First-order kinetic model of aldol reaction for different functionalised silica (APTMS).

From data shown in Figure 4.10, it appears that the linear fittings are good for all catalysts in our reaction conditions. These data were then analysed using the linear regression and the results are used to estimate the rate of the reaction and turn over frequency (TOF) at time zero and the results can be seen in Table 4.8.

Table 4.8. The change of the activity with the surface coverage.

Samples	BET surface area (m ² /g)		Amine concentration (mmol/g)	(Theoretical Surface Coverage) ^a (m ² /g)	Theoretical Surface Coverage (%)	Linear regression Equation of the first order rate	TOF (h ⁻¹) ^b
	Raw	Grafted					
SiO ₂ -NH ₂ (S1)	290	230	1.6	481	166	y = -0.0281x + 4.6756 R ² = 0.9974	21 +/- 1.07
SiO ₂ -NH ₂ (S1.1)	290	219	1.9	572	197	y = -0.0107x + 4.6416 R ² = 0.99	7.8 +/- 0.40
SiO ₂ -NH ₂ (S1.2)	290	257	1.0	301	105	y = -0.0345x + 4.6363 R ² = 0.9986	25 +/- 1.25
SiO ₂ -NH ₂ (S1.3)	290	267	0.9	271	90	y = -0.0131x + 4.658 R ² = 0.9873	9.6 +/- 0.48
SiO ₂ -NH ₂ (S1.4)	1290	284	0.6	181	62	y = -0.0066x + 4.598 R ² = 0.9986	4.8 +/- 0.24

(a) Area occupied by amine at 0.50 nm² per molecule (b) confidence limits on TOF +/- 0.05

As shown in Table 4.8, the highest activity was obtained when the nominal surface coverage by catalytic groups was 301 m²/g which is very close (within 3%) to the surface area of the support (290 m²/g). Other catalysts showed lower activities as their surface coverage results

were lower or higher than the original surface area of the support. The catalytic activity vs nominal (theoretical) surface coverage is shown in Figure 4.11.

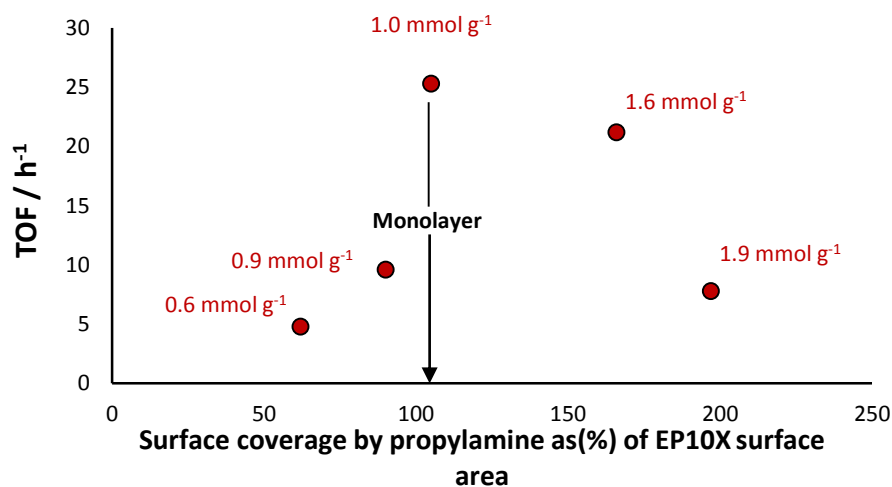


Figure 4.11. TOF for amine supported on EP10X in the nitroaldol reaction vs the nominal (theoretical) % of the surface of the silica functionalised.

Generally, the results showed that higher catalytic activity can be obtained by controlling the quantity of aminopropylsilane groups on silica support surface and the optimum loading can be calculated prior to synthesis. However many other aspects need to be understood such as the condition of the grafting reaction (temperature and stirring power), solvent type (polar vs. nonpolar) and the crystal structure (ordered vs. amorphous).

4.3.5. Discussion of monolayer optimisation:

According to the data in section (4.3.1) and section (4.3.3), it is clear that monolayer of aminopropylsilane coverage of a silica support can be obtained by carefully matching the surface coverage of each aminopropylsilane group with the support surface. It seems that more or less than 100% coverage of aminopropylsilane leads to form less active catalyst as mentioned earlier. Although nano-powder silica (S3) and EP10X (S1) silica were optimised to give here highest catalytic activity, EP10X (S1) showed higher activity than nano-powder silica (S3) when both catalysts have 100% coverage of aminopropyl groups. This results showed that activity is not only dependent on amine groups but there could be other factors coming from the support, such as the physical properties: surface area, pore size and pore volume, in line with previous reports,^{12, 21-23} the effects of which have not been investigated in this work.

4.4. Conclusion

Different silica gel supports with various surface characteristics were studied before and after functionalization with aminopropylsilane groups.

The catalytic activities showed a level of dependency on surface area, amount of active sites, pore size and pore volume.

However, one of the key variables to affect the catalytic activity was the surface coverage.

The highest specific catalytic activity was obtained at a level of functionalization corresponding to the saturation of the support surface with a single layer of functional groups.

It is concluded that loading a support above this maximum value results in a rapid decrease in activity. This approach, in which optimum loadings can be calculated, can be applied to other support materials.

4.5. References

1. T. Yokoi, T. Karouji, S. Ohta, J. N. Kondo and T. Tatsumi, *Chemistry of Materials*, 2010, **22**, 3900-3908.
2. M. Ferré, R. Pleixats, M. W. C. Man and X. Cattoën, *Green Chemistry*, 2016.
3. X. Zhao, G. Lu, A. Whittaker, G. Millar and H. Zhu, *The Journal of Physical Chemistry B*, 1997, **101**, 6525-6531.
4. Z. A. ALothman, *Materials*, 2012, **5**, 2874-2902.
5. A. Stein, B. J. Melde and R. C. Schrodin, *Advanced Materials*, 2000, **12**, 1403-1419.
6. Y. Huang, 2009.
7. Y. Mori and T. J. Pinnavaia, *Chemistry of materials*, 2001, **13**, 2173-2178.
8. M. H. Lim and A. Stein, *Chemistry of Materials*, 1999, **11**, 3285-3295.
9. T. Yokoi, H. Yoshitake and T. Tatsumi, *Journal of Materials Chemistry*, 2004, **14**, 951-957.
10. T. Yokoi, Y. Kubota and T. Tatsumi, *Applied Catalysis A: General*, 2012, **421**, 14-37.
11. M. Kruk, T. Asefa, M. Jaroniec and G. A. Ozin, *Journal of the American Chemical Society*, 2002, **124**, 6383-6392.
12. T. S. Zemanian, G. E. Fryxell, J. Liu, S. Mattigod, J. A. Franz and Z. Nie, *Langmuir*, 2001, **17**, 8172-8177.
13. M. Benaglia, Recoverable and recyclable catalysts, *Wiley Online Library*, 2009.
14. H. Salmio and D. Brühwiler, *The Journal of Physical Chemistry C*, 2007, **111**, 923-929.
15. A. N. Kursunlu, E. Guler, H. Dumrul, O. Kocyigit and I. H. Gubbuk, *Applied Surface Science*, 2009, **255**, 8798-8803.
16. A. G. Prado and C. Airolti, *Journal of colloid and interface science*, 2001, **236**, 161-165.
17. S. Brunauer, P. H. Emmett and E. Teller, *Journal of the American chemical society*, 1938, **60**, 309-319.
18. R. Denoyel, M. Barrande and I. Beurroies, *Studies in surface science and catalysis*, 2007, **160**, 33-40.
19. M. Etienne and A. Walcarius, *Talanta*, 2003, **59**, 1173-1188.
20. E. F. Vansant, P. Van Der Voort and K. C. Vrancken, Characterization and chemical modification of the silica surface, Elsevier, 1995.

CHAPTER 4

- 21 E. L. Margelefsky, R. K. Zeidan and M. E. Davis, *Chemical Society Reviews*, 2008, **37**, 1118-1126.
22. S. L. Hruby and B. H. Shanks, *Journal of Catalysis*, 2009, **263**, 181-188.
- 23 I. G. Shenderovich, G. Buntkowsky, A. Schreiber, E. Gedat, S. Sharif, J. Albrecht, N. S. Golubev, G. H. Findenegg and H.-H. Limbach, *The Journal of Physical Chemistry B*, 2003, **107**, 11924-11939

Chapter 5

EFFECT OF DIFFERENT AMINOPROPYLETHOXY SILANES WITH DIFFERENT GEOMETRICAL STRUCTURE AND THEIR EFFECT ON CATALYTIC ACTIVITY.

5.1. Introduction

The introduction of reactive organic groups into the pores of mesoporous silica is generally considered one of the important methods to prepare mesoporous catalysts. Among the mesoporous catalysts, amino-functionalized mesoporous materials heterogeneous catalysts have received growing interest.¹

Organosilanes are the reagents of choice for stable and reliable functionalization of most organic supports. Aminopropylalkoxysilanes are widely used as coupling agents and among the most commonly used precursors for the modification of silica surfaces due to their bifunctional (alkoxy and amino groups) nature and low cost.²

Aminopropylalkoxysilane (and some analogues) are water-miscible and make the functionalized supports hydrophilic.³ Their applications in aqueous media have been developed at a rapid pace because of the increasing relevance of surface chemistry to environmental sciences.^{3,4}

The three most widely used and studied aminosilanes are (3-aminopropyl) triethoxysilane (APTES), 3-Aminopropyl(diethoxy)methylsilane(APDEMS), 3-(Ethoxydimethylsilyl)propylamine. (APDMES). Due to the presence of a single alkoxy moiety (usually methoxy or ethoxy) in each aminopropylalkoxysilanes molecule, its reaction with surface hydroxyl groups is easier to control and should result in amine functionalized monolayers.^{4,5}

There are several conditions to deposition of aminopropylalkoxysilane such as reaction temperature, nature of the aminosilane (mono-, di-, or trialkoxy), silane concentration, incubation time, role of solvent, role of catalysts, postcuring,⁶ and, in particular, the amount of adsorbed water all affect the final structure of the adsorbed aminosilane layer.^{6,7}

The control of the distribution of functional groups on mesoporous silica is essential for applications of these materials in various fields including catalysis.⁸

The introduction of functional groups by grafting to mesoporous material is a versatile modification method, as the desired pore-size distribution, pore system dimensionality, particle size, and particle morphology can be obtained in a straightforward manner. However, the control of the functional-group distribution poses a particular challenge.⁹

In the previous chapter, a detailed study of the effect of the loading amount of aminopropylsilane on two silica supports was carried out by varying the amount of APTMS in the reaction medium (toluene) to obtain different surface coverage. On the basis that the fractional coverage of the silica surface by catalytically active groups is key to controlling overall catalytic activity in base-catalysed reactions, a series of different tethering aminosilanes is studied here, differing in the number and type of alkoxy groups that are on the silica atom and are available for condensation with surface silanol groups. It was stated in the previous chapter that when a trialkoxysilane compound such as (3-aminopropyl)trimethoxysilane is used, then each tethering compound occupies about 0.50 nm^2 ^{10,11} on the surface. The rationale of the work described here is that silanes with fewer than three alkoxy groups would still be able to react with the surface but would not take up as much surface per molecule, and this would allow more functional groups to populate the surface without having to exhibit multilayer functionalization, which it appears could be responsible for reduced specific activity at high coverages. The compounds used here are shown in Figure 5.3.

Although they are not the most reactive organosilanes, the methoxysilanes and ethoxysilanes are the most widely used organofunctional silanes for surface modification. 3-Aminopropyl(diethoxy)methylsilane (APDEMS) and 3-(Ethoxydimethylsilyl)propylamine (APDMES) are only available with ethoxy group in the market therefore from this chapter most of the work will be done with precursors containing ethoxy groups instead of methoxy groups. Therefore a comparison between (3-aminopropyl)trimethoxysilane and (3-aminopropyl)triethoxysilane, should illustrate the effect of increasing the size of the alkoxy group. Since this largely condenses and is lost as the associated alcohol, it might be expected to influence the ultimate packing of functional groups on the surface.

3-Aminopropyl(diethoxy)methylsilane and 3-(Ethoxydimethylsilyl)propylamine, exhibit two (rather than three) and one alkoxy group that can take part in the tethering reaction, so would more realistically be expected to affect the way the tethered amines can pack on the silica surface.

In this work two forms of silica are used. They have been chosen to represent extreme forms of the support. One is an amorphous silica gel, EP10X, chosen as a representative silica gel with porosity centred in the large mesoporous range. The second is very different and is the mesoporous molecular sieve SBA-15.

SBA-15 is a mesoporous silica sieve based on uniform hexagonal pores with a narrow pore size distribution and a tunable pore diameter of between 5 and 15 nm. The high internal surface area of typically 400–900 m²/g makes SBA-15 a well suited material for various applications.¹² It will be used as a support material, which can exhibit different intrinsic acidity or basicity and this would certainly add more about the role the surface plays in helping or hindering the activity of the supported amine groups.

Catalytic activities have been assessed using the following base-catalysed reactions; nitroaldol condensation between nitromethane and benzaldehyde to afford nitrostyrene (Figure 5.1).

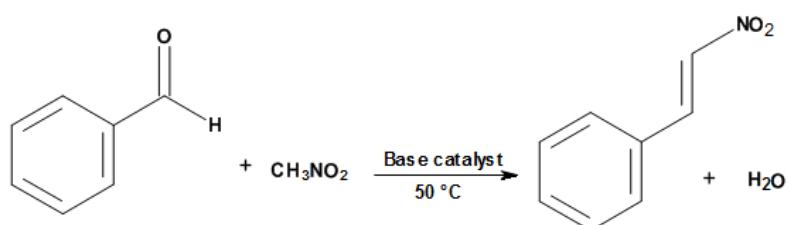


Figure 5.1. Henry reaction (nitroaldol reaction).

The Knoevenagel condensation reaction, between benzaldehyde and ethyl cyanoacetate in the presence of the toluene as the solvent to form ethyl 2-cyano-3-phenylacrylate (Figure 5.2). The mechanism of Knoevenagel reaction is similar to the mechanism of Henry reaction therefore, the same behaviour is expected for the catalysts with respect to the activity.

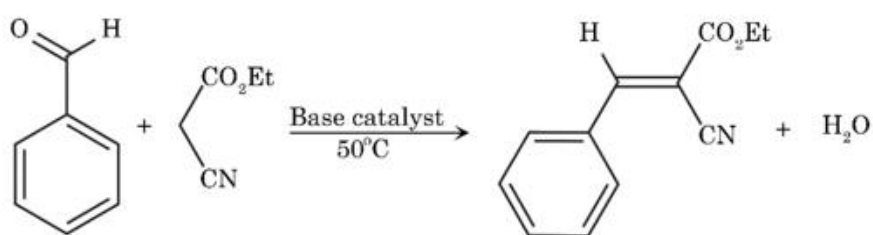


Figure 5.2. Knoevenagel condensation reaction.

5.2. Experimental and techniques

5.2.1. Materials

Different aminopropylalkoxysilanes were used for surface modification. Several types of aminopropylalkoxysilanes with interesting properties are commercially available (Figure 1). The purpose of the first part of this work was to compare the grafting behaviour of these silanes. (3-Amino-propyl)trimethoxysilane (APTMS), (3-Amino-propyl)triethoxysilane (APTES), 3-aminopropyl(diethoxy)methylsilane (APDEMS), 3-(Ethoxydimethylsilyl)propylamine (APDMES), dry toluene, o-xylene, nitromethane, and ethanol 99.5% were purchased from Sigma Aldrich and benzaldehyde was purchased from Acros and HCl at 37% was purchased from Fischer. Deionized water was used in all experiments.

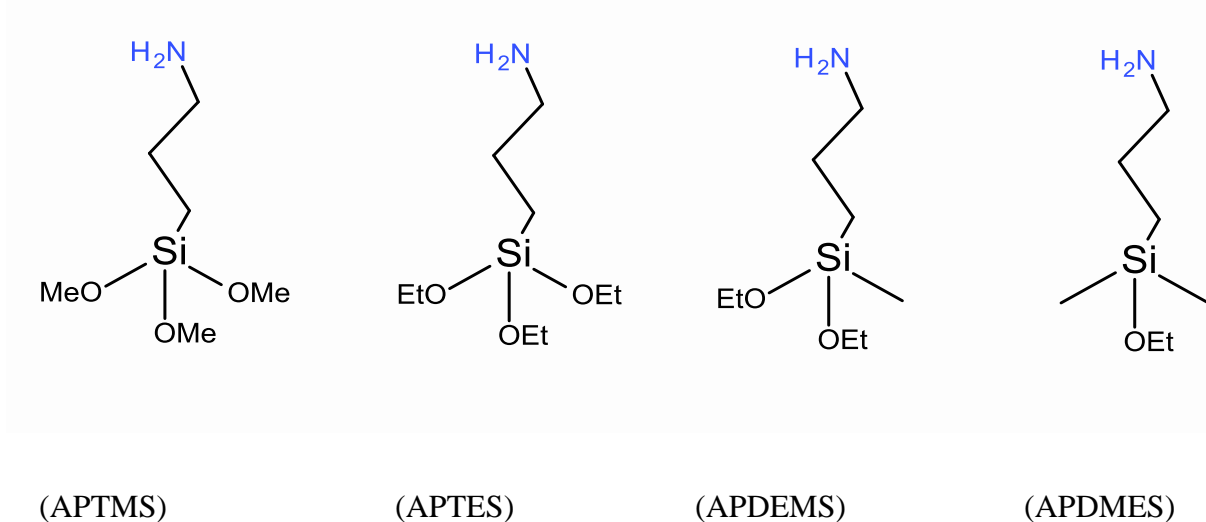


Figure 5.3. Chemical structures and abbreviations of the silanes studied in this report.

Table 5.1. Mesoporous silica supports used in this study (both from commercial suppliers).

EP10X Silica (INEOS Silicas)	SBA-15 (Glantreo Ltd)
Average surface area = 290 m ² /g	Average surface area = 557 m ² /g
Average pore volume = 1.57 cm ³ /g	Average pore volume = 0.85 cm ³ /g
Average pore size = 17.25 nm	Average pore size = 6.3 nm

5.2.2. Activation of silica supports

Silica gel was treated by acid where 30.0 g of raw silica support was refluxed in 150 ml stock HCl (37%) for 4 h at 100 °C to generate silanols groups on the surface and dissolve any metal impurities which could be active in the reactions. The activated silica support was washed in copious amounts of distilled water to remove all acid residues before being dried for 24 h.¹³

5.2.3. Synthesis of solid base catalysts with (3-aminopropyl)trimethoxysilane (APTMS)

A sample of 5 g of activated silica gel was suspended in 50 ml dry toluene, and 1.0 ml (3-aminopropyl)trimethoxysilane was added to this suspension. The mixture was refluxed in nitrogen atmosphere for 72 h at 110 °C and the modified silica gel was filtered off, washed with toluene and dried for 24 h.¹⁴ The materials labelled SiO₂-NH₂. Similar materials were prepared by same method with 1.0, 1.6 and 1.9 mmol g⁻¹ of (3-aminopropyl)trimethoxysilane. The materials are named SiO₂-NH₂ (S1.2), SiO₂-NH₂ (S1) and SiO₂-NH₂ (S1.1) respectively.

5.2.4. Synthesis of solid base catalysts with (3-aminopropyl)triethoxysilane (APTES)

A sample of 5 g of activated silica gel was suspended in 50 ml dry toluene, and 1.0 ml (3-aminopropyl) trimethoxysilane was added to this suspension. The mixture was refluxed in nitrogen atmosphere for 72 h at 110 °C and the modified silica gel was filtered off, washed with toluene and dried for 24 h.¹⁴ The materials labelled SiO₂-NH₂ (T) which is meaning 3-aminopropyltriethoxysilane. Similar materials were prepared by same method with 1.5, 1.0, 1.3, 0.5, and 1.88 mmol g⁻¹ of (3-aminopropyl) triethoxysilane. The materials are named SiO₂-NH₂ (T1), SiO₂-NH₂ (T2), SiO₂-NH₂ (T3), SiO₂-NH₂ (T4) and SiO₂-NH₂ (T5) respectively.

5.2.5. Synthesis of solid base catalysts with (3-aminopropyl)-diethoxymethylsilane (APDEMS)

A sample of 1 gm of activated silica gel was suspended in 50 ml dry toluene, and 1 ml (3-aminopropyl)-diethoxymethylsilane was added to this suspension. The mixture was treated as above and the material is labelled SiO₂-NH₂ (D) which is meaning Diethoxysilane. Similar materials were prepared by same method with 1.3, 1.0, 1.2, and 0.8 mmol g⁻¹ of (3-aminopropyl)-diethoxymethylsilane. The materials are named SiO₂-NH₂ (D1), SiO₂-NH₂ (D2), SiO₂-NH₂ (D3) and SiO₂-NH₂ (D4) respectively.

5.2.6. Synthesis of solid base catalysts with 3-(Ethoxydimethylsilyl)propylamine (APDMES).

A sample of 1.0 g of activated silica gel was suspended in 50 ml dry toluene, and 1 ml (3-aminopropyl) dimethylethoxysilane was added to this suspension. The mixture was treated as above and the material is labelled SiO₂-NH₂ (M) which is meaning Monoethoxysilane. Similar materials were prepared by same method with 1.3, 1.0, 0.8, and 0.6 mmolg⁻¹ of (3-aminopropyl)-dimethylethoxysilane. The materials are named SiO₂-NH₂ (M1), SiO₂-NH₂ (M2), SiO₂-NH₂ (M3) and SiO₂-NH₂ (M4) respectively.

5.2.7. Synthesis of base ordered mesoporous silica (SBA-15-NH₂)

A sample of 2.5 g of activated SBA-15 was suspended in 50 ml dry toluene, and 1.0 ml (3-aminopropyl)triethoxysilane was added to this suspension. The mixture was refluxed in nitrogen atmosphere for 72 h at 110 °C and the modified silica was filtered off, washed with toluene and dried for 24 h. The material is labelled SBA-15-NH₂ (T1). Similar materials were prepared by same method with 1.5, 1.0, 0.8, 0.5 and 2.0 mmolg⁻¹ of (3-aminopropyl)triethoxysilane. The catalysts have been named according to type and amount of amine used in each catalyst, as follows: SBA-15-NH₂ (T1), SBA-15-NH₂ (T2), SBA-15-NH₂ (T3), SBA-15-NH₂ (T4) and SBA-15-NH₂ (T5) respectively. The catalysts are summarised in Table 5.2

Table 5.2. Catalysts have been used in this chapter are shown with shorthand names, type of support and amount of amine that were used.

Names of catalysts	Type of Support	Type of Amine	Amount of Amine (mmol/g) (-NH ₂) ^a
SiO ₂ -NH ₂ (T1)	EP10X	(3-Aminopropyl)triethoxysilane (APTES)	1.5
SiO ₂ -NH ₂ (T2)	EP10X	(3-Aminopropyl)triethoxysilane (APTES)	1.0
SiO ₂ -NH ₂ (T3)	EP10X	(3-Aminopropyl)triethoxysilane (APTES)	1.3
SiO ₂ -NH ₂ (T4)	EP10X	(3-Aminopropyl)triethoxysilane (APTES)	0.5
SiO ₂ -NH ₂ (T5)	EP10X	(3-Aminopropyl)triethoxysilane (APTES)	1.9
SiO ₂ -NH ₂ (D1)	EP10X	3-Aminopropyl(diethoxy)methylsilane (APDEMS)	1.3
SiO ₂ -NH ₂ (D2)	EP10X	3-Aminopropyl(diethoxy)methylsilane (APDEMS)	1.0
SiO ₂ -NH ₂ (D3)	EP10X	3-Aminopropyl(diethoxy)methylsilane (APDEMS)	1.2
SiO ₂ -NH ₂ (D4)	EP10X	3-Aminopropyl(diethoxy)methylsilane (APDEMS)	0.8
SiO ₂ -NH ₂ (M1)	EP10X	3-(Ethoxydimethylsilyl)propylamine (APDMES)	1.3
SiO ₂ -NH ₂ (M2)	EP10X	3-(Ethoxydimethylsilyl)propylamine (APDMES)	1.0
SiO ₂ -NH ₂ (M3)	EP10X	3-(Ethoxydimethylsilyl)propylamine (APDMES)	0.8
SiO ₂ -NH ₂ (M4)	EP10X	3-(Ethoxydimethylsilyl)propylamine (APDMES)	0.6
SiO ₂ -NH ₂ (T1)	SBA-15	(3-Aminopropyl)triethoxysilane (APTES)	1.5
SiO ₂ -NH ₂ (T2)	SBA-15	(3-Aminopropyl)triethoxysilane (APTES)	1.0
SiO ₂ -NH ₂ (T3)	SBA-15	(3-Aminopropyl)triethoxysilane (APTES)	0.8
SiO ₂ -NH ₂ (T4)	SBA-15	(3-Aminopropyl)triethoxysilane (APTES)	0.5
SiO ₂ -NH ₂ (T5)	SBA-15	(3-Aminopropyl)triethoxysilane (APTES)	2.0
SiO ₂ -NH ₂ (S1)	EP10X	(3-Aminopropyl)trimethoxysilane (APTMS)	1.6
SiO ₂ -NH ₂ (S1.1)	EP10X	(3-Aminopropyl)trimethoxysilane (APTMS)	1.9
SiO ₂ -NH ₂ (S1.2)	EP10X	(3-Aminopropyl)trimethoxysilane (APTMS)	1.0

(a)Estimated by back titration and each value represents the average of three repeats (all values are to +/- 0.1 mmol g⁻¹)

5.2.8. Catalyst characterization:

Nitrogen adsorption–desorption isotherms were measured at 77 K on a Micrometrics ASAP-2020 after evacuation at 423 K for 5 h. The surface area was calculated using the BET method as before¹⁵. BJH analysis, based on the Kelvin equation (see chapter 2) was applied to the desorption branch for the mesopore and small macropore size range to give pore size distributions, average pore diameters and pore volumes.^{15, 16}

Levels of functionalization were assessed by two methods. The first method was via nitrogen, carbon and hydrogen elemental analysis (MEDAC Ltd), which provided the total amount of amine groups on the surface.

The second method was aqueous back titration, where a sample of 100 mg of base catalyst was stirred in 20 ml 0.0100 mol dm³ HCl solution for 4 hr. Then 10 ml of the supernatant solution was extracted and added to 10 ml distilled water and then titrated with 0.0100 mol dm³ of NaOH solutions using phenolphthalein indicator.

This method was used to estimate the number of reactive amine groups on the surface.

5.2.9. Catalytic activity measurement:

5.2.9.1. Henry reaction:

Catalysts were activated before use under static air at 120 °C for 2 h. A mixture of benzaldehyde (0.1 ml), nitromethane (5 ml) and *o*-xylene as internal standard (0.1 ml) were kept at 70 °C under an atmosphere of nitrogen and magnetic stirring for 30 min. After that, 50 mg of the selected catalyst was added to the mixture to start the reaction. The reaction mixture was then stirred under an atmosphere of nitrogen and aliquots of the sample mixture were removed with a filter syringe. The samples were stored at 0 °C in an ice bath and analysed by a calibrated gas chromatography-flame ionisation detector (GC-FID) as soon as possible (invariably within minutes of extraction). The final product was fully identified by GC-MS.

5.2.9.2. Knoevenagel condensation reaction

Catalysts were activated before use under static air oven at 120 °C for 2 h. A mixture of 5 mmol (0.53 g) benzaldehyde, 5 mmol ethyl cyanoacetate (0.50 g) 10 mL toluene as the solvent and *o*-xylene as internal standard (0.1 ml) were kept at 50 °C under an atmosphere of nitrogen and magnetic stirring for 30 min. After that, 50 mg of the selected catalyst was added to the mixture to start the reaction. The reaction mixture was then stirred under an atmosphere of nitrogen and aliquots of the sample mixture were removed with a filter syringe and analysed by a calibrated gas chromatography-flame ionisation detector (GC-FID). The final product was fully identified by GC-MS.

5.3. Results and discussion:

5.3.1. Characterisation of studied base catalysts

Silica (EP10X) support was functionalised using the amino silane reagents APTMS, APTES, APDEMS and APDMES. Their surface areas, pore diameters and pore volume of the samples distribution before and after grafting were characterized by N₂ adsorption-desorption experiments. This data appears in Table 5.3. It was observed that all samples showed type IV isotherms, characteristic of mesoporous structures. In comparison with the original support (raw), the surface area, pore size, and pore volume of the functional materials decrease as might be expected, consistent with the incorporation of organoamine groups into the framework of EP10X and SBA-15 supports.

To simplify the data presentation and the discussion, the catalysts are classified according to type of amino group grafted as shown in Table 5.3.

Table 5.3. Textural parameters for supported base catalysts. Note the numbers represent the relative levels at which the supports have been functionalised.

Types of base catalysts	Surface Area (m ² /g)		Pore Size (nm)		Pore Volume (cm ³ /g)	
	Raw	Grafted	Raw	Grafted	Raw	Grafted
SiO ₂ -NH ₂ (T1)	290	213	17.25	15.79	1.57	1.19
SiO ₂ -NH ₂ (T2)	290	233	17.25	17.00	1.57	1.50
SiO ₂ -NH ₂ (T3)	290	264	17.25	17.08	1.57	1.50
SiO ₂ -NH ₂ (T4)	290	269	17.25	17.10	1.57	1.53
SiO ₂ -NH ₂ (T5)	290	280	17.25	17.02	1.57	1.55
SiO ₂ -NH ₂ (D1)	290	212	17.25	17.00	1.57	1.30
SiO ₂ -NH ₂ (D2)	290	220	17.25	17.12	1.57	1.42
SiO ₂ -NH ₂ (D3)	290	239	17.25	17.02	1.57	1.50
SiO ₂ -NH ₂ (D4)	290	249	17.25	17.09	1.57	1.47
SiO ₂ -NH ₂ (M1)	290	172	17.25	17.08	1.57	1.11
SiO ₂ -NH ₂ (M2)	290	193	17.25	17.17	1.57	1.31
SiO ₂ -NH ₂ (M3)	290	218	17.25	17.00	1.57	1.40
SiO ₂ -NH ₂ (M4)	290	249	17.25	17.17	1.57	1.38
SBA-15-NH ₂ (T1)	557	218	6.37	5.48	0.85	0.41
SBA-15-NH ₂ (T2)	557	230	6.37	6.02	0.85	0.75
SBA-15-NH ₂ (T3)	557	388	6.37	5.93	0.85	0.60
SBA-15-NH ₂ (T4)	557	397	6.37	6.20	0.85	0.65
SBA-15-NH ₂ (T5)	557	462	6.37	6.04	0.85	0.80
SiO ₂ -NH ₂ (S1)	290	230	17.25	15.91	1.57	1.27
SiO ₂ -NH ₂ (S1.1)	290	219	17.25	14.96	1.57	1.06
SiO ₂ -NH ₂ (S1.2)	290	257	17.25	17.17	1.57	1.55

The average uncertainty for these measurements is approximately +/- 5% for surface area, 2% for average pore size and 0.2% for pore volume.

5.3.2. Quantification of aminopropyl groups on studied catalysts

The basicity of grafted amine-silica supports was estimated by the back titration method. The results are summarised in Table 5.4.

Table 5.4. Concentration of amine on silica supports estimated by back titration.

Samples	Amine concentration (mmol/g) ^a
SiO ₂ -NH ₂ (T1)	1.5
SiO ₂ -NH ₂ (T2)	1.0
SiO ₂ -NH ₂ (T3)	1.3
SiO ₂ -NH ₂ (T4)	0.5
SiO ₂ -NH ₂ (T5)	1.9
SiO ₂ -NH ₂ (D1)	1.3
SiO ₂ -NH ₂ (D2)	1.0
SiO ₂ -NH ₂ (D3)	1.2
SiO ₂ -NH ₂ (D4)	0.8
SiO ₂ -NH ₂ (M1)	1.3
SiO ₂ -NH ₂ (M2)	1.0
SiO ₂ -NH ₂ (M3)	0.8
SiO ₂ -NH ₂ (M4)	0.6
SBA-15-NH ₂ (T1)	1.5
SBA-15-NH ₂ (T2)	1.0
SBA-15-NH ₂ (T3)	0.8
SBA-15-NH ₂ (T4)	0.5
SBA-15-NH ₂ (T5)	2.0
SiO ₂ -NH ₂ (S1)	1.6
SiO ₂ -NH ₂ (S1.1)	1.9
SiO ₂ -NH ₂ (S1.2)	1.0

(a) all values are to +/- 0.1 mmol g⁻¹

Elemental analysis was only carried out on a selection of the catalysts, mainly as a check on the valued determined by back titration. Results for three representative catalysts appear in Table 5.5, showing nitrogen and carbon % w/w values. Nitrogen content reflects the amine content and the carbon content, or more specifically the molar ratio of carbon to nitrogen, can be used to identify the way in which the functional group is bound to the silica surface.

$$C_{\text{NH}_2} = (\text{N}\% / 14.0) \times 10 \text{ mmol g}^{-1}$$

(Equation 1)

Table 5.5. Elemental analysis data for three samples of functionalised silica EP10X.

Samples	N% w/w	N, mmol/g	C% w/w	C, mmol/g	C/N
SiO₂-NH₂ (T3)	1.93	1.3	5.1	4.3	3.0
SiO₂-NH₂ (D3)	1.58	1.1	6.3	5.3	4.8
SiO₂-NH₂ (M3)	1.06	0.75	4.8	4.0	5.3

(a) Each value represents the average of several repeats +/- 0.1.

As shown in table 5.5. The ratio between carbons to nitrogen for SiO₂-NH₂ (**T3**) of 3.0 is consistent with the loss of the three ethyl groups when ethoxy groups condense (leaving just the three propyl carbons per amine nitrogen). This is important because it means we can be confident that trialkoxy silane tethers do indeed bind through all three tethering groups. The value of 4.8 on the SiO₂-NH₂ (**D3**) is higher than expected (C:N would be 4:1 if the single methyl group remained unreacted but both ethoxy groups had condensed). The value of 5.3 for the dimethylethoxysilane (**M3**) tether suggests that there are about five carbon atoms remaining on each tether once bound to the surface, absolutely consistent with binding through the only alkoxy group on the original silane.

Table 5.6. The number of active sites on silica EP10 supports estimated by back titration and confirmed by elemental analysis.

Base catalysts	Number of active sites (mmol g ⁻¹)	
	By titration (NH ₂ /mmol g ⁻¹)	By elemental analysis (NH ₂ /mmol g ⁻¹) ¹
SiO ₂ -NH ₂ (T3)	1.3	1.3
SiO ₂ -NH ₂ (D3)	1.2	1.1
SiO ₂ -NH ₂ (M3)	0.8	0.75

In Table 5.6, the concentrations of amine groups determined by back titration and by elemental analysis are shown. It is clear that, within experimental error, values from the two methods are in agreement.

5.3.3. Catalytic activities of studied base catalysts

All synthesised catalysts were studied in the nitroaldol condensation reaction between nitromethane and benzaldehyde to produce nitrostyrene. The conversion of benzaldehyde was plotted against the time of reaction. Benzaldehyde is the limiting reagent and the reaction is expected to be first order with respect to this reagent.

5.3.3.1. A comparison between three catalysts made using EP10X and (3-aminopropyl) triethoxysilane (APTES) and three made using (3-aminopropyl) trimethoxysilane (APTMS) (ie “Ethoxy vs. Methoxy”)

The activity of EP10X-NH₂ catalysts made from (3-aminopropyl) triethoxysilane and (3-aminopropyl) trimethoxysilane were studied in order to investigate the effect of precursor leaving group (ethyl vs methyl) on the final coverage level and activity of the catalysts.

Figure 5.4 shows benzaldehyde conversion against time for the EP10X-NH₂ catalysts made from (3-aminopropyl) triethoxysilane and (3-aminopropyl) trimethoxysilane activity in the nitroaldol reaction. It is important to point out that in the reactions, the amount of each catalyst added to the reaction was calculated to obtain equal number of active sites in all reactions.

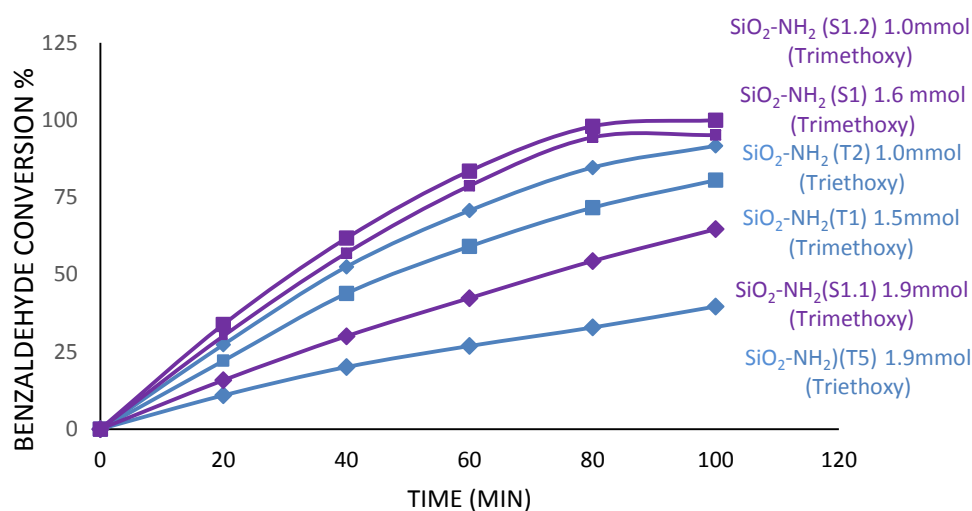


Figure 5.4. Kinetic data for the reaction of nitromethane with benzaldehyde in the presence of o-xylene over (T1), (T2), (T5), (S1), (S1.1) and (S1.2)

As shown in figure 5.4 the catalysts made from trimethoxysilanes are more active than those made from triethoxysilanes. It should be remembered that these conversion data are all for the same amine loadings so rates are all specific rates (effectively per amine group). The result is very surprising because, of course, there is no residue of the ethoxy or methoxy groups in the catalysts as used so they might be expected to be the same, regardless of the precursor.

A possible explanation is that the bulky precursor triethoxy is unable to access quite the same number of surface sites as the smaller trimethoxy precursor so the ultimate distribution of active sites on the silica surface might be rather different, especially in small pores where the triethoxy precursor might be precluded from reacting. Therefore, the catalyst produced with aminotrimethoxysilane has a more even distribution of amine groups over the surface

It is possibly worth mentioning another factor here that is related to the relative reactivity of methoxysilanes and ethoxysilanes, although in the catalysts used in these experiments it does appear that, with both the 3-aminopropyltrimethoxysilane and 3-aminopropyltriethoxysilane reaction between the three alkoxy groups and surface silanols was complete in both cases. It is however a fact that methoxysilanes are generally more reactive than ethoxysilanes because ethoxysilanes are more bulky than the corresponding methoxysilanes. The methoxysilanes are capable of reacting with substrates under dry, aprotic conditions, while the less reactive ethoxysilanes require specific conditions for suitable reactivity. The low toxicity of ethanol as a by-product of the reaction favours the ethoxysilanes in many commercial applications. So if it were the case that some of the 3-aminopropyltriethoxysilane ethoxy groups remained unreacted and therefore hanging off the tether groups, these unreacted bulky ethoxy groups could hinder the diffusion of reactants to active sites compared to methoxy groups.

In Table 5.7 the catalytic activities of the six catalysts used is quantified. Initial rates have been converted to turnover frequencies, based on the amine contents of the catalysts.

Table 5.7. Turnover frequency (TOF) and the amine contents of the catalysts used to generate the data in Figure 5.3.

Samples	Amine concentration (NH ₂ /mmol g ⁻¹) ^a	TOF (h ⁻¹) ^b 1 st Order Kinetics
SiO ₂ -NH ₂ (S1)	1.6	21.2 +/- 1.07
SiO ₂ -NH ₂ (S1.1)	1.9	7.8 +/- 0.40
SiO ₂ -NH ₂ (S1.2)	1.0	25 +/- 1.25
SiO ₂ -NH ₂ (T1)	1.5	8.8 +/- 0.44
SiO ₂ -NH ₂ (T2)	1.0	20 +/- 1.0
SiO ₂ -NH ₂ (T5)	1.9	3.6 +/- 0.18

(a) Estimated by back titration, (b) confidence limits on TOF values were +/-5%

The level of amine groups on support was essentially the same for both methoxysilane and ethoxysilane precursors despite of the fact that methoxysilanes react faster than ethoxysilanes but this could be due to the long reaction time (72 h) and the fixed amount of precursor in the reaction medium. The TOF values vary a great deal. With both types of tethering precursor the TOF falls with increasing amine loading. In work reported earlier in the thesis the TOF goes through a maximum at amine loading of typically 1.0 mmol g⁻¹. The catalysts studied here all have loadings of 1.0 or more mmol g⁻¹ so it is quite possible that they too go through a maximum and the values at 1.0 mmol g⁻¹ are close to those maxima.

5.3.3.2. The effect of amine loading on EP10X using (3-aminopropyl)triethoxysilane (i.e. T1, T2, T3, T4 and T5)

The conversions of benzaldehyde with the time with catalysts with different loading of amine groups on the support surface are shown in Figure 5.5.

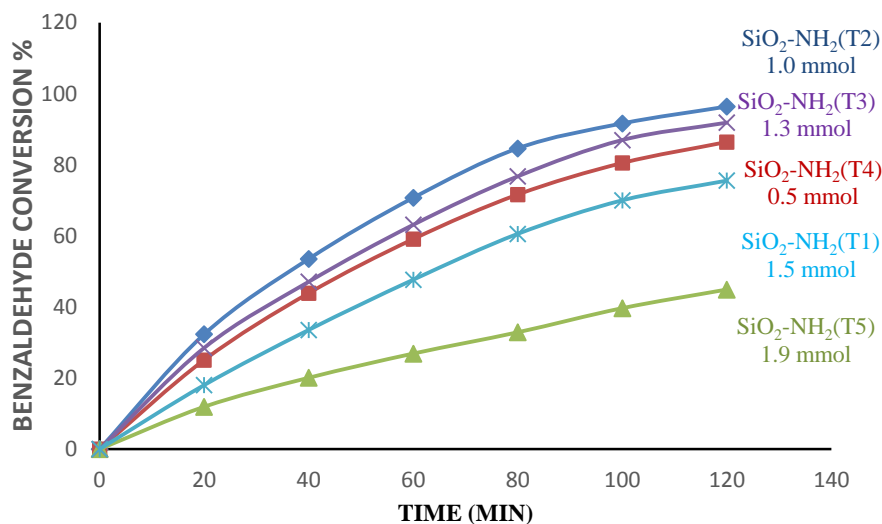


Figure 5.5. Activity of SiO₂-NH₂ in nitroaldol reaction at 50 °C.

Turnover frequencies and rate constants from this data, taken from initial rates at time zero, appear in Table 5.8.

Table 5.8. Amine loading, first order rate constants and TOF values for the SiO₂-NH₂ (T series) catalysts.

Samples	Amine concentration (mmol/g) (-NH ₂) ^a	1 st order rate constant (k /h ⁻¹)	TOF (h ⁻¹) ^b 1 st Order Kinetics
SiO ₂ -NH ₂ (T1)	1.5	0.012	8.8 +/- 0.45
SiO ₂ -NH ₂ (T2)	1.0	0.027	20 +/- 1.0
SiO ₂ -NH ₂ (T3)	1.3	0.021	15 +/- 0.75
SiO ₂ -NH ₂ (T4)	0.5	0.017	12 +/- 0.60
SiO ₂ -NH ₂ (T5)	1.9	0.005	3.6 +/- 0.18

(a)Estimated by back titration, (b) confidence limits on TOF +/-5%

As shown in Table 5.8, the activity increases with increasing loading to a certain concentration then it falls. This phenomenon has been seen and described in chapters 3, 4 and possible explanations have been put forward. The highest catalytic activity was obtained at a level of

functionalization corresponding to saturation of the surface with a single layer of functional groups then decreases as the organoamine loading amount increase. This lower activity might be as result of multilayer formation of aminopropylsilane on the silica support surface.

5.3.3.3. The effect of amine loading on EP10X using (3-aminopropyl) diethoxymethylsilane (i.e. D1, D2, D3 and D4)

Data is shown in Figure 5.6 and initial rate constants and TOF values are given in Table 5.9.

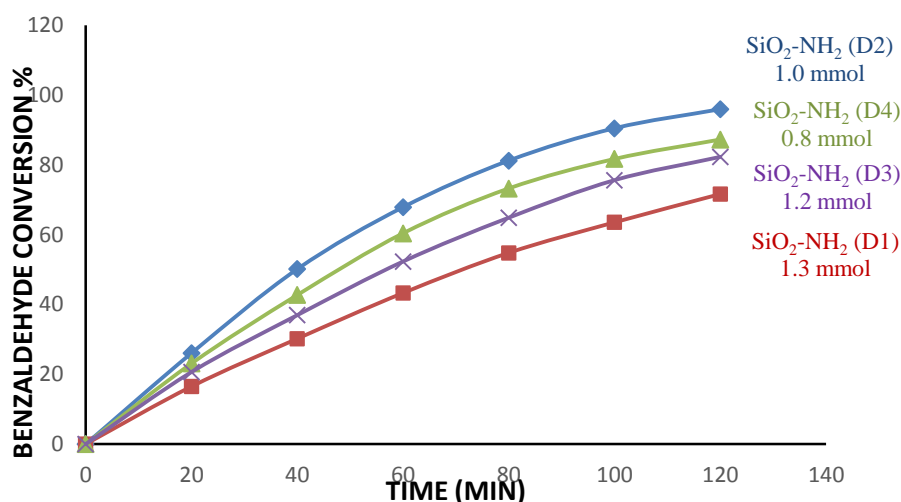


Figure 5.6. Activity of SiO₂-NH₂ in nitroaldol reaction at 50 °C.

Table 5.9. Turnover frequencies with surface amine concentrations for the SiO₂-NH₂ (D series) catalysts. The TOF was used to judge the activity of the catalysts and the basicity of the catalysts was estimated by back titration.

Samples	Amine concentration (mmol/g) (-NH ₂) ^a	1 st order rate constant (k /h ⁻¹)	TOF (h ⁻¹) ^b 1 st Order Kinetics
SiO ₂ -NH ₂ (D1)	1.3	0.010	7.4 +/- 0.37
SiO ₂ -NH ₂ (D2)	1.0	0.023	17.1 +/- 0.86
SiO ₂ -NH ₂ (D3)	1.2	0.014	10.2 +/- 0.51
SiO ₂ -NH ₂ (D4)	0.8	0.017	12.6 +/- 0.64

(a) Estimated by back titration, (b) confidence limits on TOF +/-5%

Again, a maximum in activity is seen at around 1.0 mmol g⁻¹. Similar behaviour was observed for all the catalysts in this work.

5.3.3.4. The effect of amine loading on EP10X using (3-Aminopropyl) dimethylethoxysilane (i.e. M1, M2, M3 and M4)

The conversion of benzaldehyde with the time at different loading of amine groups on the support surface is shown in Figure 5.7.

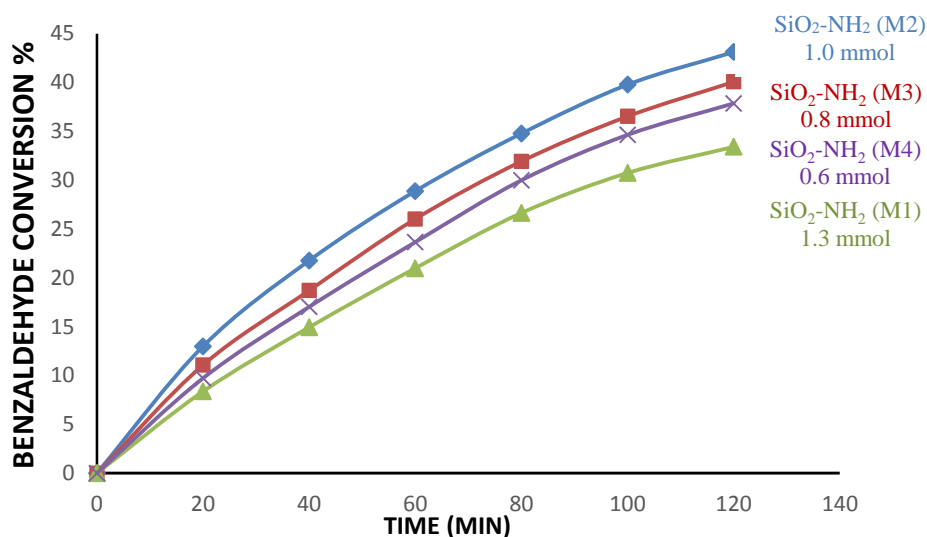


Figure 5.7. Activity of SiO₂-NH₂ in nitroaldol reaction at 50 °C.

Turn over frequency (TOF) was then calculated for all studied catalysts by using the rate of reaction where the rate of the reaction can be estimated by applying the second-order kinetic model.

Table 5.10. Amine loading, first order rate constants and TOF values for the SiO₂-NH₂ (M series) catalysts. The TOF was used to judge the activity of the catalysts and the basicity of the catalysts was estimated by back titration.

Samples	Amine concentration (mmol/g) (-NH ₂) ^a	1 st order rate constant (k /h ⁻¹)	TOF (h ⁻¹) ^b 1 st Order Kinetics
SiO ₂ -NH ₂ (M1)	1.3	0.006	4.4 +/- 0.22
SiO ₂ -NH ₂ (M2)	1.0	0.01	7.3 +/- 0.37
SiO ₂ -NH ₂ (M3)	0.8	0.009	6.6 +/- 0.33
SiO ₂ -NH ₂ (M4)	0.6	0.007	5.1 +/- 0.26

(a) Estimated by back titration, (b) confidence limits on TOF +/-5%

These catalysts show similar behaviour as other catalysts. The catalytic activities reach its maximum at a certain number of active sites. However comparisons between all the catalysts are present in section.

5.3.3.5. The effect of amine loading on SBA-15 using (3-aminopropyl)triethoxysilane (i.e. T1, T2, T3, T4 and T5)

The conversion of benzaldehyde with the time at different loading of amine groups on the support surface is shown in Figure 5.8.

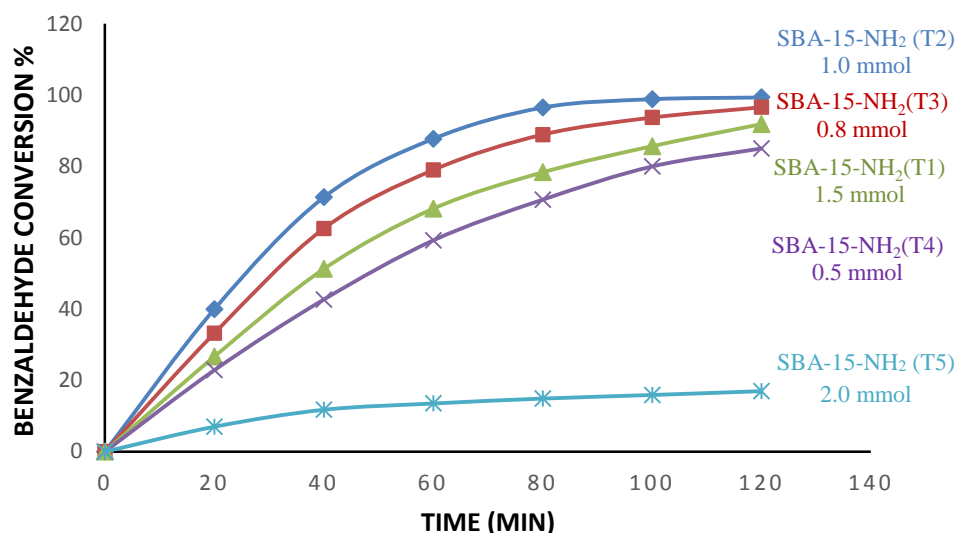


Figure 5.8. Activity of SiO₂-NH₂ in nitroaldol reaction at 50 °C.

Turn over frequency (TOF) was then calculated for all studied catalysts by using the rate of reaction where the rate of the reaction can be estimated by applying the second-order kinetic model.

Table 5.11. Turn over frequency was calculated for each catalyst with a number of active sites.

Samples	Amine concentration (mmol/g) (-NH ₂) ^a	1 st order rate constant (k /h ⁻¹)	TOF (h ⁻¹) ^b 1 st Order Kinetics
SBA-15-NH ₂ (T1)	1.5	0.021	15.2 +/- 0.76
SBA-15-NH ₂ (T2)	1.0	0.041	30.4 +/- 1.52
SBA-15-NH ₂ (T3)	0.8	0.028	21 +/- 1.07
SBA-15-NH ₂ (T4)	0.5	0.016	11.9 +/- 0.60
SBA-15-NH ₂ (T5)	2.0	0.0018	1.3 +/- 0.07

(a) Estimated by back titration, (b) confidence limits on TOF +/-5%

The catalysts prepared using the ordered mesoporous molecular sieve support show very high activities compared to all other catalysts with the non-ordered mesoporous support. The catalytic activity reach its maximum when the concentration of amine groups on the surface is again about 1.0 mmol g⁻¹

5.3.3.6. Comparison between the activities of SiO₂-NH₂ (T), SiO₂-NH₂ (D) and SiO₂-NH₂ (M), SBA-15-NH₂ (T) with different amine loadings in the nitroaldol reaction

In this section all the synthesised catalysts are compared with respect to their activities and the concentration of active sites (figure 5.9).

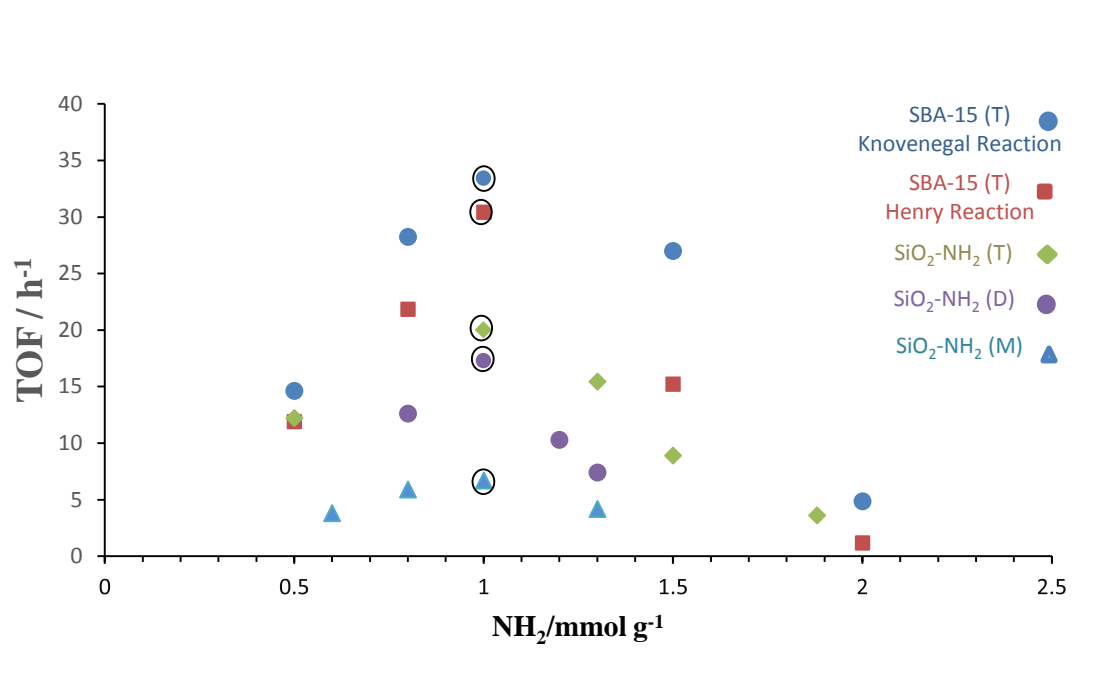


Figure 5.9. TOF as a function of the loading concentration of amine groups in all catalysts using the following base-catalysed reactions; nitroaldol reactions and Knoevenagel condensation reaction

There are several aspects of the data in Figure 5.9.

1. All the catalysts shown exhibit a strong dependence of specific activity (expressed as TOF) on amine loading, all exhibiting a clear loading that corresponds to maximum activity in the reaction between benzaldehyde and nitromethane.
2. The amine loading corresponding to maximum activity appears to be the same for all amine tethering groups, whether they bind via three, two or one oxygen bridge to the surface (trialkoxo, dialkoxo and monoalkoxo precursors).
3. The amine loading corresponding to maximum activity appears to be the same for the two silica supports, despite the fact that the two catalysts exhibit very different surface areas available for functionalisation.

4. Based on the SBA-15 catalysts, the amine loading corresponding to maximum activity appears to be the same for a second base-catalysed reaction. That is the Knoevenagel reaction between benzaldehyde and ethyl cyanoacetate.

5. The maximum activity of supported amines (at the optimum loading – in all cases around 1.0 mmol g^{-1}) varies a great deal, depending on the amine tether precursor, with the amines originating from 3-aminopropyltrialkoxysilanes and therefore held to the surface by three tethering groups, showing highest activity, followed by those held by “two” and then “one”.

6. The maximum activity (at optimum loading) is very much higher for the SBA-15 supported catalysts than for the amorphous silica supported catalysts. The surface area of SBA-15 is $557 \text{ m}^2 \text{ g}^{-1}$ compared to $299 \text{ m}^2 \text{ g}^{-1}$ for the silica EP10X.¹⁷

The explanation for all these observations are not obvious. It seems likely that the reason activity decreases at very high loadings might be because of multilayer functionalization as discussed in chapters 3 and 4 but why specific activity of amine groups should increase as loading increases at low loadings is less clear.

The higher activity of amine groups tethered by three, compared to two and one, group to the surface may be linked to steric factors in which the unbound ethyl group that remains bound to the silica on the functionalising group when it binds to the surface somehow impedes reaction or perhaps generates a hydrophobic region which is less reactive towards benzaldehyde and nitromethane.

The most surprising result is that for the loading corresponding to maximum activity. This is the same for both support materials and yet the activity of amines on SBA-15 are very much higher than on silica EP10X. It seems likely that there is some involvement of surface silanol groups in controlling activity but it is not clear how.

Although this optimum loading was observed in many of the studies, few researchers have attempted to offer explanation for it.^{8, 9, 24-26} Most authors relate catalytic activity to the available surface area and sometimes to pore volume;¹⁸⁻²⁰ however, some of the more recent investigations relate the catalytic performances to the synergetic catalytic effect of surface silanols with the introduced reactive groups, such as amines.²¹⁻²³ Therefore, as far as I am aware we are the first group related the catalytic activity with surface coverage for this type of catalysis.

5.4. Conclusion

In conclusion, eighteen amine functional mesoporous catalysts were synthesized with two different supports crystalline silica SBA-15 and amorphous silica EP10X. By adjusting the organoamine precursor or support dosage, the amine loading amount can be controlled. An optimum organoamine loading amount exists for each amine series catalysts. However, the optimum organoamine loading amount varies with the amine type and the area it takes from the surface, the surface area of the support and the crystal structure of the support. In case of ordered mesoporous silica SBA-15, the highest activity (TOF: 30.4 h^{-1}) was obtained with the catalyst contains 1.0 mmol of aminopropyltriethoxysilane while in case of amorphous mesoporous silica EP10X, the highest activity (TOF: 20.0 h^{-1}) obtained with the catalyst contains 1.0 mmol of aminopropyltriethoxysilane which prove that the order structure has increased the activity of the material 35 % higher than the amorphous structure. The reason for that could be the surface area available for the reaction after grafting which is larger in case of SBA-15 compared to EP10X when both have optimum loading.

The effect of grafting on surface area shows significant results. 60% of SBA-15 surface decreased with 1.5 mmol loading of aminopropyltriethoxysilane while only 25 % of EP10X surface decreased with same loading of aminopropyltriethoxysilane, we might expect that the pore blocking effect in case of SBA-15 as the pore size is 50% smaller than the pore size of EP10X. Pore volume change support this reason as in case of SBA-15 with 1.5 mmol loading, there was more than 50% pore volume reduction while only 25 % pore volume reduction in case of EP10X. This indicates that 25% more pores in case of SBA-15 completely blocked.

Finally, using 3-Aminopropyl(diethoxy)methylsilane and 3-(Ethoxydimethylsilyl)propylamine instead of (3-Amino-propyl)triethoxysilane had no effect on the optimum loading amount which was 1.0 mmol with the three precursors. However the turnover frequency decreased with decreasing the binding sites in the precursors (ethoxy groups). In case of the precursor with three ethoxy groups TOF was 20.0 h^{-1} while it decreased to 17.0 h^{-1} and 7.3 h^{-1} when diethoxy and monoethoxy precursors are used. Also surface area further decreased when three ethoxy precursor are replaced with the diethoxy and monoethoxy precursor which could explain the decrease in activity represented by TOF.

5.5. References

1. W. Lang, B. Su, Y. Guo and L. Chu, *Science China Chemistry*, 2012, **55**, 1167-1174.
2. P. Zucca and E. Sanjust, *Molecules*, 2014, **19**, 14139-14194.
3. Y.-P. Wang, K. Yuan, Q.-L. Li, L.-P. Wang, S.-J. Gu and X.-W. Pei, *Materials Letters*, 2005, **59**, 1736-1740.
4. E. Asenath Smith and W. Chen, *Langmuir*, 2008, **24**, 12405-12409.
5. A. Y. Fadeev and T. J. McCarthy, *Langmuir*, 2000, **16**, 7268-7274.
6. S. Naviroj, S. Culler, J. Koenig and H. Ishida, *Journal of colloid and interface science*, 1984, **97**, 308-317.
7. L. White and C. Tripp, *Journal of Colloid and Interface Science*, 2000, **232**, 400-407.
8. A. Taguchi and F. Schüth, *Microporous and mesoporous materials*, 2005, **77**, 1-45.
9. N. Gartmann and D. Brühwiler, *Angewandte Chemie International Edition*, 2009, **48**, 6354-6356.
10. M. Etienne and A. Walcarius, *Talanta*, 2003, **59**, 1173-1188.
11. E. F. Vansant, P. Van Der Voort and K. C. Vrancken, *Characterization and chemical modification of the silica surface*, Elsevier, 1995.
12. J. P. Thielemann, F. Girgsdies, R. Schlögl and C. Hess, *Beilstein journal of nanotechnology*, 2011, **2**, 110-118.
13. A. N. Kursunlu, E. Guler, H. Dumrul, O. Kocyigit and I. H. Gubbuk, *Applied Surface Science*, 2009, **255**, 8798-8803.
14. A. G. Prado and C. Airoidi, *Journal of colloid and interface science*, 2001, **236**, 161-165.
15. S. Brunauer, P. H. Emmett and E. Teller, *Journal of the American Chemical Society*, 1938, **60**, 309-319.
16. R. Denoyel, M. Barrande and I. Beurroies, in *Studies in Surface Science and Catalysis*, eds. F. R.-R. J. R. P.L. Llewellyn and N. Seaton, Elsevier, 2007, vol. Volume **160**, pp. 33-40.
17. Vizcaino, A.; Carrero, A.; Calles, J., *Proceedings of 16th World Hydrogen Energy*

Conference, Lyon, France, 2006.

- 18 Leofanti, G.; Padovan, M.; Tozzola, G.; Venturelli, B., *Catalysis Today* 1998, **41**, 207-219.
- 19 F. Fakhfakh, L. Baraket, A. Ghorbel, J. M. Fraile, C. I. Herrerías and J. A. Mayoral, *Journal of Molecular Catalysis A: Chemical*, 2010, **329**, 21-26.
- 20 W. Tang, Y. Deng, W. Li, J. Li, G. Liu, S. Li, X. Wu and Y. Chen, *Catalysis Science & Technology*, 2016, **6**, 1710-1718.
- 21 E. L. Margelefsky, R. K. Zeidan and M. E. Davis, *Chemical Society Reviews*, 2008, **37**, 1118-1126.
22. S. L. Hruby and B. H. Shanks, *Journal of Catalysis*, 2009, **263**, 181-188.
- 23 I. G. Shenderovich, G. Buntkowsky, A. Schreiber, E. Gedat, S. Sharif, J. Albrecht, N. S. Golubev, G. H. Findenegg and H.-H. Limbach, *The Journal of Physical Chemistry B*, 2003, **107**, 11924-11939.
- 24 Y. Mori and T. J. Pinnavaia, *Chemistry of materials*, 2001, **13**, 2173-2178.
25. M. H. Lim and A. Stein, *Chemistry of Materials*, 1999, **11**, 3285-3295.
26. T. Yokoi, H. Yoshitake and T. Tatsumi, *Journal of Materials Chemistry*, 2004, **14**, 951-957.

Chapter 6

EFFECT OF SILANOL GROUPS ON THE CATALYTIC ACTIVITIES OF SOLID BASE CATALYSTS.

The main goal in this chapter is to determine whether silanol groups can cooperatively participate in the key steps in base catalytic reactions.

6.1. Introduction

Mesoporous silicas have received widespread interest because of their potential applications in catalysis, separation, selective adsorption, novel functional materials, and for their use as hosts to confine guest molecules, due to their extremely high surface areas combined with large pore sizes.¹

The mesoporous silica support can be designed at will to improve the catalytic activity. Factors such as the pore size in meso structured materials, the hydrophilic and hydrophobic balance and the presence of surface silanol groups may indeed strongly influence the catalytic activity.²

There are two types of mesoporous silica: amorphous mesoporous silica and ordered mesoporous silica. Among the most frequently used ordered mesoporous silica-based materials have been the ordered hexagonal porosity labelled SBA-15 (Santa Barbara Amorphous type material) with a surface area and pore diameter of up to 1500 m²/g and 25 nm respectively.^{3,4}

Post-synthetic surface functionalization is usually carried out through grafting procedures, under anhydrous conditions. There are other strategies, for instance hydrosilylation⁵ which can also be used, but they are less common than surface grafting.⁶

The surface of the silica support can itself play a large role in the catalytic activity of heterogeneous catalysts. The weakly acidic silanol groups can form hydrogen bonds to reactants or transition states, leading to cooperative catalysis with surface organic groups.⁷ Weakly acidic silanol groups can act in concert with, for example, grafted amine groups.⁸ A synergistic acid-base catalytic mechanism has been proposed for aminopropyl-functionalized silica gel in the Henry reaction.⁹ The consequence is that the balance between the amount of amine and amount of free silanol groups needs to be considered when optimising catalytic activities.¹⁰ To investigate the effect of surface silanols as acidic sites and specifically the ability of silanol groups to activate the substrates in the reaction, several catalytic experiments have been carried out with heterogeneous catalysts whose surface silanols were capped with trimethylsilyl (TMS) groups to passivate them. The differences in activities between catalysts in which silanols are capped and uncapped gives an indication of the effects of the silanol groups on catalytic activity.¹¹ In this earlier work, additional comparison was made with free propylamine in homogeneous solution.⁸

Another aspect of the catalytic properties of silica-supported catalysts is the hydrophilic/hydrophobic nature of the catalyst. This too can be controlled to some extent by silylation of the free silanol groups and this has been studied by others.¹²

One of the most common silylation agents is trimethoxymethylsilane (TMMS) used to cap silanols and it makes the silica surfaces hydrophobic (Figure 6.1). This reagent is used in the work reported in this thesis to determine the effects of the silanols on the catalyst's activity. Other reagents, for instance, hexamethyldisilazane and chlorosilanes may also be used.^{13, 14}

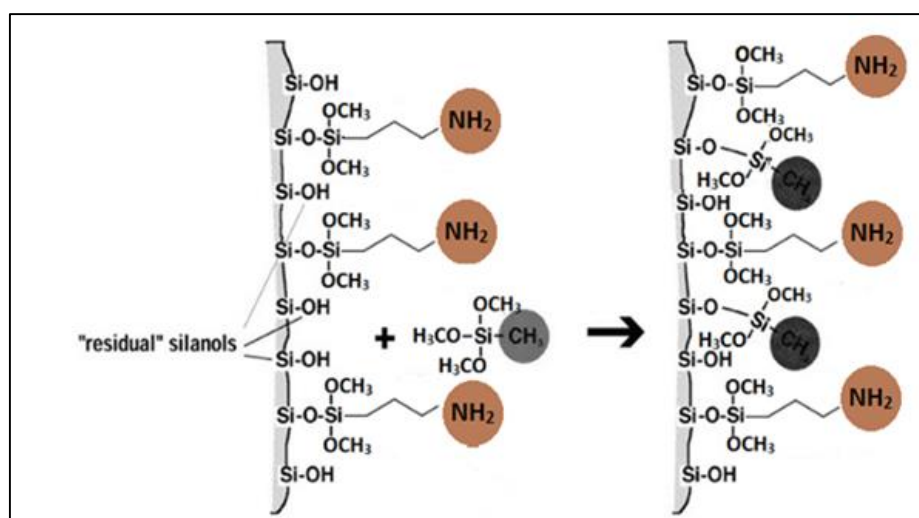


Figure 6.1. The silanol capping process with trimethoxymethylsilane.

The cooperative effect of silanol groups was thought to improve the catalytic activity of mesoporous silica-supported amines in base-catalysed reactions such as Michael addition, nitroaldol (Henry) condensation and Knoevenagel condensation.⁹

In a synthetic system, the principles of bifunctional cooperativity are demonstrated in the work of Katz and co-workers.¹⁵ They studied the synthesis of organoamine-functionalized silica gel catalysts that contain silanol groups, where bifunctional catalysts showed increase in performance and selectivity for the Michael and Henry reactions compared to the corresponding materials without silanols.

An important question over the potential role of silanol groups in these, fundamentally base-catalysed, reactions is whether the silanols are important because of the hydrophilicity they impart to the catalyst surface or whether they play a synergistic role in a cooperative acid-base catalytic mechanism.¹⁶ This is a question that is to be addressed in this chapter.

One way of probing this is to investigate the impact on activity of changing the polarity of the reaction solvent, and also to investigate the proposed cooperative effect for other reactions where reactants have different polarities. All along, an important comparison is between the catalytic activity the amine that is functionalised on the silica surface and the same amine used alone in homogeneous solution.⁸

A further approach still, that is useful in studying the role of weakly acidic silanol groups, is to change the support slightly so that the strength of the surface acid groups is changed slightly.¹⁰ Motokura *et al.*¹⁷ have demonstrated that this approach is actually possible. They used a silica–alumina support, which is more acidic than the silica, with aminopropyl groups, it is concluded that, the use of acidic silica-alumina as a support for basic amine catalyst enables coexistence of strong acid and base sites on the solid surface. The catalysts that have been prepared by silica-alumina possessed high catalytic activities compared to the catalysts obtained by using silica alone for various carbon-carbon bond-forming reactions.

Sharma *et al.*⁶ synthesized aminopropyl functionalized mesoporous silica prepared by the grafting technique using different amount of aminoorganosilanes. The Henry reaction of benzaldehyde and nitromethane was used to test the catalytic performances of the catalysts. They found the highest catalytic properties were obtained for samples containing an optimum number of grafted groups, 0.8-1.5 mmol g⁻¹ of grafted alkylamine, which was called the critical density of the grafted organic groups.

6.1.1. Specific objectives

In the work reported in this chapter the question of the effect of silanol on the activity of amine groups on the silica support is addressed. The approach taken has been to cap the silanol groups on the surface of the catalyst by using trimethoxymethylsilane (TMMS) and compare it with the uncapped catalyst. The possibility that the role of the silanol groups is nothing more than to control the hydrophilicity of the surface is also considered. This has been addressed in this work by modifying the reaction medium and the reactants from relatively polar to relatively non-polar, to enhance or suppress the simple importance of the silica surface polarity (which is to a large extent controlled by the presence of surface silanol groups). The idea is that, if the silanols do no more than assist in the adsorption of polar reactant to the surface, then their absence (brought about by capping) should have a greater effect on reactions involving polar reactants than on reactions that involve non-polar reactants. Also in this work the solid catalyst

was compared with analogue homogeneous catalyst and a mixture of homogeneous catalyst and silica support to study the effect of silica support.

In the work reported in this thesis, a contribution is made to the study of cooperative actions of supported alkylamine groups and surface silanol groups in setting the catalytic properties of amino-functionalized silicas. The catalysts have been tested in carbon-carbon coupling reactions. The first one is the aldol condensation reaction between 4-nitromethane and benzaldehyde to produce nitrostyrene.

The second test reaction is the Knoevenagel condensation reaction, between benzaldehyde and ethyl cyanoacetate in the presence of the toluene as the solvent to form ethyl 2-cyano-3-phenylacrylate (as mentioned in section 5.1 (chapter 5)).

6.2. Experimental

6.2.1. Materials

(3-Aminopropyl) trimethoxysilane (APTMS), (3-Aminopropyl) triethoxysilane (APTES), trimethoxymethylsilane (TMMS), dry toluene, o-xylene, nitromethane, nitroethane, nitropropane and ethanol 99.5%, were purchased from Sigma Aldrich and HCl at 37% was purchased from Fischer. Unless noted otherwise, all chemicals were at least 99% pure and used as received. Deionized water was used in all experiments.

Table 6.1. Silica supports used in this work ^a.

EP10X Silica (INEOS Silicas) ^a	SBA-15 (Glantreo Ltd) ^a
Average surface area = 290 m ² /g	Average surface area = 557 m ² /g
Average pore volume = 1.57 cm ³ /g	Average pore volume = 0.85 cm ³ /g
Average pore size = 17.2 nm	Average pore size = 6.3 nm

(a) Data supplied by manufactures

6.2.2. Activation of silica supports (EP10X, SBA-15)

Silica samples were treated by acid where 5.0 g of raw silica support was refluxed in 50 ml stock HCl (37%) for 4 h at 100 °C to generate silanols groups on the surface. The activated silica support was washed in copious amounts of distilled water to remove all acid residues before being dried for 24 h.¹⁸

6.2.3. Synthesis of solid base catalysts with APTMS (EP10X-NH₂)

A sample of 5 g of activated silica gel was suspended in 50 ml dry toluene, and (3-aminopropyl)trimethoxysilane was added to this suspension. The mixture was refluxed in nitrogen atmosphere for 72 h at 110 °C and the modified silica gel was filtered off, washed with toluene and dried for 24 h. The following amounts of APTMS were added to four separate 5 g amounts of silica: (1.65 ml, 1.89 mmol g⁻¹), (1.85 ml, 2.11 mmol g⁻¹), (0.84ml, 0.964 mmol g⁻¹) and (0.2 ml, 0.57 mmol g⁻¹). These amounts were chosen on the basis that, if they react fully, they would yield amine loadings on the supports of 1.6, 1.9, 1.0 and 0.6 mmol g⁻¹.

6.2.4. Synthesis of silylated mesoporous solid base catalysts (EP10X-NH₂-CH₃)

SiO₂-NH₂ (1g) was added to a dry toluene solution containing trimethoxymethylsilane (TMMS) (1.0 ml, 7mmol) and the solution left for 12 h at 110 °C under a nitrogen atmosphere. The solid was filtered and washed with dry toluene and dried in the oven at 120 °C for 24 h. The new material was named SiO₂- NH₂-CH₃ (Figure 6.1).

6.2.5. Synthesis of solid base catalysts on SBA-15 (SBA-15-NH₂)

A sample of 2.0 g of activated SBA-15 was suspended in 50 ml dry toluene, and (3-aminopropyl)triethoxysilane was added to this suspension. The mixture was refluxed in nitrogen atmosphere for 72 h at 110 °C and the modified silica was filtered off, washed with toluene and dried for 24 h. The material is labelled SBA-15-NH₂. The following amounts of APTES were added to four separate 2.0 g amounts of silica: (0.85 ml, 1.8 mmol⁻¹g), (0.5 ml, 1.06 mmol⁻¹g), (0.2 ml, 0.42 mmol⁻¹g) and 0.65 ml, 1.38 mmol⁻¹g). These amounts were chosen on the basis that, if they react fully, they would yield amine loadings on the supports of 1.5, 1.0, 0.5 and 1.3 mmol.

6.2.6. Synthesis of silylated base catalysts on SBA-15 (SBA-NH₂-CH₃)

SBA-NH₂ (1g) was added to a dry toluene solution containing trimethoxymethylsilane (TMMS) (1.0 ml, 7mmol) and the solution left for 12 h at 110 °C under a nitrogen atmosphere. The solid was filtered and washed with dry toluene and dried in the oven at 120 °C for 24 h. The new material was named SBA- NH₂-CH₃ (Figure 6.1).

Table 6.2. Catalysts have been used in this chapter are shown with shorthand names, type of support and amount of amine that were used.

Type of Silica Support EP10X			Type of Silica Support SBA-15		
Names of catalysts	Amine concentration (measured) (mmol/g) (NH ₂) ^a	Type of amine	Names of catalysts	Amine concentration (measured) (mmol/g)(NH ₂) ^a	Type of amine
SiO ₂ (S) (Raw)	-	-	SiO ₂ (T) (Raw)	-	-
SiO ₂ -NH ₂ (S1)	1.6	APTMS	SiO ₂ -NH ₂ (T1)	1.5	APTES
SiO ₂ -NH ₂ (S1.1)	1.9	APTMS	SiO ₂ -NH ₂ (T2)	1.0	APTES
SiO ₂ -NH ₂ (S1.2)	1.0	APTMS	SiO ₂ -NH ₂ (T4)	0.5	APTES
SiO ₂ -NH ₂ (S1.4)	0.6	APTMS	SiO ₂ -NH ₂ (T6)	1.3	APTES
SiO ₂ -NH ₂ -CH ₃ (S1-R)	1.6	APTMS+TMMS	SiO ₂ -NH ₂ -CH ₃ (T1-R)	1.5	APTES+TMMS
SiO ₂ -NH ₂ -CH ₃ (S1.1-R)	1.9	APTMS+TMMS	SiO ₂ -NH ₂ -CH ₃ (T2-R)	1.0	APTES+TMMS
SiO ₂ -NH ₂ -CH ₃ (S1.2-R)	1.0	APTMS+TMMS	SiO ₂ -NH ₂ -CH ₃ (T4-R)	0.5	APTES+TMMS
SiO ₂ -NH ₂ -CH ₃ (S1.4-R)	0.6	APTMS+TMMS	SiO ₂ -NH ₂ -CH ₃ (T6-R)	1.3	APTES+TMMS

(a) Estimated by back titration and each value represents the average of three repeats (all values are to +/- 0.1 mmol g⁻¹)

6.2.7. Catalyst characterization

Nitrogen adsorption–desorption isotherms were measured at 77 K on a Micromeritics ASAP-2020 after evacuation at 423 K for 5 h. The surface area was calculated using the BET method.¹⁹ BJH analysis was employed to determine pore size and specific pore volume using desorption data, .^{19, 20}

To investigate the hydrophilicity characteristics of the catalysts, they were tested by the Dynamic Vapour Sorption (DVS) technique where the catalyst was subjected to different levels of humidity (RH) between 0–95% at 25 °C. This determines the amount and rate of adsorption of a solvent by a sample. This gravimetric technique measures the change in mass as the concentration of vapour surrounding the sample is increased. Subsequently, isotherms are plotted.

Powder XRD patterns were recorded on a Bruker D-8 diffractometer using Cu K α radiation (1.5418 Å) at 40 kV and 20 mA. The patterns were collected over the range 1.5-10 2θ with a step size of 0.02 $^\circ$ at a scanning speed of 2 $^\circ$ per min.

Levels of functionalization were assessed by two methods as before, by nitrogen, carbon and hydrogen elemental analysis (MEDAC Ltd) and by back titration as described in section 2.9.1.

6.2.8. Catalytic activity measurement

6.2.8.1. Nitroaldol (Henry) reaction

Catalysts were ground in a pestle and mortar and then activated before use under static air at 120 $^\circ\text{C}$ for 2 h in still air. A mixture of benzaldehyde (0.1 ml), nitromethane (5 ml) and o-xylene as internal standard (0.1 ml) were kept at 50 $^\circ\text{C}$ under an atmosphere of nitrogen and magnetic stirring for 30 min. The reaction vessel was a 100 ml round bottom flask, fitted with a condenser and with a dry nitrogen feed. Temperature was controlled using an oil bath in which the flask was immersed on a hotplate controlled by a temperature probe immersed in the oil and feeding back to the hotplate. The activated catalyst was added to the reaction mixture and aliquots of the mixture were removed with a filter syringe at regular intervals. The filter ensured that reaction mixture was separated from catalyst at the time of extraction. The samples were stored at 0 $^\circ\text{C}$ in an ice bath and analysed by gas chromatography (FID, 25 m BPI column) which was calibrated previously (see appendix C). The final product was fully identified by GC-MS in advance of the experiments and it was established that nitrostyrene was the exclusive product. Kinetic data was henceforth reported in terms of the conversion of benzaldehyde, the limiting reagent. Pseudo first order kinetics were assumed as nitromethane was in large excess.

The same materials were tested with the nitroaldol reaction and the same conditions, but in this time nitroethane and nitropropane have been used instead of nitromethane in two different reactions, using the same molar amounts.

6.2.8.2. Homogeneous catalyst reaction

A homogeneous reaction was conducted by adding free APTMS (14.3 mg) and activated silica gel alone (50 mg) to a mixture of benzaldehyde (0.1 ml), nitromethane (5 ml) and o-xylene as internal standard (0.1 ml). The amount of APTMS used was chosen because it is equal to the amount of active sites on SiO $_2$ -NH $_2$ (S1.2) which is approximately 0.08 mmol $^{-1}$ /g. The reaction was kept at 50 $^\circ\text{C}$ under an atmosphere of nitrogen and magnetic stirring for 30 min. The

reaction mixture was then stirred under an atmosphere of nitrogen and 0.1 ml aliquots of the sample mixture were periodically removed with a filter syringe and analysed as above.

Another experiment was performed with SiO₂ (S) (Silica raw) only to ensure the inactivity of the support where 50 mg of SiO₂ (S) was added to Henry reaction and the reaction was monitored for 2 h.

6.2.8.3. Knoevenagel condensation reaction

Catalysts were activated before use under static air oven at 120 °C for 2 h. A mixture of 5 mmol (0.53 g) benzaldehyde, 5 mmol ethyl cyanoacetate (0.50 g) 10 mL toluene as the solvent and o-xylene as internal standard (0.1 ml) were kept at 50 °C under an atmosphere of nitrogen and magnetic stirring for 30 min. After that, 50 mg of the selected catalyst was added to the mixture to start the reaction. The reaction mixture was then stirred under an atmosphere of nitrogen and aliquots of the sample mixture were removed with a filter syringe and analysed as above. The final product was fully identified by GC-MS.

6.3. Results and discussion.

6.3.1. Characterisation of the base catalysts

6.3.1.1. Surface area and pore size determination by nitrogen porosimetry

The nitrogen adsorption–desorption isotherms at 77 K for S, S1.2, S1.2-R and T, T2, T2-R are shown in Figure 6.2.

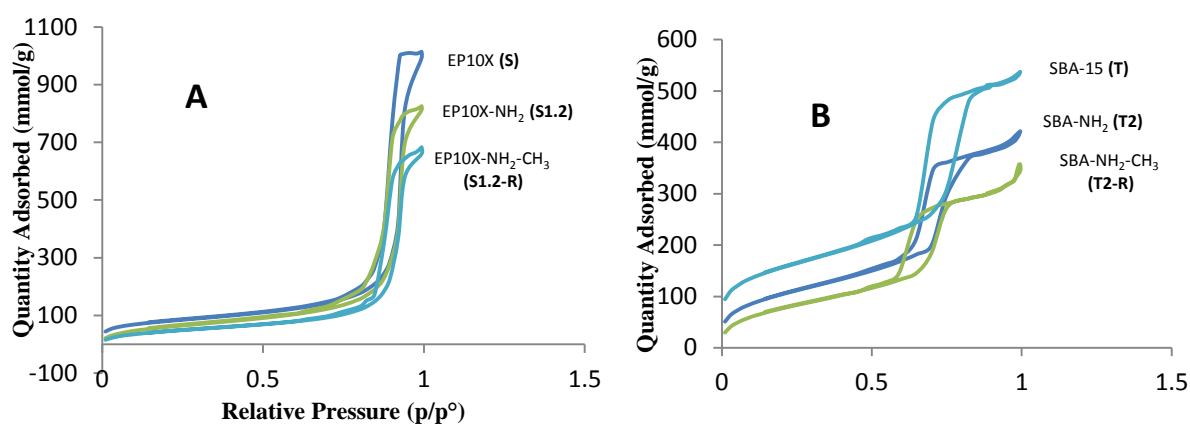


Figure 6.2. N₂ adsorption–desorption isotherms for S, S1.2 and S1.2-R (A) and T, T2 and T2-R (B).

As shown in Figure 6.2, SiO₂ (S) and SiO₂ (T) show type IV and V isotherms before and after grafting the amine groups according to the IUPAC classification.²¹ The type IV isotherm is typical for mesoporous adsorbents.

The main observation from these isotherm sets is that they remain broadly the same as we move from the parent support material to the amine-functionalised and then to the amine-functionalised and capped materials, but with progressively less adsorption consistent with a falling surface area and pore volume as the functionalisation proceeds. Significantly, the “height” of the isotherm falls most in the p/p₀ 0.5+ region suggesting that the reduction in mesopore volume is the main (but not the only) effect of functionalisation.

The hysteresis observed on the adsorption-desorption isotherms for all samples are characteristic. The hysteresis shapes for SiO₂ (T), before and after functionalisation, are indicative of cylindrical pores (as would be expected from the SiO₂ (T) structure, and those for the amorphous silica samples are typical of more disordered pore structures, as would be expected.

The specific (BET) surface areas, the average pore diameters and the total pore volumes calculated from the corresponding nitrogen sorption isotherms along for the six catalysts are shown in Table 6.3.

Table 6.3. Surface characteristics of S1.2, T2 uncapped and S1.2-R, T2-R capped.

Types of base catalysts	Surface Area (m ² /g)			Average Pore Size (nm)			Average Pore Volume (cm ³ /g)		
	Raw SiO ₂	Grafted SiO ₂ -NH ₂	Capped SiO ₂ -NH ₂ -CH ₃	Raw SiO ₂	Grafted SiO ₂ -NH ₂	Capped SiO ₂ -NH ₂ -CH ₃	Raw SiO ₂	Grafted SiO ₂ -NH ₂	Capped SiO ₂ -NH ₂ -CH ₃
SiO₂-NH₂ (S1.2)	290	257	178	17	17	16	1.6	1.6	1.1
SiO₂-NH₂ (T2)	557	230	6.37	6.0	0.85	0.75	557	230	6.37

The average uncertainty for these measurements is approximately +/- 5% for surface area, 2% for average pore size and 0.2% for pore volume.

Surface areas, pore sizes and pore volumes decrease on grafting aminopropyl groups to the surface and decrease further when the methyl groups are added. The decrease in average pore size is consistent with the observation made above that functionalisation seems to mainly reduce the mesopore volume.

The amount of active -NH₂ sites on the silica surfaces was estimated from back titration with HCl/NaOH and is given in Table 6.4.

Table 6.4. The concentration of active sites on silica supports estimated by back titration for the (S1.2), (S1.2-R) and (T2), (T2-R) catalysts.

Base catalysts	Titration (NH ₂ /mmol g ⁻¹) ^a
SiO₂-NH₂ (S1.2)	1.6
SiO₂-NH₂-CH₃ (S1.2-R)	1.5
SiO₂-NH₂ (T2)	1.0
SiO₂-NH₂-CH₃ (T2-R)	0.9

(a) All values are to +/- 0.1 mmol g⁻¹

There is no significant difference between the number of active sites on SiO₂-NH₂ (S1.2) compared to SiO₂-NH₂-CH₃ (S1.2-R) and SiO₂-NH₂ (T2) compared to SiO₂-NH₂-CH₃ (T2-R) indicating that adding methyl groups to the surface did not result in significant leaching of amine groups from the surface. (Table 6.4)

Elemental analysis results for two representative catalysts appear in Table 6.4, showing N, C and H % w/w values. Nitrogen content reflects the amine content, the carbon and the hydrogen content, or more specifically the molar ratio of carbon to nitrogen and carbon to hydrogen.

The first thing to note is the comparison between the amine contents by titration and the amine contents based on N content were 95 to 100 % similar, nearly identical in both methods. It is clear that, within experimental error, values from the two methods are in agreement (Table 6.6).

Amine group concentration was calculated as shown in Equation 1.

$$C_{\text{NH}_2} = (\text{N\%} / 14.0) \times 10 \text{ mmol g}^{-1} \quad (\text{Equation 1})$$

Elemental analysis for some studied catalysts was performed to confirm the titration results.

Table 6.5. Elemental analysis data for two samples of functionalised for SiO₂-NH₂ (S1.2) uncapped and SiO₂-NH₂-CH₃ (S1.2-R) capped.

	N% w/w	mmol/g	C% w/w	mmol/g	H% w/w	mmol/g	C/N	H/N
SiO ₂ -NH ₂ (S1.2)	2.27	1.6	5.88	4.9	1.83	18.3	3.0	11.4
SiO ₂ -NH ₂ -CH ₃ (S1.2-R)	1.97	1.4	7.76	6.4	2.01	20.1	4.5	14.3

(a) Each value represents the average of several repeats +/- 0.1.

The second observation is based on the molar ratio of C to N on each catalyst. The importance of this measurement can be used to identify the way in which the functional group is bound to the silica surface.

From elemental analysis data in Table 6.5, the carbon-to-nitrogen molar ratio is 3.0 which is consistent with bonding of silane to three silanols, with all three methoxy groups on the original silane having been eliminated (as methanol). This is shown in the third example given in Figure 6.3. This is good evidence of effective functionalisation of the silica surface.

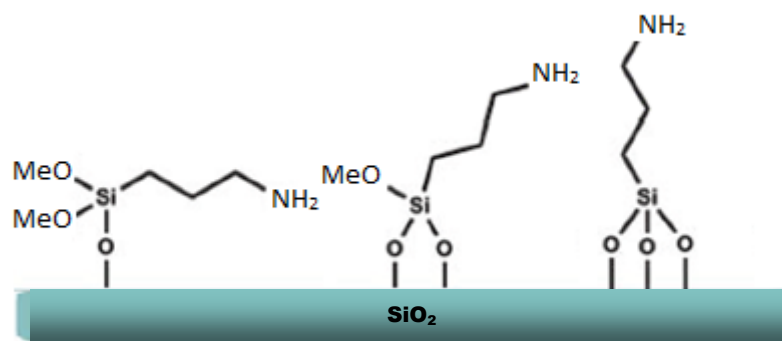


Figure 6.3: Possibilities of linkage through one, two or three hydroxyl groups on the silica support.

Table 6.6. The number of active sites in two of the studied catalysts as measured by back titration and confirmed by elemental analysis.

Base catalysts	Number of active sites (mmol g^{-1})	
	By titration $\text{NH}_2/\text{mmol g}^{-1}$	By elemental analysis. $\text{NH}_2/\text{mmol g}^{-1}$
$\text{SiO}_2\text{-NH}_2$ (S1.2)	1.6	1.6
$\text{SiO}_2\text{-NH}_2$ (S1.2-R)	1.5	1.4

A comparison between the carbon contents of the catalysts before and after the capping of silanol groups with trimethoxymethylsilane (TMMS) gives an indication of the effectiveness of the methyl capping process.

Table 6.7. Elemental analysis data of base catalysts.

Base catalysts	Carbon (C) mmol g^{-1}
$\text{SiO}_2\text{-NH}_2$ (S1.2)	4.9
$\text{SiO}_2\text{-NH}_2\text{-CH}_3$ (S1.2-R)	6.4
$\text{SiO}_2\text{-NH}_2$ (T2)	2.9
$\text{SiO}_2\text{-NH}_2\text{-CH}_3$ (T2-R)	4.8

Assuming that the trimethoxymethylsilane also binds to the silica with the elimination of all three methoxy groups, the additional molar carbon content is a direct measure of the surface concentration of methyl capping groups. The difference between $\text{SiO}_2\text{-NH}_2\text{-CH}_3$ (S1.2-R) and $\text{SiO}_2\text{-NH}_2$ (S1.2) is 1.5 mmol g^{-1} of carbon. This implies that the concentration of capping methyl groups is also 1.5 mmol g^{-1} . On the same basis for $\text{SiO}_2\text{-NH}_2\text{-CH}_3$ (T2-R), the capping methyl group concentration is 1.9 mmol g^{-1} . This suggests that more unfunctionalised silanol groups were available on $\text{SiO}_2\text{-NH}_2$ (T2) compared to $\text{SiO}_2\text{-NH}_2$ (S1.2) for subsequent reaction with TMMS and functionalisation with capping groups. This is reasonable because $\text{SiO}_2\text{-NH}_2$ (T2) has a lower concentration of amine groups on the surface than $\text{SiO}_2\text{-NH}_2$ (S1.2) (Table 6.4).

6.3.1.2. The p-XRD patterns of SiO_2 (T), $\text{SiO}_2\text{-NH}_2$ (T1), $\text{SiO}_2\text{-NH}_2$ (T2), $\text{SiO}_2\text{-NH}_2$ (T4), and $\text{SiO}_2\text{-NH}_2$ (T6).

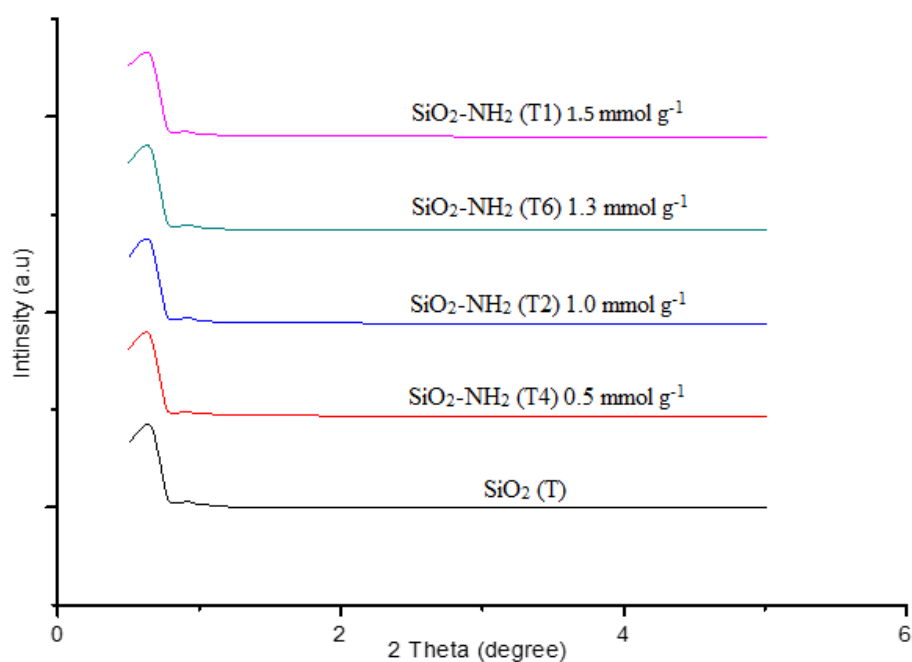


Figure 6.4. – XRD diffraction patterns of (T), (T1), (T2), (T4) and (T6).

Typical powder x-ray diffraction patterns of SiO_2 (T), $\text{SiO}_2\text{-NH}_2$ (T1) 1.5 mmol g^{-1} , $\text{SiO}_2\text{-NH}_2$ (T6) 1.3 mmol g^{-1} , $\text{SiO}_2\text{-NH}_2$ (T2) 1.0 mmol g^{-1} and $\text{SiO}_2\text{-NH}_2$ (T4) 0.5 mmol g^{-1} in range from $0.5^\circ > 2\theta < 5^\circ$ are shown in Figure 6.4. They exhibit very similar patterns with well-resolved diffraction peaks at 0.8° due to reflections from (100) planes. The peaks due to the (110) and (200) planes were not clearly resolved. Thus, the mesoporous structure was not destroyed during the surface amino-functionalization process. Similar patterns were also reported in the literature.²²

6.3.1.3. Investigation of hydrophilicity characteristic of catalyst SiO_2 (S), $\text{SiO}_2\text{-NH}_2$ (S1.2) and $\text{SiO}_2\text{-NH}_2\text{-CH}_3$ (S1.2-R), by using dynamic vapour sorption data (DVS)

To investigate the hydrophilicity characteristic of samples SiO_2 (S), $\text{SiO}_2\text{-NH}_2$ (S1.2) and $\text{SiO}_2\text{-NH}_2\text{-CH}_3$ (S1.2-R), the catalysts were tested by dynamic vapour sorption data (DVS) where the catalyst was subjected to different levels of humidity at room temperature. Water uptake data for S, S1.2 and S1.2-R were measured by DVS (Figure 6.5).

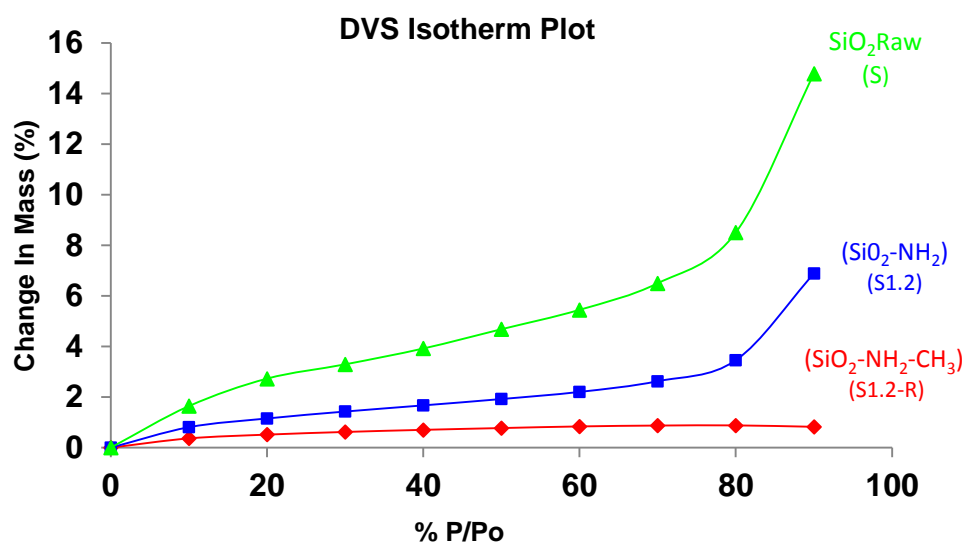


Figure 6.5. Water sorption isotherm obtained at 298 K on S, S1.2 and S1.2-R.

Water sorption yielded type IV isotherms, which are indicative of weak adsorbate–adsorbent interactions. The lower uptake of water in $\text{SiO}_2\text{-NH}_2$ (S1.2) than in SiO_2 (S) is indicative of increased hydrophobicity of this material. A further major decrease in water uptake is observed when $\text{SiO}_2\text{-NH}_2$ (S1.2) is silylated to form $\text{SiO}_2\text{-NH}_2\text{-CH}_3$ (S1.2-R). The decrease in water uptake on functionalising with amine only may indeed indicate that the surface is more hydrophobic than before functionalisation but the reduced surface area of the material may also be partly responsible. The functional aminopropyl groups have an element of hydrophilicity and an element of hydrophobicity in their structures so it is not easy to say whether their presence would enhance or diminish hydrophilicity. In contrast, adding the methyl capped silanes to the surface would undoubtedly increase hydrophobicity and this is reflected in the dramatic reduction in water uptake associated with this second functionalisation step as seen in Figure 6.5.

6.3.2. Catalytic activity

The activities of the catalysts were studied in the Henry reaction between benzaldehyde and nitromethane, using an excess of nitromethane. The amount of the catalyst utilized in each experiment was carefully determined on the basis of the measured amount of amine groups on the surface in order to introduce the same amount of supported propyl amine in the different experiments.

Benzaldehyde conversion for catalysts are shown for four catalysts in Figure 6.6. It is clear from this data that $\text{SiO}_2\text{-NH}_2$ (T2) and $\text{SiO}_2\text{-NH}_2$ (S1.2) in which the free silanol groups have been capped with $-\text{CH}_3$ groups (ie $\text{SiO}_2\text{-NH}_2\text{-CH}_3$ (T2-R) and $\text{SiO}_2\text{-NH}_2\text{-CH}_3$ (S1.2-R)) exhibited very much reduced activities compared to the uncapped catalysts.

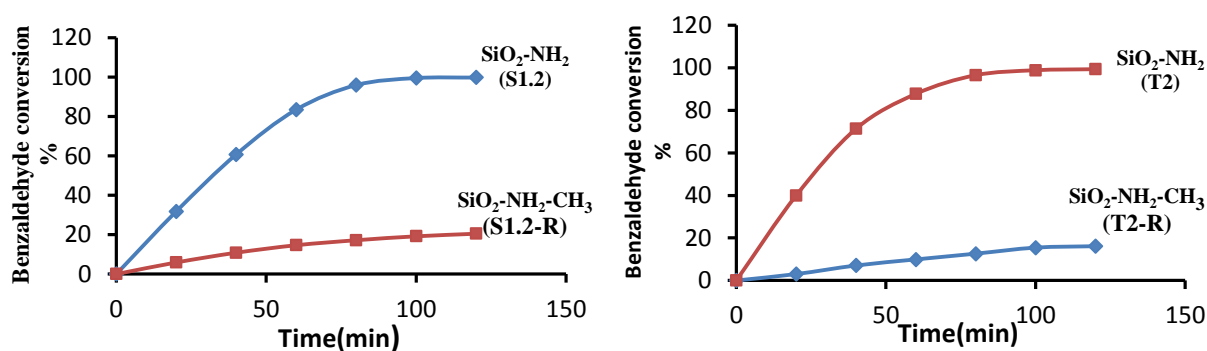


Figure 6.6 Benzaldehyde conversion vs.time using T2 and S1.2 capped and uncapped in the nitroaldol reaction at 50 °C.

The crucial question is whether this significant change in activity is the simple consequence of the hydrophobic nature of the catalysts, or does it suggest a significant role of free silanol groups on the catalyst surface alongside the aminopropyl groups in accelerating the nitroaldol reaction as suggested by Motokura *et al*, Sharma *et al* and Hruby *et al*.^[7-9]

Katz *et al*.²³ suggested a mechanism in which the acid group of Bronsted acid silanol interacts with the lone pair of electrons on the carbonyl oxygen in the benzaldehyde to give the protonated form (α -hydroxy carbocation), which is more stable than the ordinary carbocation. Then, the grafted amine nucleophilically attacks the acid stabilized aldehyde carbonyl, producing an iminium ion intermediate. At the same time, a grafted amine group deprotonates nitromethane to give the nucleophilic $^-\text{CH}_2\text{NO}_2$ anion which condenses with the iminium ion through an ion pairing mechanism to produce the final product (Figure 6.7).

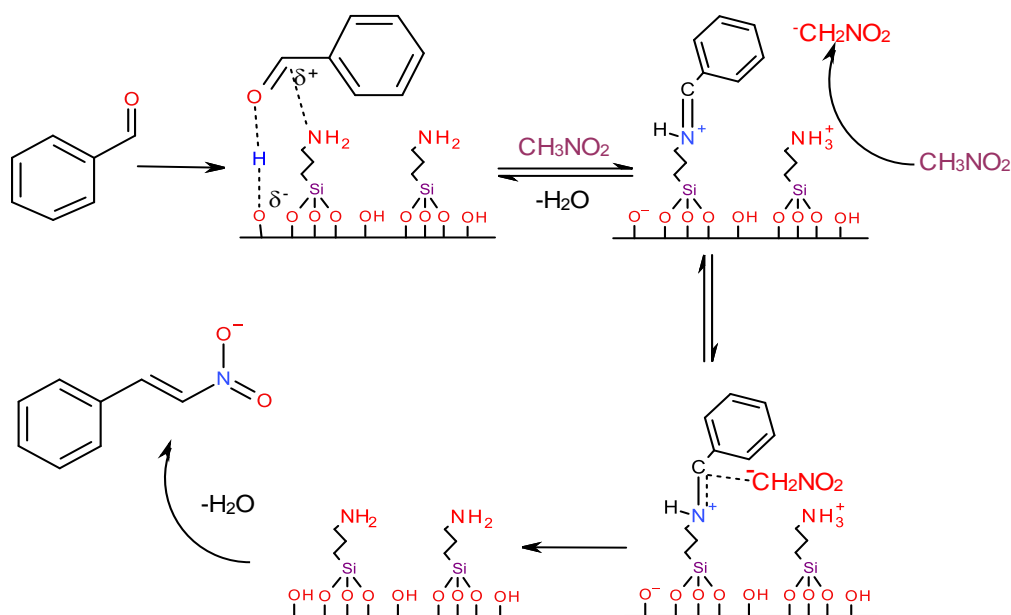


Figure 6.7. Imine catalytic mechanism for Henry reaction catalysed by amines on silica

This mechanism suggests a cooperative mechanism between silanol groups and amine groups on the surface, and takes no account of the possible effect of possible activity enhancement due simply to the higher hydrophilicity of the catalyst surface when free silanol groups are present.

6.3.2.1. Comparison between supported amine catalysts and homogeneous catalysis using APTMS in nitroaldol condensation reaction.

The same reaction was monitored under catalysis by $\text{SiO}_2\text{-NH}_2$ and compared with the reaction catalysed by the same amount of amine in the form of direct addition of homogeneous APTMS to the reaction mixture. Furthermore, an experiment was performed in which APTMS was added as a homogeneous catalyst and activated silica SiO_2 (S) was also added to the reaction mixture to investigate possible synergistic effects. In another experiment activated SiO_2 (S) alone was added to the reaction to ensure the inactivity of the support. There was no product after 2h therefore, it was confirmed that the support alone is inactive. For the other experiments benzaldehyde conversion data is shown in Figure 6.8.

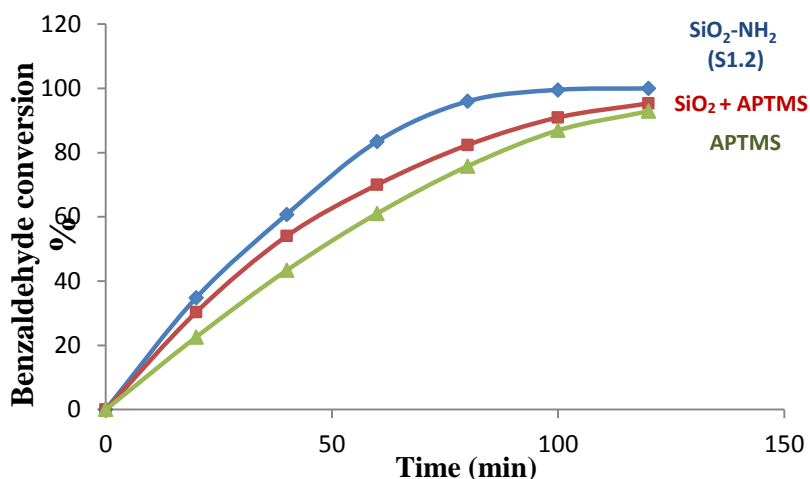


Figure 6.8. Benzaldehyde conversion vs time using SiO₂-NH₂ (S1.2), SiO₂ + APTMS and APTMS alone (all with an equivalent number of supported propylamine, 0.08 mmol) in the nitroaldol reaction at 50°C.

The results show that the supported catalyst (S1.2) is significantly more active than the same amount (0.080 mmol) of amine catalyst added as a homogeneous catalyst by 20%. This high activity of the heterogeneous amine catalyst compared to the homogeneous amine suggests that the silica surface is playing a catalytic role. In one way, this evidence supports the idea that the silanol groups are playing a role in a cooperative mechanism rather than simply enhancing the hydrophilicity of the catalyst surface since, if it were the latter, it would seem unlikely that, even with a highly hydrophilic surface, the activity of the supported amines would be comparable with that of the homogeneous amine (which is intimately mixed with the reactants and therefore, almost by definition, in better contact with reactants than surface amine groups). It may be relevant that the pK_a of silanols on functionalized silica has been reported to be between 3 and 7, depending on the type of bulk silica and the exact nature of the silanol group (isolated, geminal, vicinal, etc.)^{11, 24} so it could be the case that they are sufficiently acidic to add an element of acid catalysis, either separately or via a cooperative mechanism.

Also surprisingly, the results show that adding silica powder to the homogeneous reaction increases the activity of homogeneous amine catalysts. However the activity was lower than the immobilised amine catalyst. It is possible that some of the homogeneous amine catalyst, (3-aminopropyl)trimethoxysilane, could be adsorbing on the silica surface so that mechanism adopted by the supported catalyst could be involved. This further supports the idea of a cooperative mechanism of an acidic silanol group and amine in Henry reactions shown in Figure 6.8.

6.3.2.2. Knoevenagel condensation reaction – supported amines vs. homogeneous amine catalysts.

Similar experiments were carried out to compare homogeneous aminopropyl and supported aminopropyl catalysts in the second base-catalysed reaction between ethyl cyanoacetate and benzaldehyde in toluene a less polar reaction mixture which might be expected to be less sensitive to any enhancements in hydrophilicity if that is the key property that free silanol groups bring to the silica-supported catalysts. The results, again in terms of benzaldehyde conversion, are displayed in Figure 6.9.

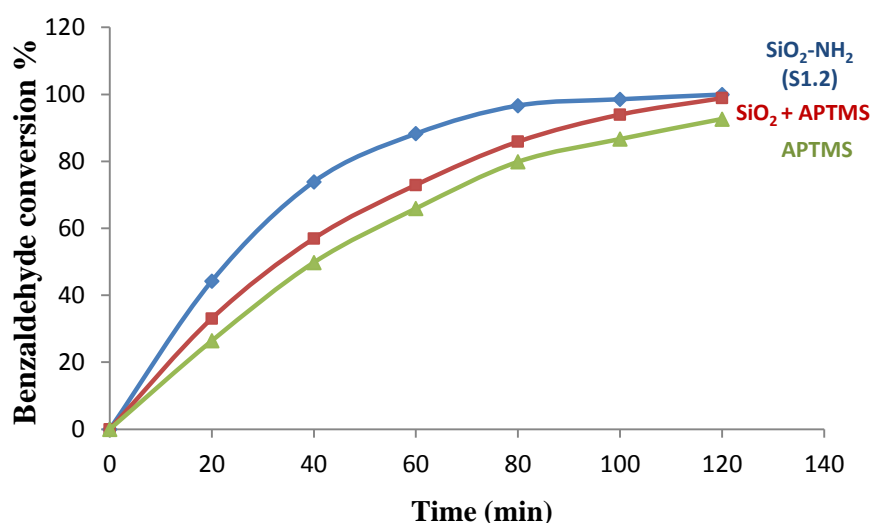


Figure 6.9. Benzaldehyde vs time for the Knoevenagel reaction studied under catalysis by SiO₂-NH₂ (S1.2), SiO₂+APTMS and APTMS alone (all with an equivalent number of supported propylamine, 0.08 mmol) in the nitroaldol reaction at 50°C.

The results show that homogeneous catalyst is again less active than the supported catalyst by 20% and they also show that separately added silica enhances the activity of the homogeneous catalyst. This suggests that the mechanism involved for the supported catalyst is due to something other than simply the effect free silanol groups have on the polarity of the catalyst surface.

6.3.2.3. Effect of capping free silanol groups on activity of silica SiO₂ (S) supported amine catalysts in the nitroaldol condensation reaction.

Various catalytic experiments were carried out with SiO₂-NH₂ catalysts with different loading whose surface silanols had been capped with trimethoxymethylsilane (TMMS). Also in this experiment the amount of the catalyst utilized in each experiment was carefully determined on the basis of the loading value in order to introduce the same amount of supported propyl amine in all experiments. Results, again in terms of benzaldehyde conversion vs. time, are shown in Figure 6.10.

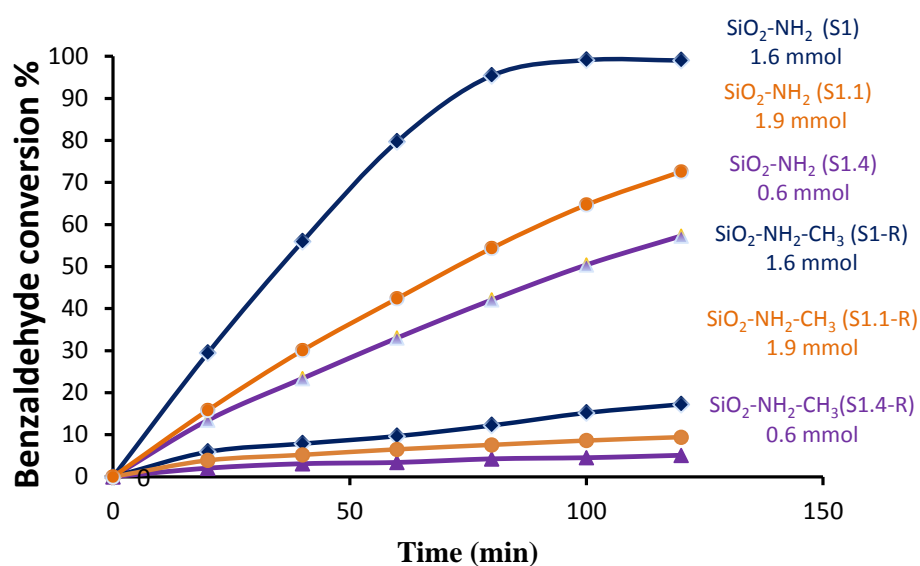


Figure 6.10. Benzaldehyde vs. time for SiO₂-NH₂ (S1, S1.1 and S1.4) and SiO₂-NH₂-CH₃ (S1-R, S1.1-R and S1.4-R), with and without surface silanol capping in the nitroaldol reaction at 50°C.

The results show that silylation resulted in a significant loss of activity for all three catalysts by up to 85%, with amine loadings from 0.6 to 1.9 mmol g⁻¹. Activities can be expressed in turn over frequency (TOF) by using the rate of reaction, assuming that the kinetics are first order in benzaldehyde and that the overall kinetics are pseudo-first order because nitromethane is used in large excess.

$$\text{Rate} = \frac{d[\text{BZ}]}{dt} = -k[\text{Nm}][\text{BZ}] \quad \text{Equation 6.1}$$

Where, Nm = Nitromethane and BZ = benzaldehyde.

$$\frac{d[\text{BZ}]}{dt} = -k'[\text{BZ}] \quad \text{when } [\text{Nm}] \gg [\text{BZ}] \text{ and } k' = k[\text{Nm}] \quad \text{Equation 6.2}$$

By integration of equation 6.2,

$$\ln [BZ] = \ln [BZ]_0 - kt \quad \text{Equation 6.3}$$

Since $[BZ] \propto [100\% \text{ conversion}]$

$$\ln [100\% \text{ conversion}] = \ln [100] - kt \quad \text{Equation 6.4}$$

Therefore by drawing $\ln [100\% \text{ conversion}]$ against time (t), a straight line with a slope equal to $-k$ will be obtained. Then by using k , TOF can be calculated by using equation 6.5.

$$\text{TOF} = \frac{k \times 60 \times \text{Initial moles of reactant (mmol)}}{\text{mmol of NH}_2} = h^{-1} \quad \text{Equation 6.5}$$

The data in the reaction progress curves for catalysts in figure 6.10 were used and the rate constants were estimated by using equation 3 as shown in Figure 6.11.

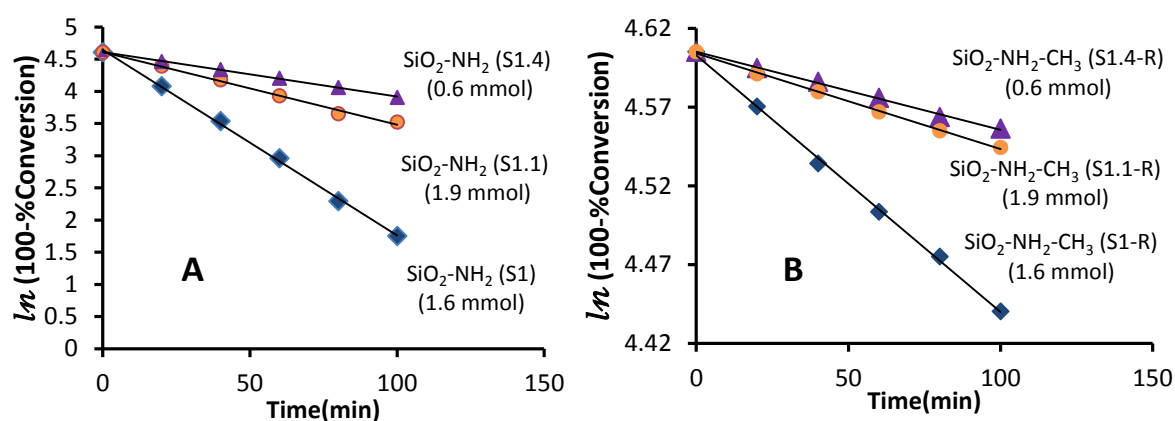


Figure 6.11. First-order plots for uncapped $\text{SiO}_2\text{-NH}_2$ (S1.4, S1.1 and S1) (A) and capped $\text{SiO}_2\text{-NH}_2\text{-CH}_3$ (S1.4-R, S1.1-R and S1-R) (B) in the nitroaldol reaction.

From data shown in Figure 6.11, appears clearly that the linear fittings are good for all catalysts in our reaction conditions as R^2 is close to 1.0. The intercept for all regression lines is approximately 4.6. These data were then analysed using the linear regression and the results are used to estimate the rate of the reaction and turn over frequency (TOF) and the results can be seen in table 6.8.

Table 6.8. First-order rate constants and TOFs for the studied catalysts in the nitroaldol reaction.

Base catalysts	Linear regression Equation of the first order rate	1 st order rate constant k (h ⁻¹) ^a	TOF (h ⁻¹) ^b 1 st order kinetics
SiO ₂ -NH ₂ (S1) (1.6 mmol)	y = -0.0289x + 4.646 R ² = 0.9987	0.0290	21 +/- 1.07
SiO ₂ -NH ₂ (S1.1) (1.9 mmol)	y = -0.0113x + 4.6106 R ² = 0.9939	0.0110	8.0 +/- 0.40
SiO ₂ -NH ₂ (S1.4) (0.6 mmol)	y = -0.0069x + 4.6082 R ² = 0.9987	0.007	4.4 +/- 0.22
SiO ₂ -NH ₂ -CH ₃ (S1-R) (1.6 mmol)	y = -0.0016x + 4.6029 R ² = 0.9985	0.0016	1.1 +/- 0.05
SiO ₂ -NH ₂ -CH ₃ (S1.1-R) (1.9 mmol)	y = -0.001x + 4.6041 R ² = 0.9986	0.0010	0.7 +/- 0.03
SiO ₂ -NH ₂ -CH ₃ (S1.4-R) (0.6 mmol)	y = -0.0005x + 4.6051 R ² = 0.9973	0.0005	0.4 +/- 0.02

(a, b) Confidence limits on k values and on TOF values are approximately +/- 5%.

The data in Table 6.8 show that capping the silanol groups decreases reaction rates to something close to only 15 % of the pre-capping values. The reduction seems to be of about the same order for all three catalysts, independent of amine content and therefore independent of the concentration of free silanol groups on the catalyst. The conclusion from this data is that the most likely role of the silanol groups on the supported catalysts is as participants in a cooperative catalytic mechanism with the amine groups. Significantly, it might be the case that a true comparison between the activities of APTMS in homogeneous solution and as aminopropyl groups supported on silica should require that the SiO₂-NH₂-CH₃ capped catalysts should be used, so that the role of silanol groups is neutralised. Had this been done, the vastly reduced activity of lower activity of SiO₂-NH₂-CH₃ would compare with the higher activity of homogeneous APTMS in a way that would be much closer to that expected from the general expectations for heterogeneous vs. homogeneous catalysis. Returning to the synergy between amine and silanol groups, it seems likely to this is the ability of silanol groups to hydrogen bond to the carbonyl groups on benzaldehyde as described above and as shown again in Figure 6.12.

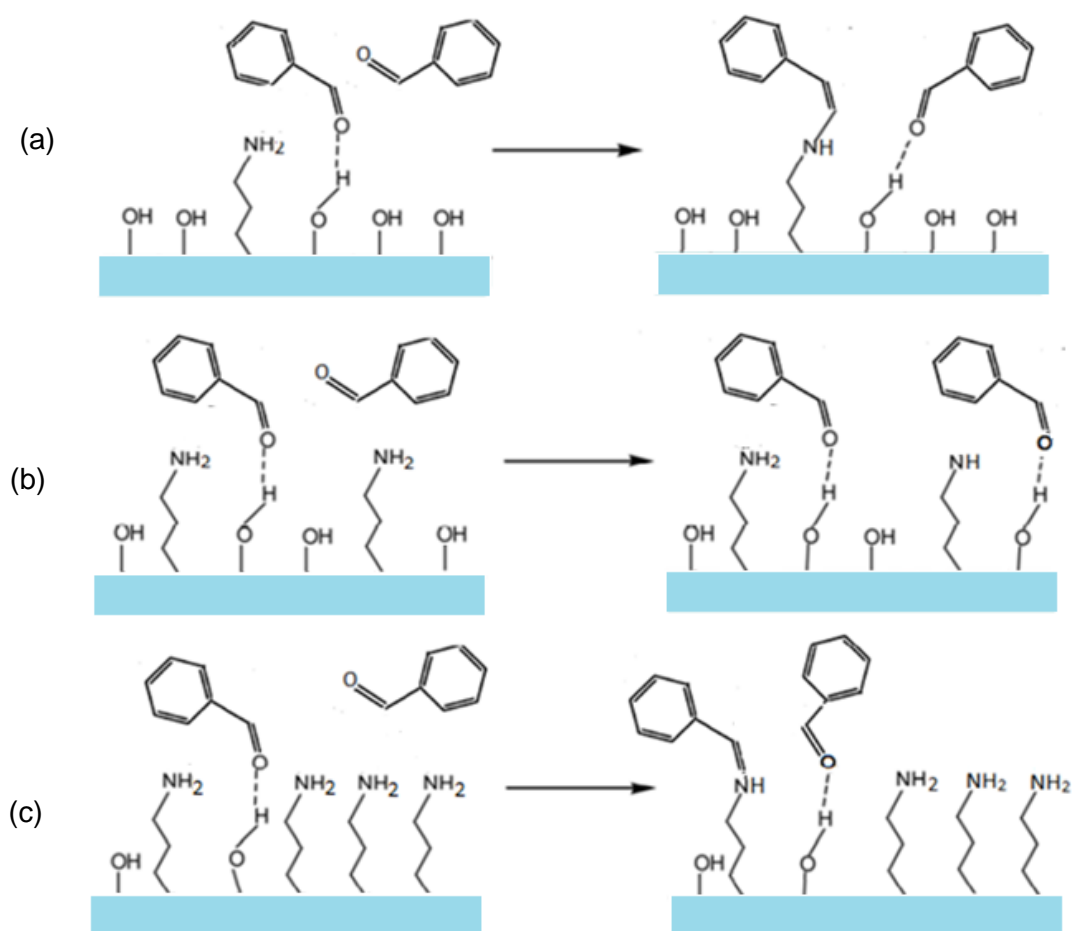


Figure 6.12. Acid-base synergistic mechanism in Henry reaction in different amine loading.

One aspect of the results that remains to be explained is why the TOFs for amine groups on catalysts where there are free silanol groups varies so much as the amine loading is varied (first three entries, final column, in Table 6.7). The effect is profound, with the TOF varying from 4.4 h^{-1} for the lowest amine loading, to 21 h^{-1} for the next and back down to 8 h^{-1} for the catalyst with the highest amine loading. It might be possible to argue that the highest amine loadings would be expected to show low activity because there are not many silanol groups available but other than that it is not really possible to offer a plausible explanation for the data observed here. The capped catalysts show TOFs in the same order, making even this explanation doubtful.

6.3.2.4. Investigation of the effect of changing the polarity of the reaction medium and the polarity of the catalyst surface.

Further experiments were designed to investigate the effect of changing the polarity of the reaction medium and the polarity of the catalyst surface. Systems were designed, using the nitroaldol reaction, to create the four sets of conditions given in Figure 6.13.

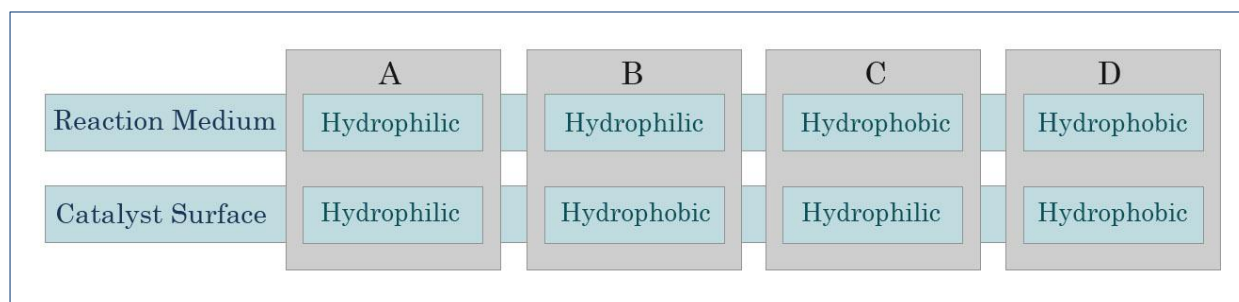


Figure 6.13. The design of experiments.

The catalytic activities were measured in four cases:

- 1- hydrophilic reaction medium with hydrophilic catalyst surface (**6.13A**)
- 2- hydrophilic reaction medium with hydrophobic catalyst surface (**6.13B**)
- 3- hydrophobic reaction medium with hydrophilic catalyst surface (**6.13C**)
- 4- hydrophobic reaction medium with hydrophobic catalyst surface (**6.13D**)

The polarity of the reaction medium was altered by replacing nitromethane with nitroethane and nitropropane.

Figure 6.14 shows the activity of $\text{SiO}_2\text{-NH}_2$ (T2) (hydrophilic surface) with nitromethane, nitroethane and nitropropane. As the reagent in excess in the nitroaldol reaction.

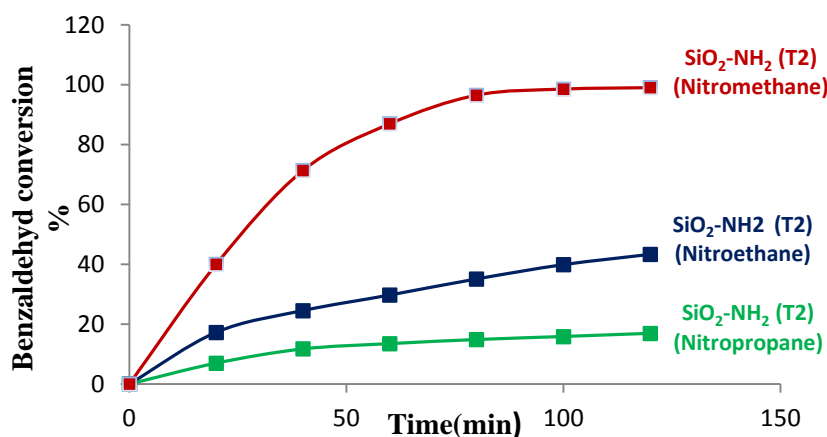


Figure 6.14. Benzaldehyd conversion vs time using $\text{SiO}_2\text{-NH}_2$ (T2), in nitroaldol reaction at 50 °C.

As shown in Figure 6.14, the catalytic activity significantly decreased when nitroethane and nitropropane were used. Turn over frequency was calculated for each catalyst and the results are summarised in Table 6.9.

Table 6.9. First-order rate constants and TOFs for the studied catalysts in the nitroaldol reaction.

Catalyst and reagent	1st order rate constant k (h^{-1}) ^a	TOF (h^{-1}) ^a 1 st order kinetics
SiO ₂ -NH ₂ (T2) / Nitromethane	0.0345	30.40 +/- 1.52
SiO ₂ -NH ₂ (T2) / Nitroethane	0.0054	3.96 +/- 0.20
SiO ₂ -NH ₂ (T2) / Nitropropane	0.0021	1.54 +/- 0.08

(a)Confidence limits on k values and on TOF values are approximately +/- 5%.

The decrease in TOF was explained first as a result of the decrease in hydrophilicity of the reaction medium, suggesting that in fact the key to controlling these catalysts is indeed controlling the match in hydrophilicity between catalyst and reagents. However, perhaps unfortunately, there may be another explanation for this which may override any conclusions of this type. And this is linked to the change of the stability in the intermediate $-\text{CH}_2\text{NO}_2$ as nitromethane goes to nitroethane and nitropropane. For the reactivities of the nitro compounds, two factors have been taken into consideration; ease of formation of the carbanion from nitroalkane, and steric hindrance of the negatively charge C in the carbanion. A stable carbanion is more easily formed than an unstable carbanion, while an unstable carbanion may be more reactive than a stable carbanion in the nucleophilic addition to the adsorbed carbonyl compound. The lower reactivity of the unstable carbanion may be the reason why the nitroethane react slower than nitromethane. Thus the founding of this experiment is not exclusive to the effect of the hydrophilicity of the reaction medium.

The effect of changing from nitromethane to nitroethane on the capped catalyst and uncapped catalyst in Henry reaction was studied as shown in Figure 6.15.

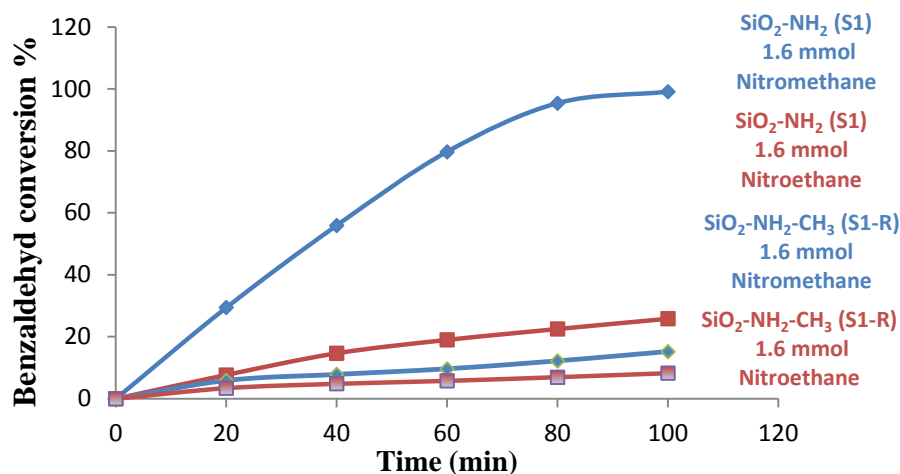


Figure 6.15. Benzaldehyde vs. time for $\text{SiO}_2\text{-NH}_2$ (S1) and $\text{SiO}_2\text{-NH}_2\text{-CH}_3$ (S1-R) catalysts with nitromethane and nitroethane, with and without surface silanol capping in the nitroaldol reaction at 50°C .

Table 6.10. The TOF was used to judge the catalytic activity of the base catalysts.

Types of base catalysts	Number of active sites (mmol g^{-1}) ^a	TOF (h^{-1}) 1 st Order Kinetics	
		Uncapped $\text{SiO}_2\text{-NH}_2$	Capped $\text{SiO}_2\text{-NH}_2\text{-CH}_3$
$\text{SiO}_2\text{-NH}_2$ (S1) Nitromethane	1.6	21 +/- 1.07	1.1 +/- 0.05
$\text{SiO}_2\text{-NH}_2$ (S1) Nitroethane	1.6	2.3 +/- 0.12	0.66 +/- 0.03

(a) Estimated by back titration and all values are to +/- 0.1 mmol g^{-1}

By comparing the activities of the catalysts in which the silanol groups are capped (and, therefore, inactive) when using nitromethane and when using nitroethane, the difference should be due only to the differences in reactivity between the two compounds. If there is an effect of the polarity due to free silanols, then the less polar nitroethane should see a smaller drop in activity than the highly polar nitromethane. From the results, the activity towards nitroethane falls by a factor of about 4 whereas the activity towards nitromethane falls by factor of about 9. This suggests that the polarity of the catalyst surface is in part controlling adsorption and hence activity, and that the role of the free silanol groups is, at least in part, to provide a polar, hydrophilic surface that concentrates the reactants near the catalytic centres.

Other experiments were designed where the hydrophilicity of the reaction medium was altered in another way, by adding a known volume of toluene to the reaction medium while keeping the total volume constant (5mL). Four catalytic reactions were performed using $\text{SiO}_2\text{-NH}_2$ (T2). The first reaction was performed without adding any toluene to the reaction medium, the

second reaction was performed with adding 2.5 mL toluene to 2.5 mL nitromethane, the third reaction was performed with adding 4 mL toluene to 1 mL nitromethane and the fourth reaction was performed with 4.8 mL to 0.2 mL nitromethane. So, other things being equal, the observed rate might have been expected to fall from “100%” to 50% to 20%.

Figure 6.16 shows the activity of $\text{SiO}_2\text{-NH}_2$ (T2) (hydrophilic surface) with the different reaction media.

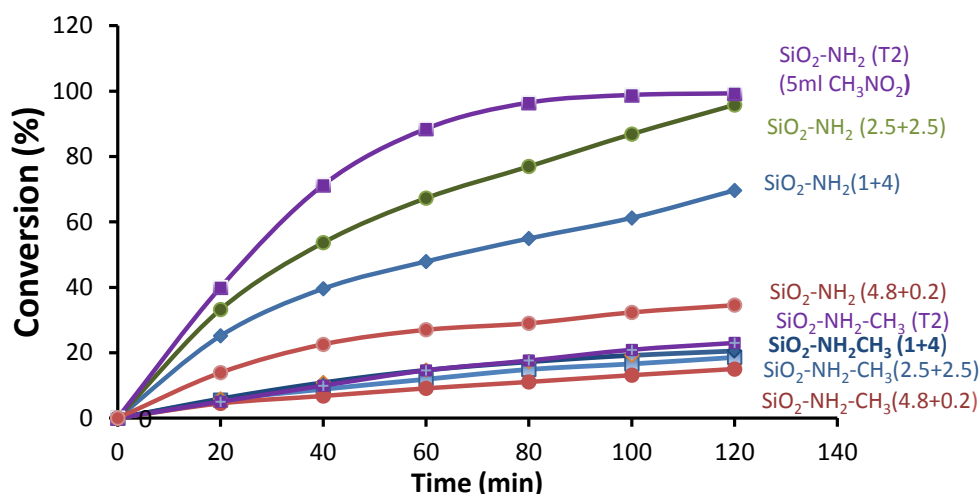


Figure 6.16. Reactivity of nitromethane with benzaldehyde in the presence of toluene over $\text{SiO}_2\text{-NH}_2$ (T2) and $\text{SiO}_2\text{-NH}_2\text{-CH}_3$ (T2-R).

The reaction progress curves in figure 6.16 were used to determine pseudo first order rate constants and TOF values. First order plots appear in Figure 6.17.

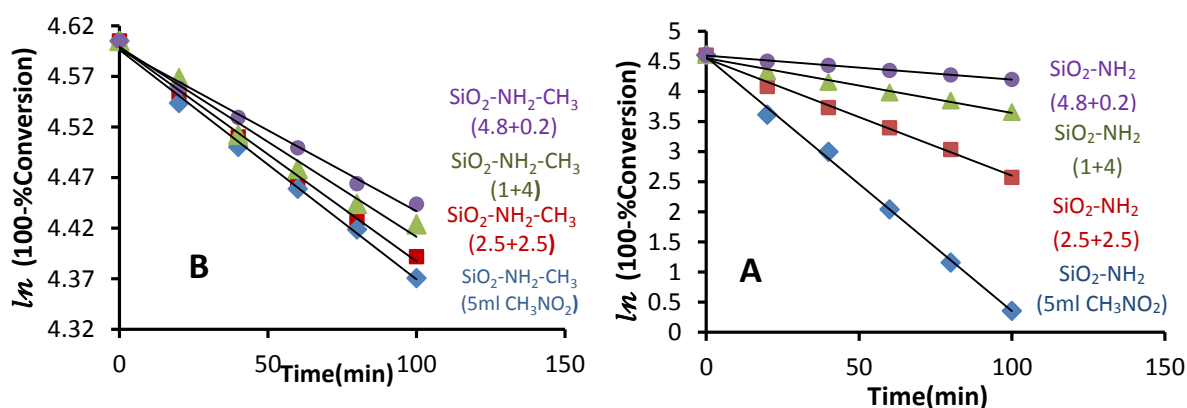


Figure 6.17. First-order kinetic model of aldol reaction for uncapped $\text{SiO}_2\text{-NH}_2$ (T2) **A** and capped $\text{SiO}_2\text{-NH}_2\text{-CH}_3$ (T2-R) **B**.

From data shown in Figure 6.17, it appears clear that the linear fittings are good for all catalysts in our reaction conditions as R^2 is close to 1.0. The intercept for all regression lines is approximately 4.6. These data were then analysed using the linear regression and the results are used to estimate the rate of the reaction and turn over frequency (TOF) and the results can be seen in Table 6.11.

Table 6.11. First-order rate constants and TOFs for the studied catalysts in the nitroaldol reaction.

Types of base catalysts	Linear regression Equation of the first order rate	TOF (h^{-1}) ^b	Linear regression Equation of the first order rate	TOF (h^{-1}) ^b
		1 st Order Kinetics		1 st Order Kinetics
		SiO ₂ -NH ₂		SiO ₂ -NH ₂ -CH ₃
SiO ₂ -NH ₂ (T2) (5ml CH ₃ NO ₂)	$y = -0.0422x + 4.5752$ $R^2 = 0.9977$	30.80 +/- 1.54	$y = -0.0023x + 4.5964$ $R^2 = 0.9951$	1.61 +/- 0.08
SiO ₂ -NH ₂ (2.5+2.5)	$y = -0.0195x + 4.5472$ $R^2 = 0.9952$	14.33 +/- 0.73	$y = -0.0021x + 4.5989$ $R^2 = 0.9964$	1.54 +/- 0.08
SiO ₂ -NH ₂ (1+4)	$y = -0.0091x + 4.5542$ $R^2 = 0.9896$	6.76 +/- 0.34	$y = -0.0019x + 4.5992$ $R^2 = 0.9816$	1.39 +/- 0.07
SiO ₂ -NH ₂ (4.8+0.2)	$y = -0.004x + 4.5964$ $R^2 = 0.9983$	2.94 +/- 0.15	$y = -0.0016x + 4.5967$ $R^2 = 0.9891$	1.17 +/- 0.06

(a, b) Confidence limits on TOF values are approximately +/- 5%.

The results in table 6.11 show that by increasing the volume of toluene in the reaction medium, TOFs fall slightly for both capped and uncapped catalysts. Within experimental error, the effect of increasing the hydrophobicity of the medium has a similar effect on the activity of the capped and the uncapped catalyst. This result is counter to that where nitroethane and nitromethane were compared in that it suggests that the hydrophilicity of the surface brought about by the free silanol groups is not key to controlling the catalytic activity of the supported amines.

6.4. Conclusion

The catalytic activities of the studied catalysts were found to significantly decrease when the silanol groups were capped with methyl groups. The capped catalysts were further investigated and compared with un-capped catalysts in different reactions designed to explore the reasons of this drop off in the activity. Nitroethane was used instead of nitromethane in the reaction and by comparing the effect of changing from nitromethane to nitroethane on the methyl capped catalyst to the effect of going from nitromethane to nitroethane on the uncapped catalysts, the relative difference observed on the uncapped catalyst was significantly greater than the difference observed on the capped catalyst thus it suggest that the polarity of the catalyst surface is in part controlling adsorption and hence activity, and that the role of the free silanol groups is, at least in part, to provide a polar, hydrophilic surface that concentrates the reactants near the catalytic centres. This finding was countered to a large extent by another designed experiment where the hydrophilicity of the reaction medium was altered by adding toluene to the reaction medium while keeping the total volume constant.

Earlier experiments in which the enhancement in activity of silica-supported amines compared to those with methyl capped silanol groups was shown to be profound in both a nitroaldol and a Knoevenagal base catalysed reaction, where the polarity of the reaction media differed significantly, also point to the relative unimportance of surface polarity in controlling activity. In overall conclusion, it seems certain that the role of free silanol groups on silica-supported amines is to participate in a cooperative base catalytic reaction mechanism with amine groups. There is potential in enhancing the synergy between the silanol and amine groups through further modifications of the support surface.

6.5. References

1. Z. A. ALothman, *Materials*, 2012, **5**, 2874-2902.
2. M. Ferré, R. Pleixats, M. W. C. Man and X. Cattoën, *Green Chemistry*, 2016.
3. J. Machado, J. Castanheiro, I. Matos, A. Ramos, J. Vital and I. Fonseca, *Microporous and Mesoporous Materials*, 2012, **163**, 237-242.
4. M. Bandyopadhyay, N. Shiju and D. Brown, *Catalysis Communications*, 2010, **11**, 660-664.
5. R. Van Grieken, J. Iglesias, V. Morales and R. García, *Microporous and Mesoporous Materials*, 2010, **131**, 321-330.
6. K. K. Sharma, R. P. Buckley and T. Asefa, *Langmuir*, 2008, **24**, 14306-14320.
7. E. L. Margelefsky, R. K. Zeidan and M. E. Davis, *Chemical Society Reviews*, 2008, **37**, 1118-1126.
8. S. L. Hruby and B. H. Shanks, *Journal of Catalysis*, 2009, **263**, 181-188.
9. J. D. Bass and A. Katz, *Chemistry of materials*, 2006, **18**, 1611-1620.
10. W. Lang, B. Su, Y. Guo and L. Chu, *Science China Chemistry*, 2012, **55**, 1167-1174.
11. I. G. Shenderovich, G. Buntkowsky, A. Schreiber, E. Gedat, S. Sharif, J. Albrecht, N. S. Golubev, G. H. Findenegg and H.-H. Limbach, *The Journal of Physical Chemistry B*, 2003, **107**, 11924-11939.
12. M. Capel-Sanchez, L. Barrio, J. Campos-Martin and J. Fierro, *Journal of colloid and interface science*, 2004, **277**, 146-153.
13. R. Anwander, I. Nagl, M. Widenmeyer, G. Engelhardt, O. Groeger, C. Palm and T. Röser, *The Journal of Physical Chemistry B*, 2000, **104**, 3532-3544.
14. A. Cauvel, G. Renard and D. Brunel, *The Journal of organic chemistry*, 1997, **62**, 749-751.
15. K. K. Sharma and T. Asefa, *Angewandte Chemie*, 2007, **119**, 2937-2940.
16. K. Motokura, M. Tada and Y. Iwasawa, *Chemistry—An Asian Journal*, 2008, **3**, 1230-1236.
17. K. Motokura, M. Tada and Y. Iwasawa, *Journal of the American Chemical Society*, 2007, **129**, 9540-9541.
18. A. N. Kursunlu, E. Guler, H. Dumrul, O. Kocyigit and I. H. Gubbuk, *Applied Surface Science*, 2009, **255**, 8798-8803.
19. S. Brunauer, P. H. Emmett and E. Teller, *Journal of the American chemical society*, 1938, **60**, 309-319.

20. R. Denoyel, M. Barrande and I. Beurroies, *Studies in surface science and catalysis*, 2007, **160**, 33-40.
21. K. S. W. Sing, D. H. Everett, R. A. W. Haul, L. Moscou, R. A. Pieroti, J. Rouquerol, T. Siemieniewska. *Pure Appl. Chem*, (1985), **57**, 603-619.
22. D. Zhang and J. Li, *Chinese Science Bulletin*, 2013, **58**, 879-883.
23. J. D. Bass, A. Solovyov, A. J. Pascall and A. Katz, *Journal of the American Chemical Society*, 2006, **128**, 3737-3747.
24. A. Méndez, E. Bosch, M. Rosés and U. D. Neue, *Journal of Chromatography A*, 2003, **986**, 33-44.

Chapter 7

SUMMARY AND CONCLUSION

7.1. Conclusion

During this research, several experiments were done to understand nature and behaviour for solid base catalysts. The physical properties of the silica support have showed a significant effect on the catalyst performance in nitroaldol reaction. In addition, the effect of chemical properties of the silica were also clear on the catalyst activity, especially in terms of how active sites of the catalyst are anchored on the surface and in the pores. This is generally confirmed the role of silanol groups on the silica surface in enhanced the catalytic performance.

In chapter 3, eight silica supports which have been functionalized by grafting 3-aminopropyl (trimethoxysilane) (APTMS), prepared from different amorphous silica gel with various structural parameters, such as surface area and porosity (dimension, distribution and shape of the pores) were studied before and after functionalization with aminopropylsilane groups.

The catalytic activity in nitroaldol reaction showed a hesitant level of dependency on surface area, amount of active sites, pore size and pore volume. However, one of the key variables to affect the catalytic activity was the surface coverage.

The results exhibited that variations of structural properties of the catalysts have a significant effect on their activity, since they influence the dispersion of the active sites, but the most interesting results were the activity of silica nanopowder $\text{SiO}_2\text{-NH}_2$ (S3) which was much lower than other catalysts, despite the amount of amine groups on the surface which was very high (2.0 mmol^{-1}) comparing to other catalysts. This lower activity may be a result of multilayer formation of aminopropylsilane on the silica support surface. This multilayer may be created when the methoxy groups from two APTMS molecules are displaced, and a siloxane bond is formed between them.

In chapter 4, the effect of the loading amount of aminopropylsilane on $\text{SiO}_2\text{-NH}_2$ (S3) and $\text{SiO}_2\text{-NH}_2$ (S1) have been studied by varying the amount of APTMS in the reaction medium (toluene) to obtain different surface coverage. The catalytic activity in nitroaldol reaction showed maximum base catalytic activity per active site was obtained with catalyst in which the amount of APTMS was calculated to completely cover the support surface in a monolayer (on the basis that one trimethoxysilane covers 0.50 nm^2), avoiding multilayers.

It is concluded that loading a support above this maximum value results in a rapid decrease in activity. This approach, in which optimum loadings can be calculated, can be applied to other support materials.

In chapter 5, eighteen amine functional mesoporous catalysts have been synthesized by grafting different aminopropylalkoxysilanes: (3-Amino-propyl) triethoxysilane (APTES), (3-aminopropyl) diethoxymethylsilane (APDEMS) and (3-Aminopropyl) dimethylethoxysilane (APDMES), with two different supports crystalline silica SBA-15 and amorphous silica EP10X. By adjusting the organoamine precursor or support dosage, the amine loading amount can be controlled. An optimum organoamine loading amount exists for each amine series catalysts. However, the optimum organoamine loading amount varies with the amine type and the area it takes from the surface, the surface area of the support and the crystal structure of the support.

In conclusion, even if using aminopropyldimethoxysilane and aminopropylmonoethoxysilane instead of aminopropyltrimethoxysilane had no effect on the optimum loading amount which was 1.0 mmol with the three precursors. However the turnover frequency decreased with decreasing the binding sites in the precursors (ethoxy groups). Also the surface area further decreased when three ethoxy precursor are replaced with the diethoxy and monoethoxy precursor which could explain the decrease in activity represented by TOF.

In chapter 6, the role of the silanol groups in aldol catalysis have been investigated, various catalytic experiments were carried out with heterogeneous catalysts whose surface silanols had been capped with trimethylsilyl (TMMS) that make the surface highly hydrophobic. The reduction in activity following silylation confirms the catalytic role played by the silanol groups. The capped catalysts were further investigated and compared with un-capped catalysts in different reactions designed to explore the reasons of this drop off in the activity, therefore it indicate that the polarity of the catalyst surface is in part controlling adsorption and hence activity, and that the role of the free silanol groups is indeed to provide a polar, hydrophilic surface that concentrates the reactants near the catalytic centres.

In conclusion, the silanol group on the surface of the catalyst were found to play a crucial role in the activity of the catalyst as they provide a polar, hydrophilic surface that concentrates the reactants near the catalytic centres and facilitate the active sites (amine groups) function.

7.2. Recommendations for future work

Further investigations are possible for all aspects this thesis, there are several ways in which this study could be expanded:

In this study, the extent of coverage of the silica supports was found to be a key property in determining activity by controlling the amount of amino groups. The same approach could be used on the other supports such as clays, aluminas, halloysite, which can exhibit different intrinsic acidity or basicity and this would certainly add more about the role the surface plays in helping or hindering the activity of the supported amine groups.

It has also been proved in this study that acid-base cooperativity between amines and silanols is crucial to the catalytic performances of the functionalized mesoporous catalysts. Therefore, a similar study can be carried out (on silicas) with supported sulfonic acids (with organic tethers) for instance to see whether silanol groups are important in enhancing or diminishing acid catalytic activity.

The possible used of another characterisation techniques such as scanning electron microscopy (SEM) could further help in identifying the nature of catalyst. Combination between SEM and XRD data might give a clear picture on any possible formation of mesoporous structures before and after.

APPENDICES

Appendices A

Calculate of Surface coverage by active sites:

Equation of calculation of Surface coverage by active sites:

$$(50 \times 10^{-20} \text{m}^2) \times (\text{Number of active sites mol g}^{-1}) \times (\text{Avogadro's number} = 6.022 \times 10^{23} \text{ mol}^{-1})^*$$

1) Silica gel – 717185: (L1)

$$(50 \times 10^{-20} \text{m}^2) \times (0.7 \times 10^{-3} \text{ mol g}^{-1}) \times (6.022 \times 10^{23} \text{ mol}^{-1}) = 221 \text{ m}^2 \text{ g}^{-1}$$

2) Silica 9536 (L2)

$$(50 \times 10^{-20} \text{m}^2) \times (0.9 \times 10^{-3} \text{ mol g}^{-1}) \times (6.022 \times 10^{23} \text{ mol}^{-1}) = 271 \text{ m}^2 \text{ g}^{-1}$$

3) Silica gel – 214396 (L3)

$$(50 \times 10^{-20} \text{m}^2) \times (0.8 \times 10^{-3} \text{ mol g}^{-1}) \times (6.022 \times 10^{23} \text{ mol}^{-1}) = 240 \text{ m}^2 \text{ g}^{-1}$$

4) Kieselgel (M1)

$$(50 \times 10^{-20} \text{m}^2) \times (1.6 \times 10^{-3} \text{ mol g}^{-1}) \times (6.022 \times 10^{23} \text{ mol}^{-1}) = 482 \text{ m}^2 \text{ g}^{-1}$$

5) Silica gel – 236845 (M2)

$$(50 \times 10^{-20} \text{m}^2) \times (1.3 \times 10^{-3} \text{ mol g}^{-1}) \times (6.022 \times 10^{23} \text{ mol}^{-1}) = 391 \text{ m}^2 \text{ g}^{-1}$$

6) Silica EP10X (S1)

$$(50 \times 10^{-20} \text{m}^2) \times (1.6 \times 10^{-3} \text{ mol g}^{-1}) \times (6.022 \times 10^{23} \text{ mol}^{-1}) = 482 \text{ m}^2 \text{ g}^{-1}$$

7) Silica Fumed (S2)

$$(50 \times 10^{-20} \text{m}^2) \times (1.3 \times 10^{-3} \text{ mol g}^{-1}) \times (6.022 \times 10^{23} \text{ mol}^{-1}) = 391 \text{ m}^2 \text{ g}^{-1}$$

8) Silica nanopowder (S3)d

$$(50 \times 10^{-20} \text{m}^2) \times (2.0 \times 10^{-3} \text{ mol g}^{-1}) \times (6.022 \times 10^{23} \text{ mol}^{-1}) = 602 \text{ m}^2 \text{ g}^{-1}$$

*M. Etienne and A. Walcarius, *Talanta*, 2003, **59**, 1173-1188.

Appendices B

Calculate the theoretical amount of APTMS which can immobilize on specific surface area of silica EP10X (S1.2):

$$\text{BET}_{(\text{Raw Silica})} = 290 \text{ m}^2/\text{g}$$

$$\text{Pore Size}_{(\text{Raw Silica})} = 17.25 \text{ nm}$$

$$\text{Pore Volume}_{(\text{Raw Silica})} = 1.57 \text{ cm}^3/\text{g}$$

One molecule of APTMS covers approximately $0.50 \text{ nm}^2 = 50 \text{ \AA}^2$

$$\text{Convert } 50 \text{ \AA}^2 \text{ to } \text{m}^2 = 0.5 \times 10^{-18} \text{m}^2$$

$$\text{Number of APTMS which could cover all surface/g} = \frac{290 \text{ m}^2}{0.5 \times 10^{-18} \text{m}^2} = 5.8 \times 10^{20} \text{ molecule g}^{-1}.$$

$$\text{Divide by Avogadro number} = \text{Atom / mol} = \frac{5.8 \times 10^{20}}{6.02 \times 10^{23}} = 0.963 \times 10^{-3} \text{ mol g}^{-1}$$

$$\text{Number of moles of APTMS} = 0.963 \times 10^{-3} \text{ mol} = 0.963 \text{ mmol g}^{-1}$$

$$0.963 \times 10^{-3} \text{ mol} \times 179.29 \text{ g/mol} = 0.173 \text{g}$$

$$0.172 \text{ g} \times \frac{1 \text{ ml}}{1.027 \text{ g}} = 0.168 \text{ ml}$$

0.168 of APTMS covered one gram of activated silica.

Appendices C

Gas Chromatography Clarus 500 Perkin Elmer

This work utilized gas chromatography technique to monitor sample (reactant and product) for nitroaldol (Henry) reaction and tandem deacetalization-Henry reaction. The GC used for this purpose was Perkin Elmer Clarus 500 with 50 m capillary column (BP1 column), equipped with FID detector.

a) Gas Chromatography operation conditions

Unit	Operating Conditions
Column	BP1 50 m
Detector	Flame Ionisation Detector (FID) at 250 °C
Oven Temperature	Initial Temp. 60 °C, hold 0 min Ramp 1 10°/ min to 160°, hold for 0 min Ramp 2 20°/ min to 290°, hold for 2 min
Carrier Gas	Helium at 2 ml min ⁻¹ Air at 450 ml min ⁻¹ H2 at 45 ml min ⁻¹
Injector	On Colum injector
Injection temperature	250 °C
Injection volume	0.5 µml
Channel Run Time	18.5 min



Gas Chromatography Clarus 500 Perkin Elmer

b) Characterization of reaction products in test reaction: Nitroaldol reaction (henry reaction).

Reactant conversions were determined from peak areas relative to that of internal standard, using calibration plots with standard solutions of o-xylene, nitrostyrene, benzaldehyde, nitrostyrene.

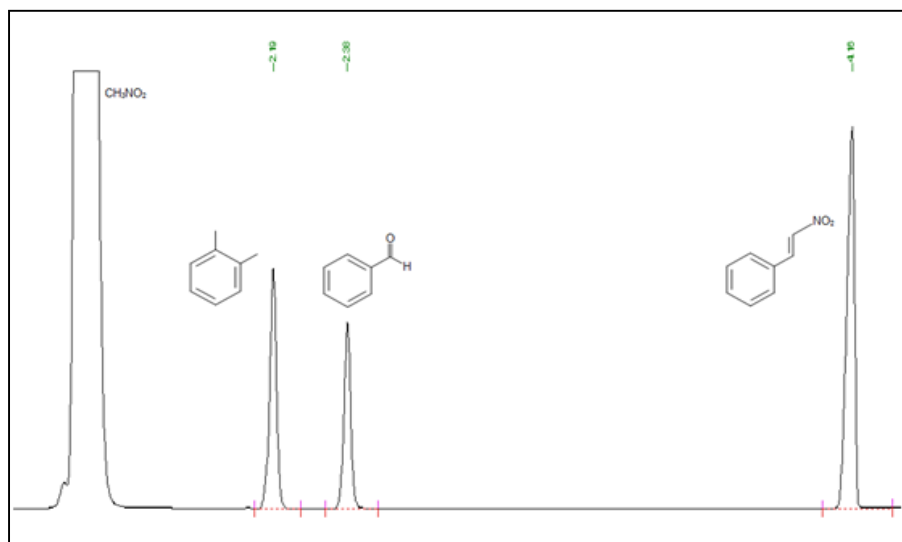


Figure X1. GC chromatograms of Nitroaldol reaction (henry reaction) to produce Nitrostyrene

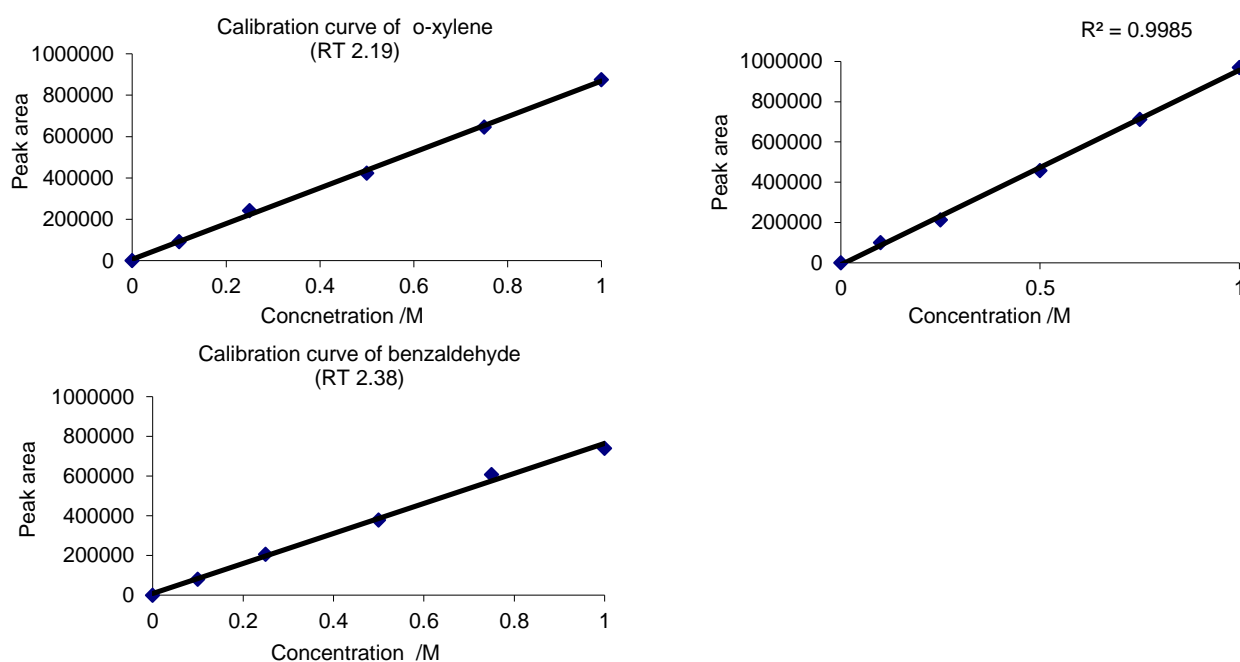
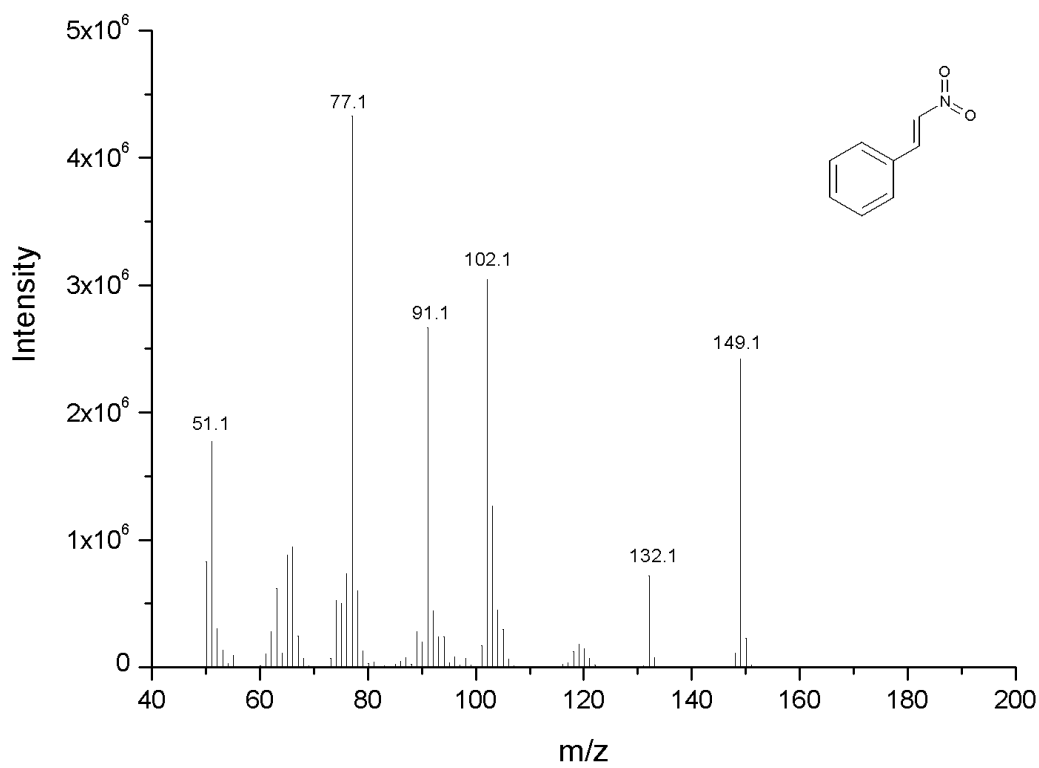
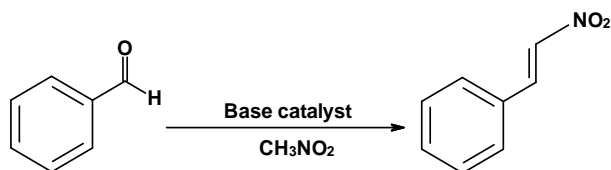


Figure X2. Calibration curves of the reactants in tandem deacetalization-henry reaction and o-xylene as internal standard

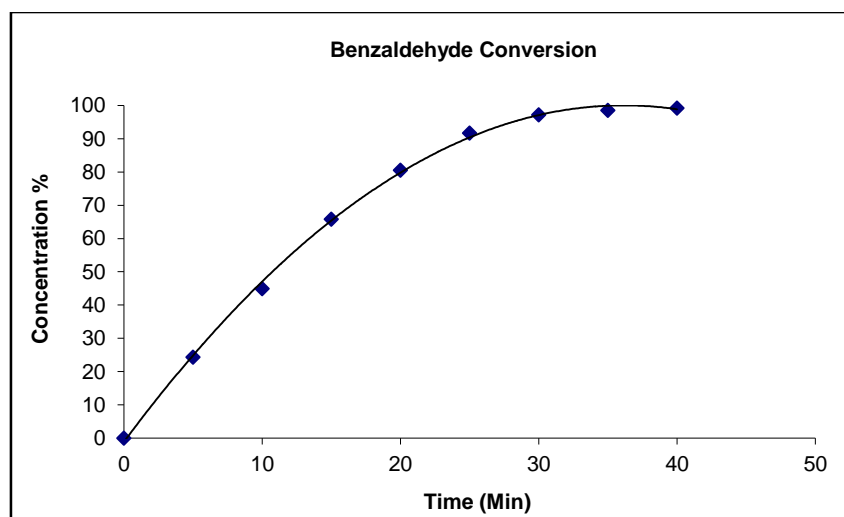
C) The identity of nitrostyrene as product was confirmed using GCMS for the peak in

Figure X1. at RI 4.10 min.**Figure X3.** Mass spectrum taken from GC peak at RI 4.10 in Fig 1S, verifying origin as nitrostyrene.

d) Monitoring the conversion using GC-FID for Henry reaction.



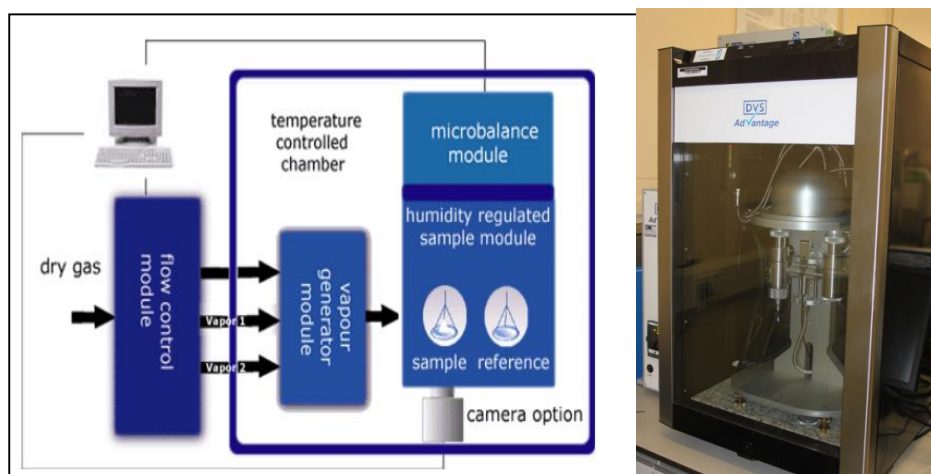
Min	SiO ₂ -NH ₂ (52.10 mg)	Peak area	Conc. M	Time min	Conc. M	Conv. %
0	Benzaldehyde	124913	0.124	0	0.124	0
	O-xylene	16303		5	0.094	24
5	Benzaldehyde	96868	0.094	10	0.068	45
	O-xylene	16712		15	0.042	66
10	Benzaldehyde	53215	0.068	20	0.024	81
	O-xylene	12624		25	0.010	92
15	Benzaldehyde	44295	0.042	30	0.003	97
	O-xylene	16923		35	0.002	99
20	Benzaldehyde	24682	0.024	40	0.001	99
	O-xylene	16586				
25	Benzaldehyde	10543	0.010			
	O-xylene	16619				
30	Benzaldehyde	3040	0.003			
	O-xylene	14091				
35	Benzaldehyde	1835	0.002			
	O-xylene	16559				
40	Benzaldehyde	1035	0.001			
	O-xylene	17585				



Appendices D

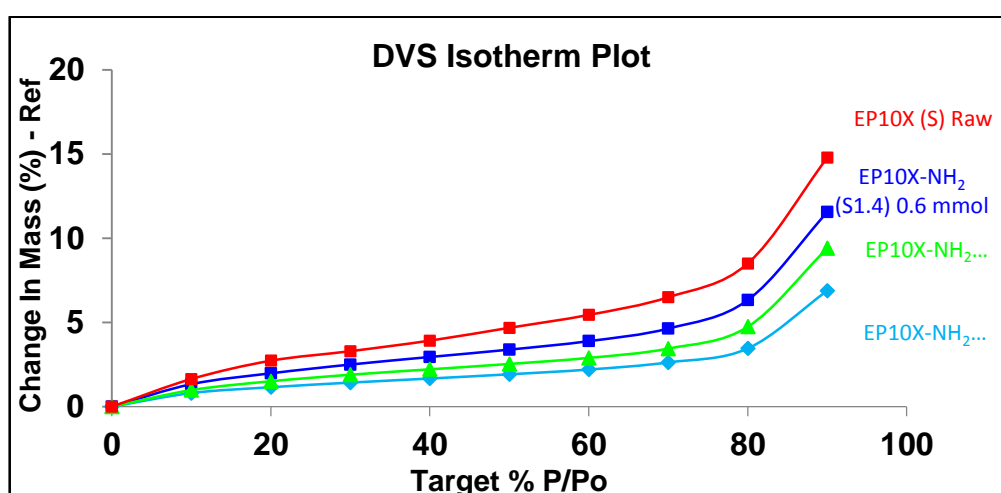
Dynamic Vapour Sorption (DVS)

Moisture sorption and desorption isotherms were generated at 25 °C using Dynamic Vapour Sorption (Surface Measurement Systems Ltd. a schematic of which is shown below).



Schematic Diagram of Dynamic Vapour Sorption Instrument

The DVS is equipped with an electronic microbalance for the accurate measurement of weight. The procedure involved 10% steps of relative humidity (RH) between 0–95% RH following an initial drying at 200 °C. Equilibrium was assumed to be established when dm/dt is equal to 0.02%; the symbol “ dm/dt ” means the criteria of sample weight change ratio (m: mass and t: time).



Water sorption isotherm obtained at 298 K on EP10X (S), EP10X-NH₂ (S1.4), EP10X-NH₂ (S1.3), EP10X-NH₂ (S1.2)

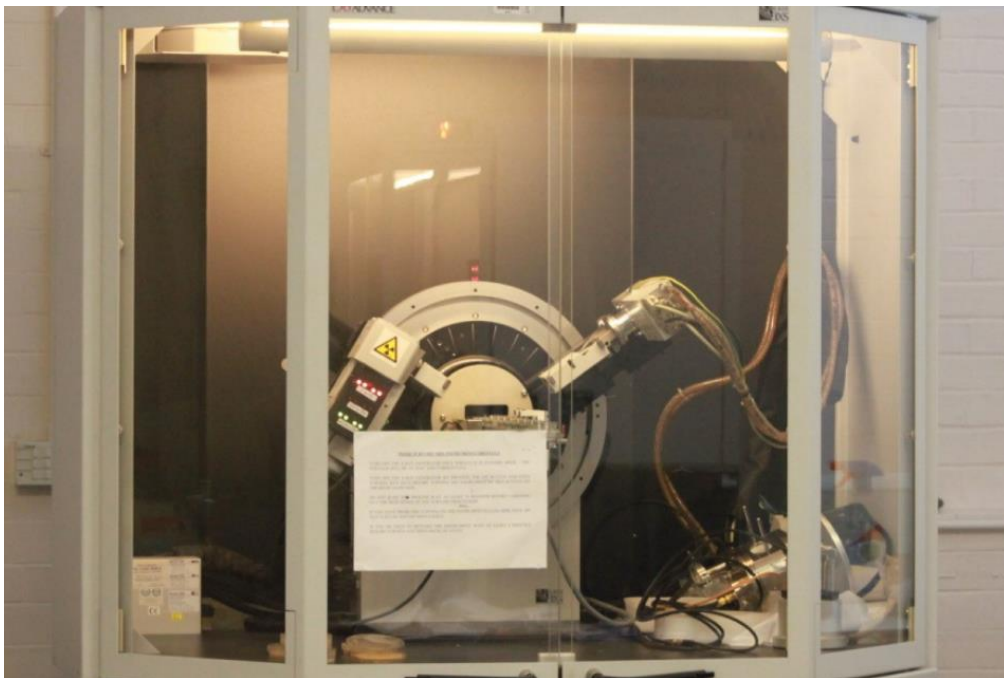
Appendices F

Powder X-ray Diffraction Bruker D8

a) Operating conditions

- Operating conditions: 40 kV, 20 mA using nickel-filtered Cu K α radiation (1.5406 Å)
- Scan Axis 2 theta
- Start 1.5 and stop 10°
- Step size: 0.02
- No. of steps: 3250
- Time/step: 1
- Total scan: 0:54:11

b) XRD –Equipment Bruker D8

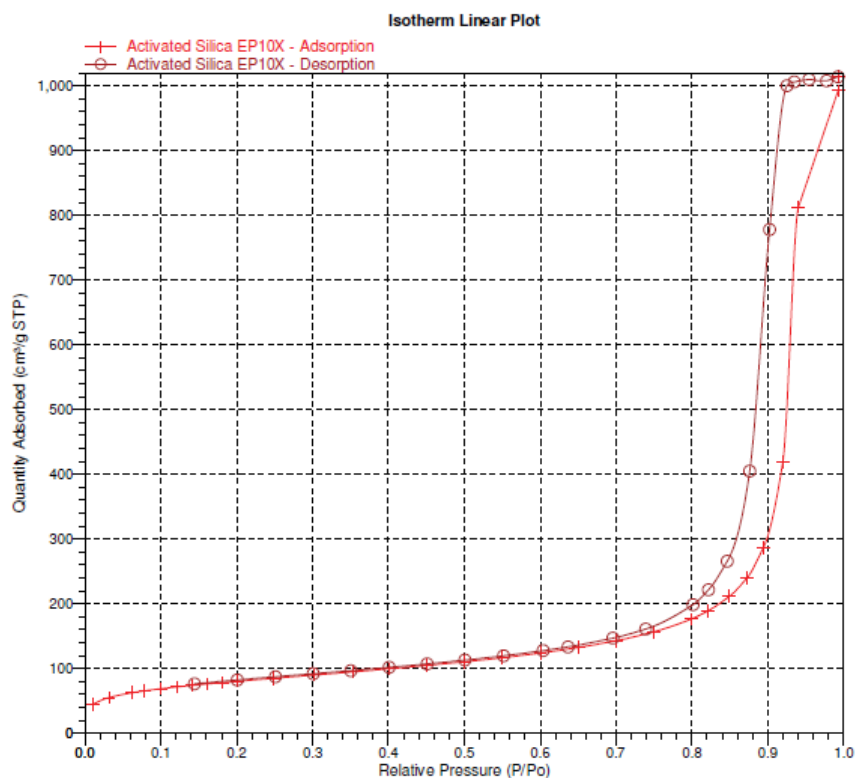


Appendices G

Nitrogen Adsorption : Micrometrics ASAP 2020

This method was used to measure BET surface area, pore volume and pore diameter of the catalyst. The analysis was run at 77 K or -196 °C.

Micrometrics ASAP 2020



Surface area report on EP10X support is shown below:

Full Report Set

ASAP 2020 V4.02 (V3.00 H)

Unit 1

Serial #: 517

Page 1

Sample: Catalyst EP10X-NH₂ 1.9 mmol (S1.1)

Operator:

Submitter:

File: C:\2020\DATA\001-518.SMP

Started: 13/04/2013 14:06:29PM	Analysis Adsorptive: N2
Completed: 14/04/2013 3:08:42PM	Analysis Bath Temp.: 77.263 K
Report Time: 06/05/2016 12:08:37PM	Thermal Correction: No
Sample Mass: 0.2041 g	Warm Free Space: 29.0005 cm ³ Measured
Cold Free Space: 88.8937 cm ³	Equilibration Interval: 10 s
Ambient Temperature: 22.00 °C	Low Pressure Dose: None
Automatic Degas: Yes	

Summary Report

Surface Area

Single point surface area at $p/p^{\circ} = 0.200516604$: 198.5577 m²/g

BET Surface Area: 219.7676 m²/g

Langmuir Surface Area: 316.2810 m²/g

t-Plot External Surface Area: 260.2613 m²/g

BJH Adsorption cumulative surface area of pores
between 17.000 Å and 3000.000 Å width: 256.110 m²/g

BJH Desorption cumulative surface area of pores
between 17.000 Å and 3000.000 Å width: 284.6130 m²/g

Pore Volume

Single point adsorption total pore volume of pores
less than 1862.804 Å width at $p/p^{\circ} = 0.989511643$: 1.035202 cm³/g

t-Plot micropore volume: -0.025720 cm³/g

BJH Adsorption cumulative volume of pores
between 17.000 Å and 3000.000 Å width: 1.051285 cm³/g

BJH Desorption cumulative volume of pores
between 17.000 Å and 3000.000 Å width: 1.064502 cm³/g

Pore Size

Adsorption average pore width (4V/A by BET): 188.4175 Å

BJH Adsorption average pore width (4V/A): 164.193 Å

BJH Desorption average pore width (4V/A): 149.607 Å